

From the Comprehensive Pneumology Center (CPC)  
in collaboration with the Department of Medicine V, University Hospital  
of the Ludwig-Maximilians-University Munich,  
the Asklepios Fachkliniken Munich-Gauting  
and the Helmholtz Center Munich



Dissertation  
zum Erwerb des Doctor of Philosophy (Ph.D.)  
an der Medizinischen Fakultät der  
Ludwig-Maximilians-Universität zu München

## **B cell-mediated autoimmunity in idiopathic pulmonary fibrosis**

vorgelegt von:

Dr. med. Gabriela Franziska Leuschner  
geboren in Landshut, Germany

2021

---

Mit Genehmigung der Medizinischen Fakultät der  
Ludwig-Maximilians-Universität zu München

**First supervisor:** Prof. Dr. med. Jürgen Behr

**Second supervisor:** Dr. Herbert Schiller

**Third supervisor:** Prof. Dr. rer. nat. Vigo Heissmeyer

**Forth supervisor:** Prof. Dr. rer. nat. Heiko Adler

**Dean:** Prof. Dr. med. Thomas Gudermann

Datum der Verteidigung:

15. März 2022

---

## Table of content

<b>Table of content</b> .....	<b>4</b>
<b>Summary</b> .....	<b>6</b>
<b>Zusammenfassung</b> .....	<b>8</b>
<b>List of figures</b> .....	<b>10</b>
<b>List of tables</b> .....	<b>16</b>
<b>List of abbreviations</b> .....	<b>17</b>
<b>1. Introduction</b> .....	<b>19</b>
1.1 Pulmonary fibrosis.....	19
1.1.1 Evolution of pulmonary fibrosis.....	19
1.1.2 Interstitial lung diseases.....	21
1.1.3 Idiopathic pulmonary fibrosis (IPF).....	22
1.1.4 Pathogenesis and risk factors for idiopathic pulmonary fibrosis (IPF).....	24
1.2 The human immune system.....	25
1.2.1 Cells of the innate and adaptive immune system.....	26
1.2.2 B cell checkpoints and break of tolerance.....	27
1.3 Autoimmunity in pulmonary fibrosis.....	30
1.3.1 Connective tissue disease related interstitial lung disease (CTD-ILD).....	30
1.3.2 Interstitial pneumonia with autoimmune features (IPAF).....	31
1.3.3 The role of autoimmunity in idiopathic pulmonary fibrosis (IPF).....	32
<b>2. Objectives</b> .....	<b>35</b>
2.1 First chapter.....	35
2.2 Second chapter.....	36
<b>3. Material and Methods</b> .....	<b>38</b>
3.1 Material and Methods for proteome profiling of human tissue fibrosis project.....	38
3.1.1 Study cohort and human patient material.....	38
3.1.2 Sample preparation for proteome analysis.....	38
3.1.3 LC-MS/MS analysis.....	40
3.1.4 Bioinformatic analysis of MS data.....	40
3.1.5 Immunohistology stainings.....	41
3.1.6 Protein isolation.....	42
3.1.7 SDS-Page and Western blot analysis.....	42
3.1.8 Statistics.....	44
3.2 Material and Methods for autoantibody discovery project.....	44
3.2.1 Study cohorts and clinical data.....	44
3.2.1 Human sample preparation.....	45
3.2.2 Differential Antigen Capture (DAC) assay.....	46
3.2.3 Mass spectrometry (MS).....	46
3.2.4 Statistics and bioinformatic analysis.....	48
<b>4. Results</b> .....	<b>49</b>

---

4.1	Characterization of the human proteome in lung and skin fibrosis.....	49
4.1.1	Introduction.....	49
4.1.2	Presence of marginal zone B and B1 cell specific protein (MZB1)-positive tissue resident plasma B cells in lung and skin fibrosis .....	51
4.1.3	Correlation of marginal zone B and B1 cell specific protein (MZB1) with state of diseases and tissue immunoglobulin G (IgG).....	57
4.1.4	IgG subclasses in ILD .....	61
4.1.5	Discussion .....	66
4.2	Autoantigen discovery in interstitial lung disease (ILD) .....	69
4.2.1	Introduction.....	69
4.2.2	Identification of lung specific autoantigens in interstitial lung disease (ILD) using a proteomic workflow .....	71
4.2.3	Study cohorts and patient characteristics .....	73
4.2.4	Discovery of unknown autoantibodies in idiopathic pulmonary fibrosis (IPF) .....	76
4.2.5	Association between novel autoantigens and transplant free survival .....	84
4.2.6	Discussion .....	95
<b>5.</b>	<b>Conclusion and future directions.....</b>	<b>99</b>
	<b>References .....</b>	<b>101</b>
	<b>Appendix: Permission to reuse figures and tables .....</b>	<b>115</b>
	<b>Acknowledgements .....</b>	<b>116</b>
	<b>Affidavit.....</b>	<b>117</b>
	<b>Confirmation of congruency .....</b>	<b>118</b>
	<b>Curriculum vitae .....</b>	<b>119</b>
	<b>List of publications .....</b>	<b>120</b>

## Summary

Fibrotic diseases are a major health concern in the developed world with only limited treatment options. Persistent tissue damage, dysregulated regeneration and repair processes or aging and autoimmunity are all factors that have been discussed as reasons for fibrosis. Fibrotic destruction of the lung leads to pulmonary fibrosis, in which the lung parenchyma scars over time. Disease progression can lead to loss of lung function, reduced pulmonary gas exchange, and ultimately organ failure. Most cases of so-called interstitial lung disease (ILD) respectively diffuse parenchymal lung disease are associated with a fibrotic remodeling of the lung parenchyma thus pulmonary fibrosis. ILDs encompass a very heterogeneous group of diseases. Since in a subgroup of ILD the cause of the disease has not been clarified yet, these types are also referred to as "idiopathic" interstitial pneumonia. Among the different types of ILDs, idiopathic pulmonary fibrosis (IPF) is characterized by a particularly progressive clinical course and a poor prognosis. As the name suggests, the genesis of IPF has not yet been fully clarified. While immunosuppressive therapy can improve many other ILDs, such therapies have been shown to be potentially harmful in IPF. There are only two antifibrotic drugs approved for IPF (pirfenidone and nintedanib) which do not cure IPF, but can slow down the disease progression. It is therefore of great interest to both clinicians and basic scientists to further explore the pathophysiology of ILDs and in particular of IPF in order to be able to identify new therapeutic approaches. In recent years, there have been increasing indications that autoimmunity might be involved in the genesis of ILD.

The aim of this work was to first analyze common and different characteristics of fibrosis in various fibrotic diseases at the molecular level. For the analysis of the tissue proteome mass spectrometry was used. Since fibrotic diseases lead to an unphysiological accumulation of extracellular matrix (ECM), this work aimed to further investigate the nature of the ECM proteome, the so called matrisome, in specific tissues and diseases. In the first part of the work, different forms of ILDs and tissue samples obtained from patients with localized scleroderma, which represents fibrosis in an autoimmune disease, were examined and compared with healthy donor samples. The analyzes detected common and disease-specific protein regulation in fibrosis. Interestingly, an elevated amount of marginal zone B and B1 specific protein (MZB1)-positive plasma B cells were found in both types of organ fibrosis. This was confirmed by immunostaining and Western blot supporting the theory of autoimmune processes in the genesis of fibrosis. In a second, larger cohort of patients with ILD, a negative correlation between tissue MZB1 levels and lung function was found, which suggests a clinical connection. There was also an association between MZB1 and total immunoglobulin G (IgG) levels in the lung parenchyma which leads to the question whether some of these IgGs could be (possibly disease-causing) autoantibodies.

The second part of the thesis continues this question and deals with the identification of potential autoantibodies in patients with IPF. Due to the limited treatment options for IPF, the detection of autoantigens associated with IPF could enable the development of suitable preclinical models to

investigate the role of specific antigens in the development of idiopathic forms of organ fibrosis. Since previous work on autoantigens in IPF has mostly been based on the use of synthetic antigens, the aim in the second part of this work was to establish a mass spectrometry-based method that can be used to screen for autoantibodies in the plasma of patients with ILD in an unbiased way and with high throughput. Our so-called Differential Antigen Capture (DAC) assay includes immunoprecipitation of proteome extracts from ILD and healthy donor lung tissue and plasma IgGs and then quantitative mass spectrometry. As a comparison, samples from patients with autoimmune-associated ILD (connective tissue disease-related ILD; CTD-ILD) and healthy controls in a total of two ILD cohorts from Munich and Hannover were examined. Using the DAC approach, disease-specific and common autoantibodies could be found in IPF and CTD-ILD, whereas patients with CTD-ILD did not have a higher number of detected autoantigens. To enable a translational approach, the results were correlated with clinical data such as lung function and survival. We found autoantigens and autoantigen signatures that were associated with worse survival in both IPF and CTD-ILD. These analyzes provide a basis for further research on autoantigens which might help to learn more about B cell-mediated autoimmunity in IPF.

## Zusammenfassung

Fibrotische Erkrankungen stellen in den Industrienationen ein großes Gesundheitsproblem mit nur begrenzten Behandlungsmöglichkeiten dar. Als Ursachen für eine Fibrose werden anhaltende Gewebeschäden, fehlregulierte Regenerations- und Reparationsvorgänge oder auch Altern und Autoimmunität diskutiert. Ein fibrotischer Befall der Lunge führt zur Lungenfibrose, bei der es mit der Zeit zu einer Vernarbung des Lungengewebes kommt. Das Fortschreiten dieser Erkrankung kann zu einem Verlust der Lungenfunktion, einem reduzierten Gasaustausch und letztendlich Organversagen führen. Die meisten Fälle der so genannten interstitiellen Lungenerkrankungen (engl.: interstitial lung diseases; ILD) beziehungsweise diffusen Lungenparenchymerkrankungen (engl.: diffuse parenchymal lung disease) gehen mit einem fibrotischen Umbau des Lungenparenchyms und somit einer Lungenfibrose einher. ILDs umfassen dabei eine sehr heterogene Gruppe von Erkrankungen. Da bei einem Teil der Patienten mit ILD die Ursache der Erkrankung bisher noch nicht geklärt ist, werden diese Formen als „idiopathische“ interstitiellen Pneumonien bezeichnet. Unter den ILDs kennzeichnet sich die idiopathische pulmonale Fibrose (IPF) durch einen besonders progressiven Verlauf und eine schlechte Prognose aus. Wie der Name vermuten lässt, ist die Genese der IPF bisher noch nicht vollständig geklärt. Während bei vielen anderen ILDs eine immunsuppressive Therapie eine Verbesserung bringen kann, kann diese bei Patienten mit IPF sogar schädlich sein. Für die Behandlung der IPF sind lediglich zwei antifibrotische Medikamente zugelassen (Pirfenidon und Nintedanib), die zwar die IPF nicht heilen, aber den Krankheitsverlauf verlangsamen können. Daher ist es sowohl für Kliniker als auch für Grundlagenwissenschaftler von höchstem Interesse die Pathophysiologie der ILDs und im Besonderen der IPF weiter zu erforschen um neue Therapieansätze identifizieren zu können. Es haben sich in den letzten Jahren zunehmend Hinweise ergeben, dass auch Autoimmunität in die Genese von ILDs involviert sein könnte.

Das Ziel dieser Arbeit war es zunächst gemeinsame und unterschiedliche Merkmale von Fibrose bei unterschiedlichen Erkrankungen auf molekularer Ebene zu analysieren. Hierfür eignet die Analyse des Proteoms mittels Massenspektrometrie. Da es bei fibrotischen Erkrankungen zu einer unphysiologischen Anhäufung von extrazellulärer Matrix (engl. extracellular matrix; ECM) kommt, war es Ziel dieser Arbeit, die Natur des ECM-Proteoms, des sogenannten Matrisoms, in bestimmten Geweben und Krankheiten weiter zu untersuchen. Im ersten Teil der Arbeit wurden sowohl verschiedene Formen von ILDs als auch Gewebeproben von Patienten mit lokalisierter Sklerodermie, welche eine Fibrose bei einer Autoimmunerkrankung darstellt, untersucht und mit gesunden Vergleichsproben verglichen. Die Analysen detektierten gemeinsame und krankheitsspezifische Proteinregulierungen bei den verschiedenen Fibroseformen. Interessanterweise wurde bei beiden Arten der Organfibrose eine erhöhte Menge von marginal zone B and B1 specific protein (MZB1) -positiven Plasma-B-Zellen gefunden. Dies konnte mittels Immunfärbung und Western blot bestätigt werden, was die Theorie unterstützt, dass autoimmune Prozesse bei der Genese von Fibrose involviert sind. In einer zweiten, größeren Kohorte von



Patienten mit ILD fand sich zudem eine negative Korrelation zwischen MZB1 Gehalt im Gewebe und der Lungenfunktion, was einen klinischen Zusammenhang vermuten lässt. Außerdem fand sich ein Zusammenhang zwischen MZB1 und dem Gesamt-Immunglobulin G (IgG) im Lungenparenchym. Daraus ergibt sich die Frage, ob es sich bei einem Teil dieser IgGs um (möglicherweise krankheitsauslösende) Autoantikörper handeln könnte.

Der zweite Teil der Arbeit knüpft direkt an dieser Stelle an und beschäftigt sich mit der Identifizierung von potenziellen Autoantikörpern bei Patienten mit IPF. Aufgrund der begrenzten Therapieoptionen bei IPF könnte die Detektion von mit IPF assoziierten Autoantigenen die Entwicklung geeigneter präklinischer Modelle ermöglichen, um die Rolle spezifischer Antigene bei der Entstehung idiopathischer Formen der Organfibrose zu untersuchen. Da bisherige Arbeiten zu Autoantigenen bei IPF meist auf der Verwendung von synthetischen Antigenen stützen, war es im zweiten Teil dieser Arbeit Ziel eine Massenspektrometrie-basierte Methode zu etablieren, mit der unvoreingenommen und mit großem Durchsatz nach Autoantikörpern im Plasma von Patienten mit ILD gesucht werden kann. Unser so genannter Differential Antigen Capture (DAC) Assay beinhaltet die Immunpräzipitation von Proteomextrakten aus ILD und gesundem Spenderlungengewebe und Plasma-IgGs, gefolgt von quantitativer Massenspektrometrie. Als Vergleich wurden Proben von Patienten mit autoimmun-assoziiertes ILD (engl.: connective tissue disease related ILD; CTD-ILD) und gesunde Kontrollen in insgesamt zwei ILD-Kohorten aus München und Hannover untersucht. Mittels DAC Ansatz konnten krankheitsübergreifende und -spezifische Autoantikörper bei IPF und CTD-ILD gefunden werden, wobei Patienten mit CTD-ILD keine höhere Anzahl an nachgewiesenen Autoantigenen aufwiesen. Um einen translationalen Ansatz zu schaffen wurden die Ergebnisse mit klinischen Daten wie Lungenfunktion und Überleben korreliert. Hier fanden sich sowohl bei IPF auch bei CTD-ILD Autoantigene und Autoantigen-Signaturen, die mit einem schlechteren Überleben vergesellschaftet sind. Diese Analysen bieten eine Grundlage um entsprechende Autoantigene in zukünftigen Arbeiten weiter zu erforschen und möglicherweise mehr zu erfahren über B Zell-vermittelte Autoimmunität bei der IPF.

## List of figures

- Figure 1.** Concept of pulmonary wound healing and tissue remodeling. Wound repair consists of four stages: **(1)** activation of platelets with clotting and coagulation, **(2)** migration of inflammatory cells and secretion of pro-fibrotic factors, **(3)** migration, proliferation and activation of fibroblasts and secretion of extracellular matrix (ECM) components by activated fibroblasts and myofibroblasts to build a provisional repair matrix and **(4)** tissue remodeling and resolution. Fibrosis can develop if any of these steps is dysregulated or when the damaging trigger persists. Figure taken and legend adapted from (Wynn 2011). .....20
- Figure 2.** Scheme of different interstitial lung diseases (ILDs). Printed in bold are types of ILD that rather experience clinical deterioration known as a “progressive-fibrosing phenotype. Abbreviations: idiopathic interstitial pneumonias (IIPs), interstitial lung disease (ILD). Figure taken and legend adapted from (Cottin et al. 2018).....22
- Figure 3.** Usual interstitial pneumonia (UIP) pattern on high-resolution computed tomography. Computed tomography depicts the typical subpleural predominance and an apicobasal gradient of honeycombing in transverse **(A-C)** and coronal reconstruction **(D)**. **(E)** A magnified view (left lower lobe) demonstrate characteristic patterns of honeycombing, comprising grouped cystic airspaces with surrounding walls and variable size. Honeycombing can occur in variable layering (see arrows). Figure taken and legend adapted from (Raghu et al. 2018). .....23
- Figure 4.** Processes potentially involved in the pathogenesis of idiopathic pulmonary fibrosis (IPF). The combination and interplay of genetic susceptibility, ageing and environmental factors lead to an epigenetic reprogramming promoting dysregulated epithelial activation potentially resulting in IPF. The process might be induced by repetitive microinjuries. Impaired wound healing then triggers a remodeling of the lungs with fibrotic tissue. Figure taken and legend adapted from (Martinez et al. 2017).....25
- Figure 5.** Cells of the immune system. The innate immunity, the first immunological mechanism to respond after contact with an infectious agent, includes soluble components (e.g. the complement system) and immune cells such as granulocytes, mast cells, macrophages, dendritic cells and natural killer cells. The adaptive immunity, consisting of antibodies, B cells, and T cells, reacts slower but in an antigen-specific manner. Further, the adaptive immunity has the ability to develop an antigen-specific memory. Cytotoxic lymphocytes (natural killer cells and  $\gamma\delta$  T cells) represent a link between innate and adaptive immune system. Figure taken and legend adapted from (Dranoff 2004). .....26
- Figure 6.** Overview of the development of autoimmune disease. Despite several central and peripheral checkpoints, a small number of autoreactive T and B cells can escape into the periphery. These cells will not be pathological unless a patient has a genetic predisposition to autoimmune disease and experiences an environmental trigger. Figure taken and legend adapted from (Wang et al. 2015) .....28
- Figure 7.** Potential ways for self-reactive B cells to bypass selection processes of the immune system. **(a)** B cells evolve in the bone marrow and periphery by passing through multiple checkpoints. Autoreactive B cells which might arise during variable/(joining)/diversity gene segment [V(D)J] recombination of the B cell receptor (BCR) might be eliminated by clonal deletion and receptor editing. In the periphery B cells have to pass further checkpoints. **(b)** Potential mechanisms which allow autoreactive B cells to escape from these checkpoints are somatic hypermutation (SHM) and cross-reactivity of T and B cells with foreign or structurally similar self-antigens. Figure taken and legend adapted from (Reijm et al. 2020) .....29
- Figure 8.** Survival of patients with idiopathic pulmonary fibrosis (IPF), interstitial pneumonia with autoimmune features (IPAF) and connective tissue disease related interstitial lung diseases (CTD-ILD). **(a)** Kaplan–Meier survival curves depict a significantly worse survival of patients with IPAF in comparison to patients with CTD-ILD. **(b)** IPAF patients with a UIP pattern (radiological and/or histological) had a similar survival curve to patients with IPF while survival of IPAF patients without UIP appeared to be similar to CTD-ILD. Abbreviations: idiopathic pulmonary fibrosis (IPF), interstitial pneumonia with autoimmune features (IPAF), connective tissue

disease related interstitial lung disease (CTD-ILD), usual interstitial pneumonia pattern (UIP). Figure taken and legend adapted from (Oldham et al. 2016) .....32

- Figure 9.** Common and disease specific genes enriched in lung and skin fibrosis. (A) A scatterplot displays the annotation enrichment scores of gene groups for patients with interstitial lung disease (ILD) (abscissa) and localized scleroderma (ordinate) in comparison to healthy controls, respectively. Shared gene categories are found in the upper right quadrant, including immunoglobulins (red text). (B) Student's t test differences of proteins in ILD (abscissa) and skin fibrosis (ordinate) in comparison to healthy controls are plotted against each other. While there were proteins enriched exclusively in ILD (orange) or scleroderma (blue), the marginal zone B and B1 cell specific protein (MZB1) was shared between both types of fibrosis. Again, in human lung and skin fibrosis several immunoglobulins were detected (purple squares). Abbreviations: false discovery rate (FDR); Kyoto Encyclopedia of Genes and Genomes. Figure and legend taken and adapted from (Schiller et al. 2017) .....52
- Figure 10.** Detection of marginal zone B- and B1-cell-specific protein (MZB1) in tissue-resident cells. Immunostainings show distribution of MZB1 in human lung fibrosis of patients with interstitial lung disease (ILD). The co-localization with CD38 characterizes MZB1-positive cells as terminally differentiated plasma B cells (indicated by arrows). Staining with 4',6-diamidino-2-phenylindole (DAPI) indicates nuclei and desmin was used to identify vascular smooth muscle cells and a few mesenchymal cells. Abbreviation: idiopathic pulmonary fibrosis (IPF). Figure and legend taken and adapted from (Schiller et al. 2017).....53
- Figure 11.** Marginal zone B- and B1-cell-specific protein (MZB1) positive cells do not express CD3 or CD20 in lung fibrosis. (A) CD3 is a lineage marker for T lymphocytes. (B) CD20 is a B cell lineage marker. (A, B) Staining with 4',6-diamidino-2-phenylindole (DAPI) indicates nuclei and desmin was used to identify vascular smooth muscle cells and a few mesenchymal cells. MZB1 positive cells are displayed by arrows. Figure taken and legend adapted from (Schiller et al. 2017) 54
- Figure 12.** Marginal zone B- and B1-cell-specific protein (MZB1) positive do not express CD45 but CD138 in human lung fibrosis. (A) CD45 is a leukocyte lineage marker. (B) CD138, also known as syndecan 1, is a plasma B cell marker. (A, B) Staining with 4',6-diamidino-2-phenylindole (DAPI) indicates nuclei and desmin was used to identify vascular smooth muscle cells and a few mesenchymal cells. MZB1 positive cells and MZB1/CD138 co-expressing cells are displayed by arrows. Figure and legend taken from (Schiller et al. 2017).....55
- Figure 13.** Marginal zone B- and B1-cell-specific protein (MZB1) positive cells co-express CD27 and immunoglobulin G (IgG) in human lung fibrosis. (A) CD27 is a plasma B cell marker. (B) IgGs are produced in plasma B cells (A, B) Staining with 4',6-diamidino-2-phenylindole (DAPI) indicates nuclei and desmin was used to identify vascular smooth muscle cells and a few mesenchymal cells. MZB1 positive cells, MZB1/CD27 double positive and MZB1/IgG co-expressing cells are displayed by arrows. Figure and legend taken from (Schiller et al. 2017) .....56
- Figure 14.** Marginal zone B- and B1-cell-specific protein (MZB1) positive do also express CD38 in skin fibrosis of localized scleroderma. CD38 is a surface marker of plasma B cells. Staining with 4',6-diamidino-2-phenylindole (DAPI) indicates nuclei and desmin was used to identify vascular smooth muscle cells and a few mesenchymal cells. MZB1 positive cells and MZB1/CD38 co-expressing cells are displayed by arrows. Figure taken and legend adapted from (Schiller et al. 2017) .....57
- Figure 15.** Identification of marginal zone B- and B1-cell-specific protein (MZB1)-positive cells in interstitial lung disease (ILD) and localized scleroderma using Western blot analysis. (A) Antibodies against MZB1 were used to perform Western blot and analyze homogenated tissues of different types of lung fibrosis due to ILD. To uncover the relationship between MZB1 positive cells and immunoglobulin G (IgG), additionally, antibodies against IgG were used. Amido black served as loading control and displayed the total protein loading of each sample. (B) *Box-and-whisker* plot is used to depict Western blot quantification of healthy donor tissue, idiopathic pulmonary fibrosis (IPF) and non-IPF ILD [raw data from (A); results are normalized to amido black] and indicates significantly more MZB1 in ILD compared to donor tissue. (C) Homogenated tissues of un-involved and involved skin from patients with localized scleroderma were subjected to Western blot analysis. Antibodies against

MZB1 and IgG were used and amido black served as loading control and displayed the total protein loading of each sample. Figure and legend taken and adapted from (Schiller et al. 2017).....59

- Figure 16.** Marginal zone B- and B1-cell-specific protein (MZB1)-positive cells correlate positively with tissue immunoglobulin G (IgG) and negatively with diffusing capacity of the lung for carbon monoxide (DLCo). **(A)** Linear regression analysis of MZB1 and IgG shows a moderate, positive correlation. **(B)** *Box-and-whisker* of MZB1 expression in a large U.S. microarray cohort (Gene Expression Omnibus dataset GSE47460 published by the Lung Tissue Research Consortium) (Bauer et al. 2015). MZB1 is significantly higher in ILD than in healthy donor tissue. **(C)** Pearson correlation of mass spectrometry data (Figure 9) shows a strong, negative correlation of MZB1 and DLCo (%). **(D)** Pearson correlation of Western blot data depicts a strong, negative correlation of MZB1 and DLCo (%). **(A, C, D)** Color code shows distribution of different forms of ILD. For MZB1 raw data see Figure 15A. Abbreviations: arbitrary units (AU); chronic obstructive pulmonary disease (COPD); connective tissue disease (CTD); hypersensitivity pneumonitis (HP); interstitial lung disease (ILD); idiopathic pulmonary fibrosis (IPF); nonspecific interstitial pneumonia (NSIP); unclassifiable ILD (unclass. ILD); Western blot (WB). Figure and legend taken and adapted from (Schiller et al. 2017).....60
- Figure 17.** The amount of marginal zone B- and B1-cell-specific protein (MZB1) is independent of demographic and therapeutic factors in human lung fibrosis. **(A)** Linear regression analysis shows no correlation between MZB1 and age. **(B)** Linear regression analysis shows no correlation between MZB1 and vital capacity (VC) in %. **(C – E)** *Box-and-whisker* identifies no relationship between MZB1 tissue level and steroids, antifibrotic therapy and gender, respectively. **(A, B)** Color code shows distribution of different forms of ILD. **(A – E)** For MZB1 raw data see Figure 15A. Figure taken and legend adapted from (Schiller et al. 2017).....61
- Figure 18.** Immunoglobulin G (IgG) and IgG subclasses distribution in the proteome profiling datasets. Raw data was taken from (Schiller et al. 2017). **(A)** Western blot analysis identified significantly more tissue IgG in interstitial lung disease (ILD) than in controls. **(B)** Quantification of IgG subclasses in proteomics data. ....62
- Figure 19.** Immunoglobulin G (IgG) subclasses in interstitial lung disease (ILD) tissue. **(A-D)** Tissue homogenates of healthy donors and different ILD entities were analysed by Western blot with antibodies against marginal zone B and B1 specific protein (MZB1) and IgG1 (A), IgG2 (B), IgG3 (C) and IgG4 (D). For quantification of the total protein loading blots were also stained with amido black. ....63
- Figure 20.** Quantification of Western blot analysis of immunoglobulin G (IgG) subclasses. **(A, B)** *Box-and-whisker* of the respective IgG subclass in the Western blot analysis, see Figure 22 A-D and the IgG1 to IgG4 ratio. ....64
- Figure 21.** Correlation of marginal zone B- and B1-cell-specific protein (MZB1) and IgG subclasses in interstitial lung disease (ILD) tissue. **(A-D)** Correlation of IgG1 (A), IgG2 (B), IgG3 (C) and IgG4 (D) and MZB1 levels identifies a positive correlation for IgG2 (B) and IgG4 (D). ....65
- Figure 22.** Experimental workflow of the Differential Antigen Capture assay (DAC). Immunoprecipitation was used to generate and enrich autoantibody-antigen complexes out of patients' plasma and native extracts from end stage interstitial lung disease (ILD). Shotgun proteomics was used to quantify differential protein detection in diseased patients versus healthy age matched controls. Figure and legend taken and adapted from (Leuschner et al. 2021).....72
- Figure 23.** A proteomic workflow detects autoantigens in patients with interstitial lung disease (ILD) with high sensitivity and specificity. **(A)** Proof of concept was successfully reached with plasma from patients with systemic sclerosis (SSc) and connective-tissue related interstitial lung disease (CTD-ILD), who were clinically characterized by Scl-70 antibodies (antigen topoisomerase I; TOP1) using an approved ELISA test. The different coloring shows the number of significant enrichments for Scl-70/TOP1 in the three replicates in the mass spectrometry (MS)-analysis. **(B)** The volcano plot is an example of a patient with SSc, in whom TOP1 was detected. Red colored points depict significantly enriched proteins (FDR <10%) in comparison to healthy age matched controls. Abscissa: x-fold difference to control-values (log<sub>2</sub>); ordinate: p-value (-log<sub>10</sub>). **(C, D)** Each patient sample in the

- proof of concept pilot experiment was processed and analyzed three times (panel B). The four-field table indicates the amount of true and false positive measurements. The ROC analysis shows that the sensitivity of significantly enriched TOP1 (detected by MS-analysis) in SSc-patients in comparison to healthy controls was 96% and the specificity 100%. Figure and legend taken and adapted from (Leuschner et al. 2021).....73
- Figure 24.** Investigation of autoantibody profiling in one cohort from Munich (cohort 1) and a second cohort from Hannover (cohort 2). Figure taken and legend adapted from (Leuschner et al. 2021).....74
- Figure 25.** Kaplan-Meier survival analysis shows a significantly better transplant-free survival in patients with connective tissue related interstitial lung disease (CTD-ILD) in comparison to patients with idiopathic pulmonary fibrosis (IPF). .....76
- Figure 26.** Protein quantification and identification of interstitial lung disease (ILD) associated autoantigens. **(A)** Number of quantified proteins in controls, idiopathic pulmonary fibrosis (IPF) and connective tissue disease related interstitial lung disease (CTD-ILD) (cohort 1). **(B)** Categories of proteins detected in IPF (left, blue colors) and CTD-ILD (right, red colors) from cohort 1 hardly differed in both diseases. **(C)** Volcano plot showing significantly different expressed genes in IPF and CTD-ILD without accounting for differences to healthy controls. Red colored points depict significantly enriched proteins (FDR <10%). **(D)** Number of quantified proteins in patients with IPF and CTD-ILD from cohort 2. Panel A, B and D taken and adapted from (Leuschner et al. 2021). .....77
- Figure 27.** Significantly enriched antigens in patients from two independent cohorts. **(A)** The amount of identified potential autoantigens (significantly enriched) in patients with idiopathic pulmonary fibrosis (IPF) and connective tissue diseases related interstitial lung disease (CTD-ILD) from the Munich (cohort 1) and Hannover (cohort 2). Patients with IPF from Munich had the highest number of autoantigens. **(B)** The bar graph shows that in IPF most antigens were only detected in 1-2 patients, while only a small number of antigens were found in more than 7 patients. This distribution pattern was similar in Munich and Hannover. Figure and legend taken and adapted from (Leuschner et al. 2021).....78
- Figure 28.** Most frequently identified autoantigens in idiopathic pulmonary fibrosis (IPF) from both cohorts. **(A-C)** In patients with IPF from the Munich cohort, RuvB-like 2 (RUVBL2) (A), Histone H3 (HIST2H3PS2) (B) and Tubulin beta-8 chain (TUBB8) (C) were the autoantigens which were most frequently detected. Differences in forced vital capacity (FVC) were only found in TUBB8 positive versus TUBB8 negative patients. **(D-E)** While the benefit for transplant-free survival for patients with RuvB-like autoantigens did not reach significance (D), the Kaplan-Meier survival showed a significantly longer time to death or transplantation for patients positive for TUBB8 (E). **(F-H)** In the Hannover IPF cohort, Ficolin-3 (FCN3) (F), 60S ribosomal protein L35 (RPL35) (G) and Alpha-1-antitrypsin (SERPINA1) (H) were most frequently detected but the FVC values were similar in patients positive and negative for the respective autoantigens. Figure taken and legend taken and adapted from (Leuschner et al. 2021).....79
- Figure 29.** Common and individual autoantigens in idiopathic pulmonary fibrosis (IPF) and connective tissue diseases-related interstitial lung diseases (CTD-ILD). Individual and common autoantigens in IPF and CTD-ILD in the Munich and Hannover cohort are displayed in a Venn diagram. The dashed rectangle provides information about the composition of IPF-specific autoantigens (n=279) of cohort 1. The majority (70.6%) of autoantigens were exclusively derived from four patients with high autoimmune signature. Figure and legend taken and adapted from (Leuschner et al. 2021).....80
- Figure 30.** Subgroup of patients with idiopathic pulmonary fibrosis (IPF) from Munich and high autoimmune signature. **(A)** Volcano plot showing enriched antigens in four individual IPF patients in comparison to the other IPF patients from cohort 1. The color code indicates the number of patients (out of four) with significantly enriched antigen. **(B)** The forced vital capacity (FVC<sub>%pred.</sub>) did not differ between the four IPF patients with high autoimmune signature and other IPF patients. **(C)** Transplant-free survival was similar between both IPF groups.....81

- Figure 31.** Identified autoantigens specific for idiopathic pulmonary fibrosis (IPF). **(A)** The bar graph shows all autoantigens specifically and exclusively detected in patients with IPF in two independent cohorts. The color code displays the distribution between Munich and Hannover. **(B)** Patients positive for Apolipoprotein A-IV (APOA4) had a higher forced vital capacity (FVC) than patients in whom APOA4 was not detected as autoantigen. **(C-Q)** The FVC showed no differences in patients with the respective autoantigen compared to all other IPF patients. Figure and legend taken and adapted from (Leuschner et al. 2021). .....82
- Figure 32.** Most commonly identified autoantigens in idiopathic pulmonary fibrosis (IPF) and connective tissue disease related interstitial lung disease (CTD-ILD). **(A)** The bar graph pictures autoantigens which were shared between all patient groups from Munich and Hannover. The color code provides information about the frequency distribution within the groups. **(B)** Bar graph shows autoantigens that were found in at least three patients in both IPF groups and were therefore the most frequently identified autoantigens in IPF. **(C)** Bar graph shows autoantigens that were found in at least two patients in both CTD-ILD groups and were therefore the most frequently identified autoantigens in CTD-ILD. **(D)** All antigens which were detected in a minimum of three patients in one of the four groups are displayed in a heat map. The color code of these most commonly identified autoantigens gives information about the so called “sum score” which was derived from the Student’s *t* test statistics of significant proteins with FDR <10%. Arbitrarily, a minimum value of >4 was chosen which resulted in a number of 116 most frequently identified autoantigens. Figure and legend taken and adapted from (Leuschner et al. 2021). .....83
- Figure 33.** Kaplan-Meier curves for survival in patients with idiopathic pulmonary fibrosis (IPF) and specific autoantigens. **(A-C)** The presence of autoantibodies against thrombospondin-1 (THBS1) (A), tubulin beta-1 chain (TUBB1) (B), or CD5L (C) was associated with a shorter transplant-free survival. Figure and legend taken and adapted from (Leuschner et al. 2021). .....85
- Figure 34.** Kaplan-Meier curves for transplant-free survival in patients with idiopathic pulmonary fibrosis (IPF) either positive or negative for thrombospondin-1 (THBS1) autoantibodies. In patients with autoantibodies against THBS1, survival was shorter in both the Munich (A) and the Hannover cohort (B), respectively. Figure and legend taken and adapted from (Leuschner et al. 2021). .....86
- Figure 35.** Hierarchical clustering of potential autoantigens in idiopathic pulmonary fibrosis (IPF). Hierarchical clustering displays 58 genes. These had to be (1) present in IPF patients from Munich and Hannover and (2) detected in a minimum of two patients in one of the two groups. Two autoantigen clusters were identified (cluster 1 and cluster 2). Figure and legend taken and adapted from (Leuschner et al. 2021). ....88
- Figure 36.** Potential predictive autoantigens in idiopathic pulmonary fibrosis (IPF). **(A)** Grouping of patients based on the same 58 proteins as used in Figure 35 by a principal component analysis (PCA). **(B)** The loadings of component 1 and 2 of the PCA from panel A are displayed with a color code for the top antigens of component 1 (blue) and component 2 (purple). **(C)** The survival curve of patients from PCA group 1 is similar to all other IPF patients. **(D)** Kaplan-Meier curve identifies IPF patients from PCA group 2 as having a significantly reduced transplant-free survival. Figure and legend taken and adapted from (Leuschner et al. 2021). .....89
- Figure 37.** Kaplan-Meier curves for survival in patients with connective tissue disease related interstitial lung disease (CTD-ILD) and specific autoantigens. **(A-B)** The presence of autoantibodies against Protein argonaute-1 (AGO1) (A) and Ficolin-3 (FCN3) (B) was associated with a shorter transplant-free survival. Patients with the respective autoantigen are shown with dashed line.....90
- Figure 38.** Hierarchical clustering of 19 potential autoantigens in patients with connective tissue disease related interstitial lung disease (CTD-ILD). The autoantigens had to be (1) present in CTD-ILD patients from Munich and Hannover and (2) detected in a minimum of two patients in one of the two groups. The clustering depicts four distinct autoantigen-cluster (cluster 1-4). .....91
- Figure 39.** Identification of predictive autoantigens in connective tissue disease related interstitial lung disease (CTD-ILD). **(A)** Based on component 1 and component 4, a principal component analysis (PCA) of the same 19 proteins as used in Figure 38 distinguishes three different groups of patients. **(B)** The loadings of component 1 and

4 of the PCA from panel A are displayed with a color code for the top antigens of component 1 (purple) and component 4 (blue). **(C)** Kaplan-Meier curve depicts CTD-ILD patients from PCA group 1 as having a significantly worse transplant-free survival. **(D)** Survival of CTD-ILD patients from PCA cluster 2 is similar to all other CTD-ILD patients. **(E)** Patients from PCA cluster 3 have a significantly shorter time to death or transplantation according to Kaplan-Meier curves.....92

**Figure 40.** Analysis of autoantibodies reveals differential V-segment usage in idiopathic pulmonary fibrosis (IPF) and connective tissue disease related interstitial lung disease (CTD-ILD). **(A-B)** Hierarchical clustering of ANOVA-significant V-segments in patients with IPF and CTD-ILD from Munich (A) and Hannover (B). The color code depicts ANOVA significance. **(C)** Survival in cohort 1 and 2 in V2-15 protein positive and negative IPF patients. ....93

## List of tables

<b>Table 1.</b> Primary and secondary antibodies for immunostaining .....	42
<b>Table 2.</b> Composition of 12% SDS polyacrylamide gels .....	43
<b>Table 3.</b> Primary and secondary antibodies for Western blot .....	44
<b>Table 4.</b> Demographics and clinical characteristics of patients with lung fibrosis included in the proteomic study. Abbreviations: idiopathic pulmonary fibrosis (IPF); hypersensitivity pneumonitis (HP); cryptogenic organizing pneumonia (COP); nonspecific interstitial pneumonia (NSIP); pulmonary function test (PFT); vital capacity (VC); total lung capacity (TLC); residual volume (RV); forced expiratory volume in 1 second (FEV1); diffusing capacity of the lung for carbon monoxide (DLCo); long term oxygen therapy (LTOT). Table taken and legend adapted from (Schiller et al. 2017).....	51
<b>Table 5.</b> Demographics and clinical characteristics of patients with lung fibrosis included in the Western blot analysis. Abbreviations: idiopathic pulmonary fibrosis (IPF); hypersensitivity pneumonitis (HP); cryptogenic organizing pneumonia (COP); nonspecific interstitial pneumonia (NSIP); pulmonary function test (PFT); vital capacity (VC); total lung capacity (TLC); residual volume (RV); forced expiratory volume in 1 second (FEV1); diffusing capacity of the lung for carbon monoxide (DLCo); long term oxygen therapy (LTOT). * n=1; ° not all patients were able to perform a DLCo. Table taken and legend adapted from (Schiller et al. 2017) .....	58
<b>Table 6.</b> Demographics and clinical characteristics of patients with idiopathic pulmonary fibrosis (IPF) and connective tissue disease related interstitial lung diseases (CTD-ILD) from Munich (cohort 1). Data is given as mean ( $\pm$ SD) or n (%). Abbreviations: percentage of forced vital capacity (FVC <sub>%pred</sub> ), percentage of diffusion capacity of carbon monoxide (DLCo <sub>%pred</sub> ). <sup>1</sup> smoking status of n=42, <sup>2</sup> smoking status of n=30, <sup>3</sup> smoking status of n=12, <sup>4</sup> FVC of n=59 (IPF n=34, CTD-ILD n=25), <sup>5</sup> DLCo of n=49 (IPF n=28, CTD-ILD n=21). Table and legend taken and adapted from (Leuschner et al. 2021). .....	75
<b>Table 7.</b> Demographics and clinical characteristics of patients with idiopathic pulmonary fibrosis (IPF) and connective tissue disease related interstitial lung diseases (CTD-ILD) from Hannover (cohort 2). Data is given as mean ( $\pm$ SD) or n (%). Abbreviations: percentage of forced vital capacity (FVC <sub>%pred</sub> ), percentage of diffusion capacity of carbon monoxide (DLCo <sub>%pred</sub> ). <sup>1</sup> smoking status of n=58, <sup>2</sup> smoking status of n=38, <sup>3</sup> DLCo of n=54 (IPF n=38, CTD-ILD n=16). Table and legend taken and adapted from (Leuschner et al. 2021).....	75
<b>Table 8.</b> Multiple regression analysis in idiopathic pulmonary fibrosis (IPF) for transplant-free survival. Autoantibodies against thrombospondin-1 (THBS1) are an independent predictor for transplant-free survival. Table taken and legend taken and adapted from (Leuschner et al. 2021).....	86



## List of abbreviations

### A

AE acute exacerbation  
AGO1 protein argonaute-1  
APOA4 apolipoprotein A-IV

### C

COPD chronic obstructive pulmonary diseases  
CTD connective tissue disease  
CTD-ILD connective tissue disease related interstitial lung disease

### D

DAC Differential Antigen Capture  
DAPI 4',6-diamidino-2-phenylindole  
DLCo diffusing capacity of the lung for carbon monoxide

### E

ECM extracellular matrix  
EDTA ethylenediaminetetraacetic acid  
ER endoplasmic reticulum

### F

FCN3 ficolin-3  
FDC follicular dendritic cells  
FDR false discovery rate  
FEV1 forced expiratory volume in 1 second  
FVC<sub>%pred.</sub> forced vital capacity % pred.

### G

GPX1 glutathione peroxidase 1

### H

HP hypersensitivity pneumonitis

### I

IFN $\gamma$  interferon gamma  
IgG immunoglobulin G  
IL interleukin  
ILD interstitial lung disease  
IPF idiopathic pulmonary fibrosis

### L

LIMS1 LIM and senescent cell antigen-like-containing domain protein 1  
LTBP1 latent-transforming growth factor beta-binding protein 1

### M

MS mass spectrometry  
MZB1 the marginal zone B and B1 cell specific protein

### N

NSIP non-specific interstitial pneumonia

### P

PBS phosphate-buffered saline  
PCA principal component analysis

### Q

QDSP quantitative detergent solubility profiling

**R**

rpm runs per minute  
RV residual volume

**S**

SDS sodium dodecyl sulfate  
SERPINA1 alpha-1-antitrypsin  
SSc systemic sclerosis

**T**

TFA trifluoroacetic acid  
TGF- $\beta$  transforming growth factor beta  
Th Thompson (unit)  
Th cells T helper cells  
THBS1 thrombospondin-1  
TLC total lung capacity  
TLN talin 1  
TNF $\alpha$  tumor necrosis factor alpha  
TRIS tris(hydroxymethyl)aminomethane  
TUBB1 tubulin beta-1 chain  
TUBB8 tubulin beta-8 chain

**U**

UIP usual interstitial pneumonia

**V**

V volt  
VC vital capacity  
V(D)J variable (diverse) joining gene segment (recombination)

**Z**

ZYX zyxin

# 1. Introduction

## 1.1 Pulmonary fibrosis

Chronic respiratory diseases affect millions of people worldwide. A study including 195 countries detected that in the past three decades, the number of deaths due to chronic respiratory disease has risen continuously (Li et al. 2020). In 2017, chronic respiratory diseases were responsible for 3.9 million deaths, which corresponds proportionally to 7% of all deaths around the world (Li et al. 2020). Although, globally, respiratory disease belongs to the most common diseases, the general awareness of the severity and extent of the disease is still insufficient. While onset and clinical course can vary enormously, many chronic respiratory diseases share similar pathological mechanisms. This includes, for example, a higher burden of disease in poorer regions of the world and further well-established risk factors like ageing, smoking, environmental pollution and body weight (Li et al. 2020). However, the knowledge about molecular mechanisms of respiratory disease is still limited.

While mortality rates for chronic obstructive pulmonary disease (COPD) and pneumoconiosis declined, the mortality rates for interstitial lung disease (ILD) and sarcoidosis raised over the last years (Li et al. 2020). ILD, also called diffuse parenchymal lung disease, are a heterogenous group of diseases, which are characterized by fibrotic and chronic inflammatory processes destructing the lung parenchyma ultimately leading to the loss of intact lung tissue and respiratory failure (Raghu et al. 2011, Behr 2013). Since therapeutic options for patients with ILD are limited it is of urgent need to better understand pathophysiological mechanisms of the disease and identify potential therapeutic targets.

### 1.1.1 Evolution of pulmonary fibrosis

In ILD, inflammatory, granulomatous and/or fibroproliferative tissue reactions result in repetitive, multifocal alveolar damage with consecutive excessive and uncontrolled wound healing (Behr 2013). Generally, wound repair is a complex biological process and an essential property of multicellular organisms (Gurtner et al. 2008). After an injury, wound healing is initiated by replacement of damaged or dead cells with connective tissue leading to the formation of a scar. This provisional matrix is an important biological process as it prevents excessive blood loss and functions as barrier for the invasion of pathogens until re-epithelialization has taken place (Hecker and Thannickal 2011). In the process of wound repair and tissue remodeling in the lung, multiple pathways are activated inducing wound healing in four distinct stages: clotting and coagulation, inflammation, fibroblast migration and new tissue formation and tissue remodeling and/or resolution (Gurtner et al. 2008, Wynn 2011) (Figure 1).

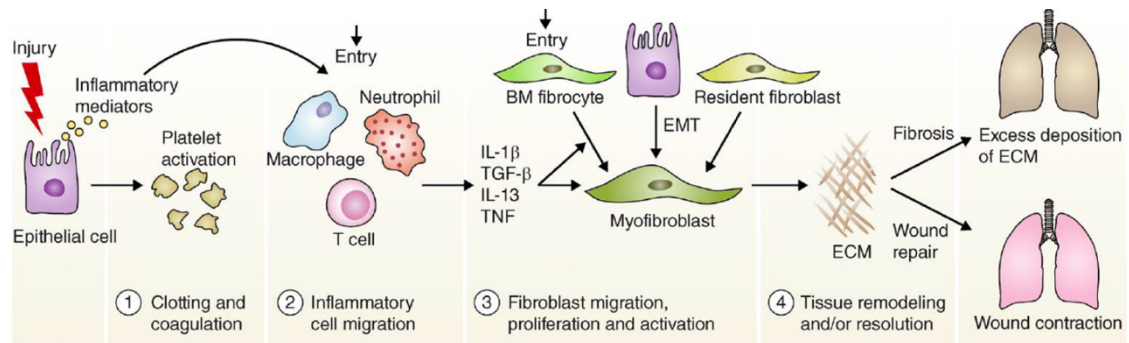


**Figure 1.** Concept of pulmonary wound healing and tissue remodeling. Wound repair consists of four stages: **(1)** activation of platelets with clotting and coagulation, **(2)** migration of inflammatory cells and secretion of pro-fibrotic factors, **(3)** migration, proliferation and activation of fibroblasts and secretion of extracellular matrix (ECM) components by activated fibroblasts and myofibroblasts to build a provisional repair matrix and **(4)** tissue remodeling and resolution. Fibrosis can develop if any of these steps is dysregulated or when the damaging trigger persists. Figure taken and legend adapted from (Wynn 2011).

The first step after tissue injury is the release of inflammatory mediators by endo- and/or epithelial cells which in turn activates circulating platelets (Wynn 2011). An antifibrinolytic coagulation cascade initiates clotting and prevents further blood and fluid loss and infection. A provisional fibrin matrix becomes the scaffold for infiltrating cells. Secondly, the aggregation and degranulation of platelets leads to the secretion of chemokines which induce the dilation of blood vessels and increase permeability which in turn allows migration of neutrophils, macrophages, lymphocytes, and eosinophils. At the site of the injury activated macrophages and neutrophils fight invading pathogens and remove cell debris (Wynn 2011). Additionally, inflammatory cells secrete various cytokines and chemokines including transforming growth factor beta (TGF- $\beta$ ), platelet derived growth factor, tumor necrosis factor alpha (TNF $\alpha$ ) and interleukin six and 13 (IL-6 and IL-13) which in turn reinforce the inflammatory response. This triggers the activation, migration, proliferation and recruitment of fibroblasts and myofibroblasts. Yet, the origin of myofibroblasts is not fully understood but includes local mesenchymal cells, so-called fibrocytes which are bone marrow progenitor cells and epithelial cells which transdifferentiate into fibroblast-like cells (Kisseleva and Brenner 2008, Wynn 2011). After activation of fibroblasts, they transform into  $\alpha$ -smooth muscle actin-expressing myofibroblasts which produce and secrete distinct extracellular matrix (ECM) components that can form new tissue. Finally, myofibroblasts induce wound contraction which triggers epithelial and endothelial cells to split up and move over the provisional ECM matrix to re-epithelialize and reconstitute the parenchymal tissue architecture (Gurtner et al. 2008, Hecker and Thannickal 2011, Wynn 2011).

However, if one of these multiple steps becomes dysregulated or if the lung-damaging stimulus persists, it can cause the formation of a persisting fibrotic scar, which consists of excess deposition of ECM components (Wynn 2011). In pulmonary fibrosis, it is currently assumed that repeated (subclinical) injury causes harm to the alveolar epithelial cells and the subsequent tissue repair response activates mesenchymal cells to produce a specialized ECM, which includes, e.g. interstitial collagens, proteoglycans, fibronectin and hyaluronic acid (Wynn 2011, Wuyts et al.

2013). The lung has a remarkable capacity to regenerate (Hogan et al. 2014), and thus, in normal physiology, the provisional ECM that was deposited after injury is being remodeled after completion of epithelial regeneration so that interstitial fibrosis resolves. Due to dysregulated repair mechanisms, in pulmonary fibrosis, however, regeneration is insufficient or incomplete, which leads to permanent scarring and remodeling of the lung interstitium (Wuyts et al. 2013).

### 1.1.2 Interstitial lung diseases

The prevalence of ILD is estimated to be 67,5 per 100.000 in females and 80,9 per 100.000 in males (Coultas et al. 1994). There are over 200 clinically defined ILD sub entities with a broad variety in terms of etiology, radio morphology, prognosis and therapeutic options among them. Since the molecular pathophysiology in most ILD entities is unclear, it is still a major challenge to diagnose and stratify patients into groups that are relevant for prognosis and therapy initiation. Only 35-40% of patients with ILD are diagnosed with a known etiology [pneumoconiosis, hypersensitivity pneumonitis, drug or radiation induced ILD or post-infectious ILD], while most ILDs have an unknown etiology (sarcoidosis, idiopathic interstitial pneumonias) (Thomeer et al. 2001). According to a consensus classification ILDs can be subdivided into four main groups: ILD with known origin (e.g. drug-induced ILD, connective tissue disease related ILD; CTD-ILD), idiopathic interstitial pneumonia, granulomatous ILD (e.g. sarcoidosis) or other ILD (e.g. lymphangioleiomyomatosis) (American Thoracic and European Respiratory 2002, Behr 2013, Travis et al. 2013).

Idiopathic interstitial pneumonias can further be subdivided into the 'rare idiopathic interstitial pneumonias' (< 1%) and 'major idiopathic interstitial pneumonias', which include chronic fibrosing idiopathic interstitial pneumonias like idiopathic pulmonary fibrosis (IPF; approx. 50%) and idiopathic non-specific interstitial pneumonia (NSIP; approx. 25%), smoking related idiopathic interstitial pneumonias (e.g. respiratory bronchiolitis ILD; approx. 10%) and acute/subacute idiopathic interstitial pneumonias like cryptogenic organizing pneumonia (COP; approx. 5%) (Travis et al. 2013, Neurohr and Behr 2015). Another 10-14% of patients with idiopathic interstitial pneumonias are so called unclassifiable idiopathic interstitial pneumonias, leaving patients and physicians dissatisfied (Ryerson et al. 2013, Troy et al. 2014, Guler and Ryerson 2018).

In some patients with ILD, pulmonary fibrosis can develop into a progressively fibrosing clinical phenotype associated with rapidly worsening dyspnea, loss of lung function, potentially reduced response to immunosuppressive treatment and limited survival (Cottin et al. 2018). Figure 2 depicts ILD entities which are more likely to develop such a progressive-fibrosing clinical phenotype, including IPF, which might be considered representative for this phenotype (Cottin et al. 2018). Given the highly diverse clinical course and therapeutic options an early and correct diagnosis of ILD is crucial for the patients' outcome.

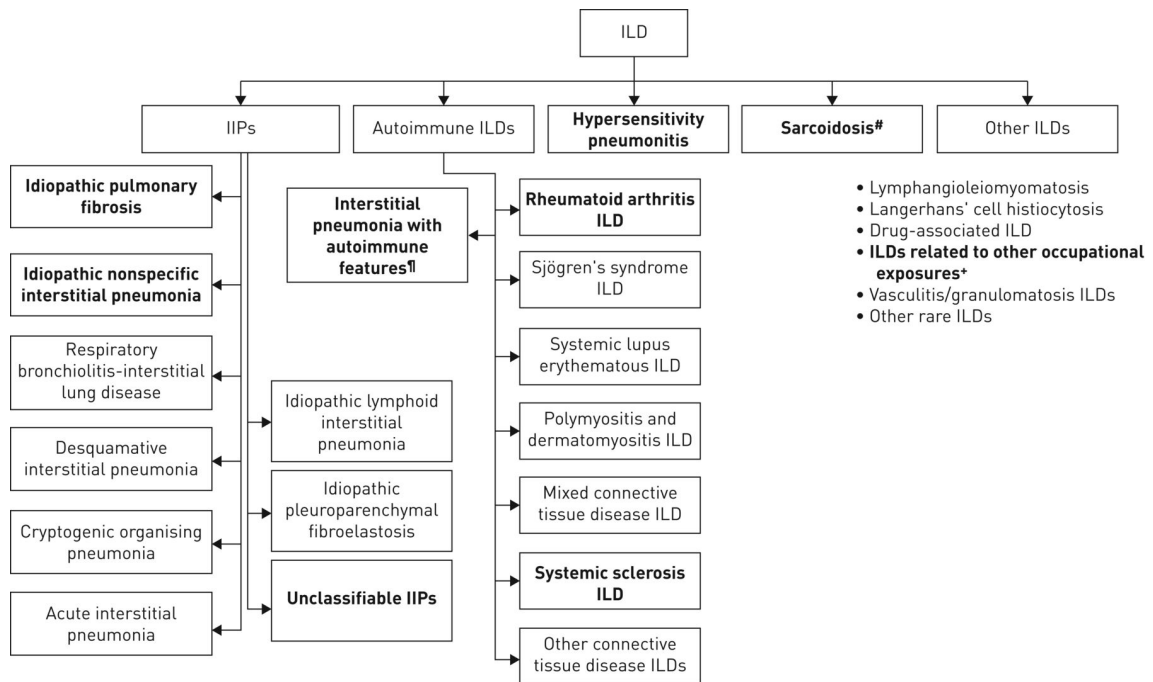


**Figure 2.** Scheme of different interstitial lung diseases (ILDs). Printed in bold are types of ILD that rather experience clinical deterioration known as a “progressive-fibrosing phenotype. Abbreviations: idiopathic interstitial pneumonias (IIPs), interstitial lung disease (ILD). Figure taken and legend adapted from (Cottin et al. 2018).

### 1.1.3 Idiopathic pulmonary fibrosis (IPF)

Idiopathic pulmonary fibrosis (IPF) is a chronic and progressive fibrotic ILD of unknown etiology (Raghu et al. 2018). In Europe, the prevalence of IPF ranges between 1.25 and 23.4 per 100.000 and the yearly incidence is estimated to range between 0.22 and 7.4 per 100.000 inhabitants, which makes it a rare disease (orphan disease) (Nalysnyk et al. 2012). Nevertheless, IPF is the most common representative of idiopathic interstitial pneumonias (Raghu et al. 2018). It is characterized by interstitial fibrosis which is confined to the lungs and associated with the typical *usual interstitial pneumonia* (UIP) pattern, which can be found on computed tomography and histopathology (Raghu et al. 2018) (Figure 3). Due to repetitive, multifocal injury to the alveolar compartment excessive reparation processes and chronic inflammation are induced (Burgstaller et al. 2017). This induces fibroblast proliferation and myofibroblast differentiation followed by an increased collagen secretion, ECM deposition as well as fibrosing and scarring of the lung parenchyma leading to an ultimately fatal disorder. The further understanding of the molecular pathophysiology in IPF is still limited. The evaluation process of IPF is complex and other reasons for ILD need to be ruled out prior to a definite, final diagnosis. IPF is most prevalent in male patients over the age of 60 years with a history of smoking, which is often years ago (Raghu et al. 2018). There is also a familial form of IPF in which two or more related family members are affected (Raghu et al. 2018). Since clinical diagnostics have evolved enormously in the past few

years, recently, an updated international guideline for the diagnosis of IPF has been published by the *American Thoracic Society, European Respiratory Society, Japanese Respiratory Society and Latin American Thoracic Society (ATS/ERS/JRS/ALAT)* (Raghu et al. 2018). Based on this guideline, the German Respiratory Society (Deutsche Gesellschaft für Pneumologie) and other associations have developed a new German-language S2k guideline (Behr et al. 2020, Behr et al. 2021).

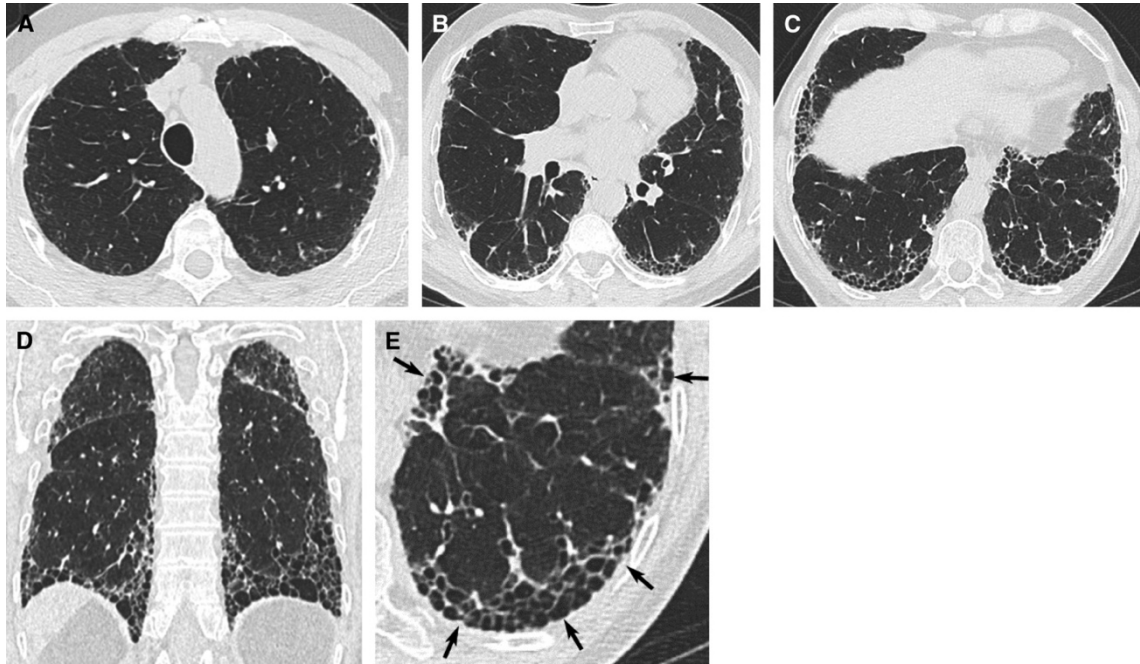


**Figure 3.** Usual interstitial pneumonia (UIP) pattern on high-resolution computed tomography. Computed tomography depicts the typical subpleural predominance and an apicobasal gradient of honeycombing in transverse (**A-C**) and coronal reconstruction (**D**). (**E**) A magnified view (left lower lobe) demonstrate characteristic patterns of honeycombing, comprising grouped cystic airspaces with surrounding walls and variable size. Honeycombing can occur in variable layering (see arrows). Figure taken and legend adapted from (Raghu et al. 2018).

IPF patients experience highly diverse clinical courses, ranging from slow to rapid progressive (King et al. 2011). If an acute exacerbation (AE) of ILD occurs, diseases progression can even be accelerated. Currently, AEs occur with unpredictable probability and they are associated with a high mortality (Collard et al. 2016). AEs are characterized by a diffuse alveolar damage and vast acute lung injury (Oda et al. 2014), which is probably caused by an intrinsic or extrinsic trigger like viral infections or micro aspiration (Collard et al. 2016).

Overall, the prognosis of IPF is limited with an estimated survival of two to five years after diagnosis (Nathan et al. 2011, Raghu et al. 2018). Although the clinical course of patients with ILD can vary enormously, even within a defined entity, the therapy of choice is usually a non-specific anti-inflammatory and immunosuppressive therapy (Behr 2013). However, in IPF,

immunosuppressive therapy is ineffective and can also be harmful as it was shown with the combined therapy of prednisone, azathioprine, and N-acetylcystein in the so-called PANTHER-IPF trial (Idiopathic Pulmonary Fibrosis Clinical Research et al. 2012, Wells et al. 2012). For only a few years now, two antifibrotic drugs, pirfenidone and nintedanib, have been approved and are recommended by the guidelines for the therapy of IPF (Raghu et al. 2015). For both medications it has been shown that in comparison to placebo the loss of lung function can be reduced and the progression-free survival is longer under therapy (Noble et al. 2011, King et al. 2014, Richeldi et al. 2014).

Regardless of the therapeutic breakthrough with antifibrotic drugs, there is no cure for IPF, yet. As antifibrotic therapies can “just” counteract the loss of lung function but cannot cure the disease, so far, the only definite therapeutic option remains a lung transplantation in patients who qualify for it (Raghu et al. 2018). Further research is therefore urgently needed in order to learn more about the pathogenesis of IPF and uncover possible targets for future therapies.

#### **1.1.4 Pathogenesis and risk factors for idiopathic pulmonary fibrosis (IPF)**

The pathogenesis of IPF is of high complexity and still poorly understood. Histological hallmarks of IPF include excessive deposition of ECM, fibroblast foci and spatially heterogenous fibrosis, which is characterized by areas of fibrosis next to normal lung tissue (Wynn 2011, Fernandez and Eickelberg 2012, Heukels et al. 2019). It is assumed that cellular homeostasis in the lungs is lost, which in turn leads to a dysregulation of wound healing and an aberrant remodeling of the alveolar wall (Hecker and Thannickal 2011). The excessive production and deposition of ECM finally leads to fibrosis of the lung tissue thereby destroying the original function of the organ (Hecker and Thannickal 2011). The organ malfunction results in an impaired gas exchange and eventually death from respiratory failure (Wynn 2011). It can be assumed that fibrosis typically only develops if these conditions persist over several weeks, months or years (Wynn 2011, Wuyts et al. 2013, Rockey et al. 2015).

Currently it is assumed that in the pathogenesis of IPF (repetitive) epithelial injury could initiate pro-fibrotic reprogramming on an epigenetic level, persistent senescence of epithelial cells and dysregulated increased production of fibrotic mediators as well as constant activation of fibroblasts in a genetically predisposed elderly person (Martinez et al. 2017). The combination of all of these factors together could lead to the uncontrolled wound repair which ultimately results in IPF (Martinez et al. 2017) (Figure 4). The pathomechanisms in IPF are multifactorial and during the development of fibrosis the innate and the adaptive immune system are also involved (Wynn 2011). One of the key-pathways in IPF is TGF- $\beta$  signaling (Heukels et al. 2019).



Despite a currently not fully understood etiology, multiple possible risk factors for IPF have been recognized such as genetic predisposition, environmental agents (e.g. viruses), behavioral factors (e.g. history of smoking >20 pack years) and asymptomatic gastro-esophageal reflux disease (Raghu et al. 2011, Behr 2013). Moreover, there is an increasing body of evidence that autoimmune processes might be involved in the genesis of IPF. However, autoimmunity and IPF leads to controversial discussions since, if IPF is suspected, a systemic autoimmune disease must be excluded prior to diagnosis (Raghu et al. 2018). In addition, as mentioned earlier, in the past it has been shown that a systemic immunosuppressive combination therapy consisting of cortisone, azathioprine and N-acetylcysteine is harmful for patients with IPF (Idiopathic Pulmonary Fibrosis Clinical Research et al. 2012). Nevertheless, there is data that autoimmune processes take place in IPF. For example, the detection of autoantibodies shows that further investigations regarding autoimmunity and IPF should be pursued.

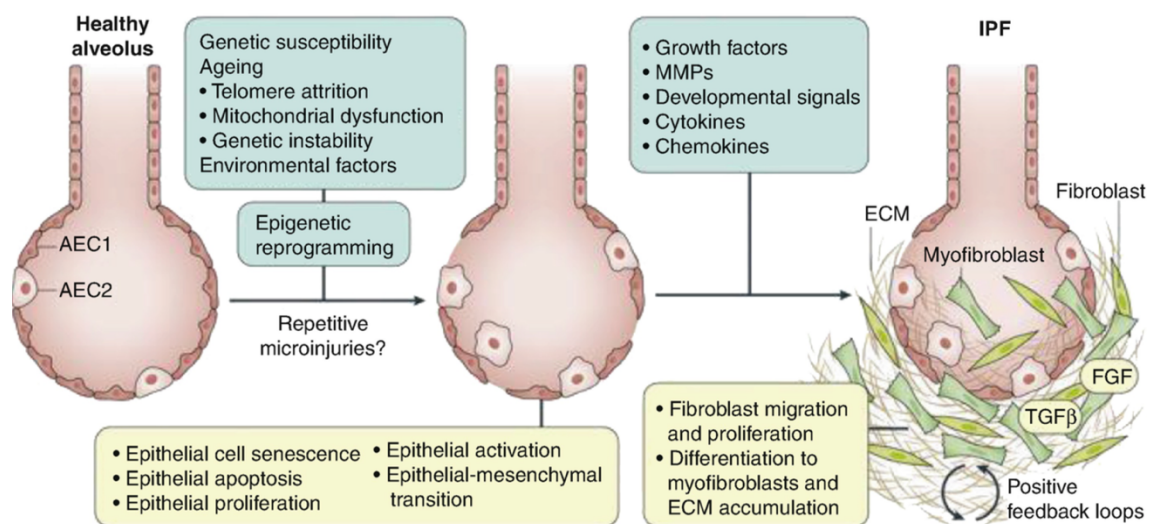


**Figure 4.** Processes potentially involved in the pathogenesis of idiopathic pulmonary fibrosis (IPF). The combination and interplay of genetic susceptibility, ageing and environmental factors lead to an epigenetic reprogramming promoting dysregulated epithelial activation potentially resulting in IPF. The process might be induced by repetitive microinjuries. Impaired wound healing then triggers a remodeling of the lungs with fibrotic tissue. Figure taken and legend adapted from (Martinez et al. 2017)

## 1.2 The human immune system

Appreciation for the potential role of immune responses in the etiology and/or progression of fibrotic diseases including ILD is growing (Hoyne et al. 2017). Hereafter, the cells of the immune system will be introduced with a specific focus on B cells including important central and peripheral checkpoints and mechanisms to escape and allow break of tolerance in these cells.

### 1.2.1 Cells of the innate and adaptive immune system

The immune system consists of innate and adaptive components and there is intensive crosstalk between these two (Figure 5). While the innate immunity reacts immediately to pathogens, the adaptive immunity is highly specific and antigen-driven. The innate immune reaction comprises dissoluble components, like the complement system, as well as immune cells like macrophages, granulocytes (basophils, eosinophils and neutrophils), dendritic cells, mast cells, and natural killer cells (Dranoff 2004, Yamauchi and Moroishi 2019). Innate immunity triggers the first immunological processes in response to the detection of bacteria, viruses, and cancer and responds within hours. This is because the innate immune response encompasses various cell-surface molecules and pattern-recognition receptors which can quickly detect microbial-derived proteins and initiate an inflammatory response (Janeway 2001, Dranoff 2004).

In contrast, the response of the adaptive immunity takes longer as it is an antigen-specific defense mechanism. While the adaptive immunity takes days to develop the immune protection is long-lasting (Yamauchi and Moroishi 2019). The adaptive immunity comprises B cell-mediated humoral immunity via antibodies and CD4<sup>+</sup> and CD8<sup>+</sup> T cell-mediated immunity (Yamauchi and Moroishi 2019). The increase of rare lymphocytes is needed as they contain somatically transformed immunoglobulin components or T cell receptors which recognize microbial constituents or peptide fractions offered and shown by major histocompatibility complex (MHC) molecules (Zinkernagel 2003).

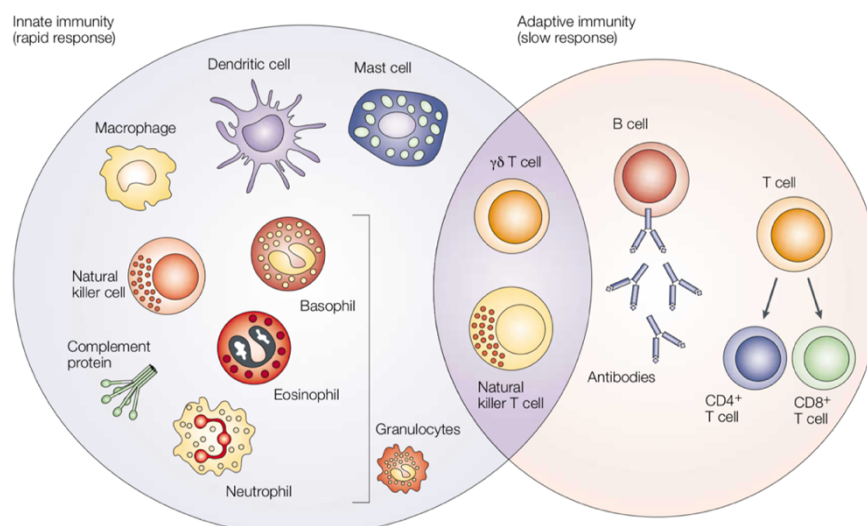


**Figure 5.** Cells of the immune system. The innate immunity, the first immunological mechanism to respond after contact with an infectious agent, includes soluble components (e.g. the complement system) and immune cells such as granulocytes, mast cells, macrophages, dendritic cells and natural killer cells. The adaptive immunity, consisting of antibodies, B cells, and T cells, reacts slower but in an antigen-specific manner. Further, the adaptive immunity has the ability to develop an antigen-specific memory. Cytotoxic lymphocytes (natural killer cells and  $\gamma\delta$  T cells) represent a link between innate and adaptive immune system. Figure taken and legend adapted from (Dranoff 2004)

Cytotoxic T lymphocytes, such as the natural killer cells and  $\gamma\delta$  T cells have their function in between innate and adaptive immunity (Dranoff 2004). Also, macrophages and dendritic cells have innate and adaptive characteristics as they are considered as professional antigen-presenting cells with the ability to induce adaptive immunity by presenting antigens to T and B cells (Yamauchi and Moroishi 2019).

### 1.2.2 B cell checkpoints and break of tolerance

The primary function of the complex interactions of the immune system is to defend the host from infection. However, there are two major scenarios where the immune system itself can cause pathology: immune deficiency syndromes and autoimmune diseases (Wang et al. 2015). The inability of the immune system to properly distinguish between self and non-self and therefore the underlying mechanism of autoimmune diseases is often termed “break of tolerance”. Autoimmune diseases affect 3-5% of the population (Wang et al. 2015). While autoimmune thyroid disease is the most common one, there are nearly 100 autoimmune diseases, some of which do only affect one organ such as primary biliary cirrhosis and others that affect multiple organs (e.g. systemic lupus erythematosus) (Yu et al. 2014).

Several mechanisms are in place to ensure immune tolerance including central tolerance, peripheral tolerance and others, such as T regulatory cells and produced cytokines and chemokines (Figure 6). The existence of autoreactive T and B cells per se does not necessarily lead to pathology which is why autoimmunity can be termed as “physiological” and “pathological” (Avrameas and Selmi 2013, Salinas et al. 2013). There are currently theories which suggest that (pathological) autoimmune diseases develop preferentially in patients with a genetic predisposition when additional environmental factors occur causing the immune system to initiate processes destructing the tissue (Wang et al. 2015).

Given the success of B cell targeting therapies, B cells seem to be crucially involved in various human autoimmune diseases, including rheumatoid arthritis (Edwards and Cambridge 2005). B cells are most likely part of the pathological processes by generating harmful autoantibodies, inducing cytokines which initiate inflammation as well as activating T cells (e.g. via antigen presentation) (Reijm et al. 2020).

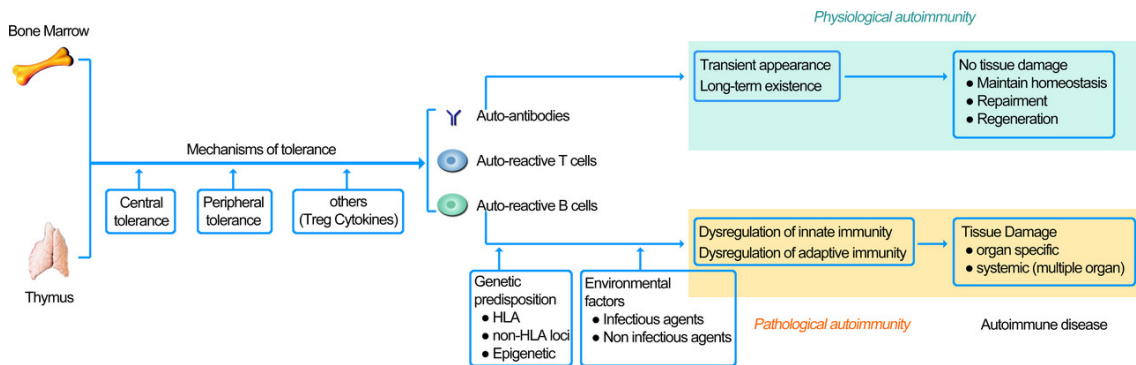


**Figure 6.** Overview of the development of autoimmune disease. Despite several central and peripheral checkpoints, a small number of autoreactive T and B cells can escape into the periphery. These cells will not be pathological unless a patient has a genetic predisposition to autoimmune disease and experiences an environmental trigger. Figure taken and legend adapted from (Wang et al. 2015)

B cell first develop in the bone marrow and begin to express B cell receptors. The part of the B cell receptor which recognizes antigens comprise so called light and heavy chains. Light chains consist of variable (V) and joining (J) gene segments, while heavy chains additionally include diversity (D) gene segments. Due to the random association of these gene segments, B cell receptors encompass highly varying antigen-binding sites (Tonegawa 1983). Further variety during V(D)J-recombination is generated using the integration of palindromic- and non-templated nucleotides (Lewis et al. 1984, Lewis et al. 1985). Moreover, the variable domain of the B cell receptor experiences additional diversity via the combination of heavy and light chains. All of these processes together allow a highly diverse B cell receptor repertoire and B cell population which is why various different structures and molecules can be specifically identified (Reijm et al. 2020). This includes self-reactive B cell receptors and therefore recognition of self-molecules.

To prevent self-reactive B cells from leaving the bone marrow, negative selection processes take place. In this B cell central tolerance mechanism receptor-editing and clonal deletion helps to remove a significant amount of self-reactive B cells (Reijm et al. 2020) (Figure 7 a). However, a certain number of self-reactive B cells will be able to “leak out” into the periphery. To prevent humoral autoimmunity there are also a number of checkpoints and peripheral tolerance processes in the periphery. Peripheral checkpoints first include follicular exclusion of immature self-reactive B cells as they are in competition with mature B cells to go in the primary follicles (Cyster and Goodnow 1995). After entering the primary follicles, B cells reach germinal centers where they get in contact with antigen-presenting follicular dendritic cells (FDC) and obtain commands to survive (Allen and Cyster 2008). In the next selection step activated B cells enter the border between T and B cells in order to show antigens while being supported by T helper cells (Reijm et al. 2020). Afterwards, B cells proliferate and experience so called somatic hypermutation followed by FDC driven selection (Mandel et al. 1981, MacLennan 1994). It is known from mouse models that selected B cells are able to leave the germinal centers or return to them as so called “*memory B cells or plasmablasts /cells*” that secrete isotype-switched antibodies with high affinity (Reijm et al. 2020). Again, for the B cell survival and activation, the presentation of antigens on

the cell surface by FDCs and the promotion of support from T helper cells are important control points in the periphery as they prompt vital signals to B cells (Reijm et al. 2020). The presence of diseases-specific autoantibodies shows that despite these central and peripheral checkpoints negative selection fails to completely eliminate all self-reactive B cells. Nevertheless, many times it is still unclear how or at which time point autoreactive B cells are activated (Reijm et al. 2020). One of the main mechanisms how B cells can escape peripheral checkpoints seem to be generation of self-reactive B cells during somatic hypermutation where the B cell receptor reactivity is directed against self-antigens (Figure 7 b). Secondly, in the event of cross-reactivity, the B cell receptor can recognize foreign microbial/environmental or structurally similar self-antigens. Since T cells, which are not autoreactive, might support these B cells, they might be able to then bypass important checkpoints (Reijm et al. 2020).

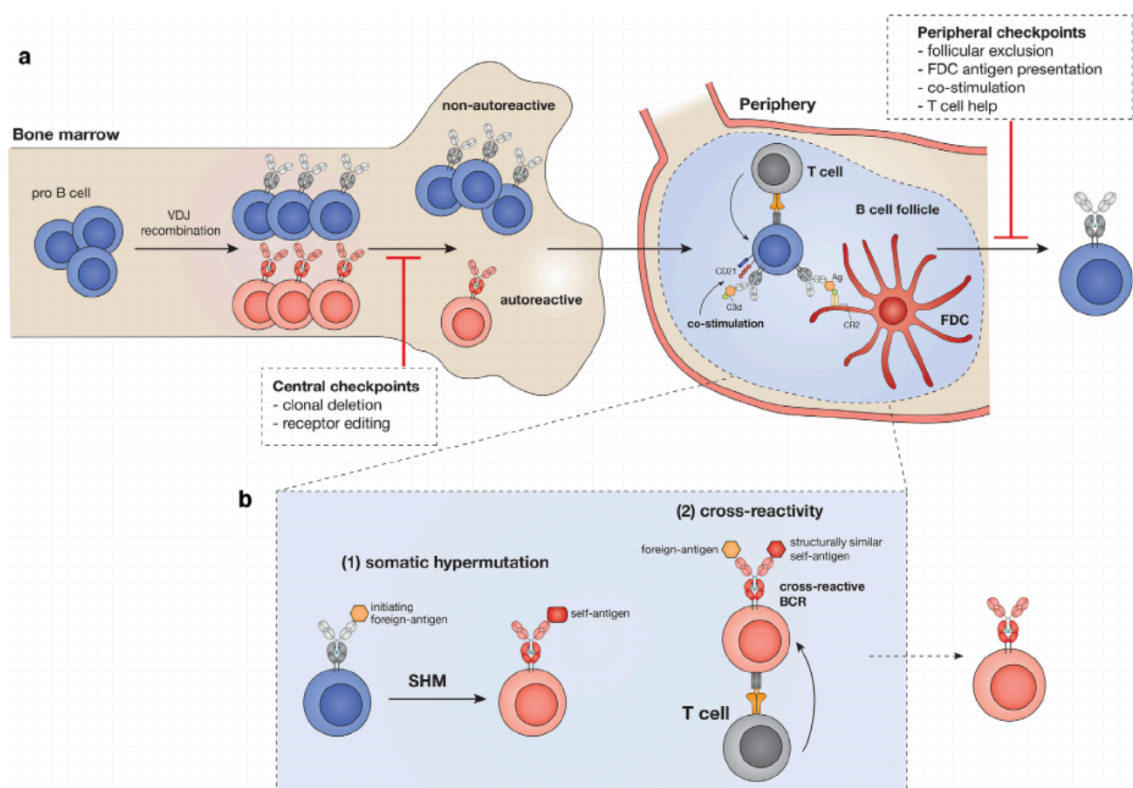


**Figure 7.** Potential ways for self-reactive B cells to bypass selection processes of the immune system. **(a)** B cells evolve in the bone marrow and periphery by passing through multiple checkpoints. Autoreactive B cells which might arise during variable/(joining)/diversity gene segment [V(D)J] recombination of the B cell receptor (BCR) might be eliminated by clonal deletion and receptor editing. In the periphery B cells have to pass further checkpoints. **(b)** Potential mechanisms which allow autoreactive B cells to escape from these checkpoints are somatic hypermutation (SHM) and cross-reactivity of T and B cells with foreign or structurally similar self-antigens. Figure taken and legend adapted from (Reijm et al. 2020)

### 1.3 Autoimmunity in pulmonary fibrosis

As mentioned above, the role of autoimmunity in the genesis of a range of fibrotic diseases is increasingly recognized (Hoyne et al. 2017). While some forms of ILD are closely connected to an underlying autoimmune disease, known as CTD-ILD, idiopathic interstitial pneumonias such as IPF do usually require the exclusion of an underlying autoimmune disease. Nevertheless, the presence of lymphoid aggregates in IPF lungs and circulating autoantibodies propose a role of immune cells in the genesis or progression of the disease (Hoyne et al. 2017). Therefore, in the following section, autoimmunity in the context of ILD will be discussed and data on B cell-mediated autoimmunity in IPF will be highlighted.

#### 1.3.1 Connective tissue disease related interstitial lung disease (CTD-ILD)

At present, in Western countries, autoimmune diseases are among the third most common causes of morbidity and mortality (Degn et al. 2017). Though connective tissue disease (CTD) comprise various immune diseases with unambiguous and distinctive characteristics, they share the presence of auto-reactive T cells and B cells which generate and secrete autoantibodies causing chronic inflammation and harm the tissue (Wells and Denton 2014, Cottin et al. 2018). It seems that the environment and genetics can contribute to the genesis of CTDs (Wells and Denton 2014).

Pulmonary involvement is a major complication in patients with autoimmune rheumatic diseases leading to an increased risk for mortality (Wells and Denton 2014). Overall, approximately 10% of all patients with ILD suffer from CTD-ILD (Grund and Siegert 2016). With idiopathic interstitial pneumonias (including IPF) being the most frequent diagnosis of patients presenting in ILD referral centers, CTD-ILD is the second most common diagnosis (Hyltdgaard et al. 2014, Ahmad et al. 2017). Around 80% of CTD-ILD patients suffer from systemic sclerosis (SSc), but also patients with rheumatoid arthritis can develop ILD (Fischer and du Bois 2012, Grund and Siegert 2016). Beside SSc and rheumatoid arthritis, CTD-ILD is most prevalent in autoimmune myositis, systemic lupus erythematosus, sjogren's syndrome and undifferentiated collagenases (Doyle and Dellaripa 2017). In this context, depending on the underlying disease and the current stage of the disease, a combination of pulmonary fibrosis and inflammation can be observed (Heukels et al. 2019). On high resolution computed tomography, NSIP is the most common pattern, but UIP pattern can also be found in CTD-ILD requiring differentiation from IPF (Cottin 2016). While dyspnea is present in 35% of patients with SSc, 32% have restrictive lung function parameters and in 52% an ILD can be found on computed tomography (Meier et al. 2012). In comparison, the prevalence of clinically significant ILD for patients with rheumatoid arthritis is lower with only 10%, but strong serum positivity and men with a history of smoking have been shown to be at risk for developing ILD (Olson et al. 2011, Kelly et al. 2014). In patients with rheumatoid arthritis, however, a UIP pattern is more frequently found on high resolution computed tomography, which in turn is

associated with poorer survival and an increased risk of AEs (Suda et al. 2009, Kelly et al. 2014, Solomon et al. 2016). Though, the increased occurrence of AEs could be due to the fact that the UIP pattern itself is associated with an increased risk of AE (Leuschner and Behr 2017). Further, data have recently been published suggesting that similar mechanisms might contribute to the genesis of lung fibrosis in IPF and ILD in rheumatoid arthritis (Juge et al. 2018).

Overall, compared to patients with IPF, patients with CTD-ILD are assumed to have a less severe disease process (de Lauretis et al. 2011). In contrast to IPF and although medical therapy does not reduce the fibrotic changes in the lungs, immunosuppressive therapy can partially slow down the progression of CTD-ILD (de Lauretis et al. 2011). Very recently, it has been shown that nintedanib can reduce FVC decline in patients with SSc-ILD, which led to the approval of the treatment with nintedanib in SSc-ILD in 2020 (Distler et al. 2019).

### **1.3.2 Interstitial pneumonia with autoimmune features (IPAF)**

Given the different prognosis and treatment options, it would be desirable that patients could always be clearly classified as CTD-ILD or idiopathic interstitial pneumonias. However, in clinical practice there are patients with ILD who present with features of CTD but cannot be formally designated as such as they do not qualify for the CTD diagnosis criteria. Recently, a European Respiratory Society/American Thoracic Society research statement introduced criteria for these patients proposing the term “interstitial pneumonia with autoimmune features” (IPAF) (Fischer et al. 2015). The statement considers the three domains “clinical” (particular extra-thoracic features), “serological” (particular autoantibodies) and “morphological” (particular chest imaging, histopathologic or pulmonary physiologic features) suggestive of CTD (Fischer et al. 2015). Classification criteria for IPAF requires (1) evidence of an interstitial pneumonia either on high resolution computed tomography or surgical lung biopsy, (2) the exclusion of an alternative etiology of ILD despite a complete clinical evaluation, (3) incomplete features of a specific CTD, and (4) a minimum of one characteristic from two or all three domains “clinical”, “serological” and “morphological” (Fischer et al. 2015).

The prevalence of IPAF among patients with ILD is reported to range between 7 and 34% (Chartrand et al. 2016, Oldham et al. 2016, Ahmad et al. 2017). In comparison to patients with CTD-ILD patients with IPAF seem to have a significantly worse survival (Oldham et al. 2016) (Figure 8 a). Interestingly, patients of the IPAF cohort without a UIP pattern show an improved survival while IPAF patients with UIP pattern have a more unfavorable survival (Figure 8 b). Due to the fact that data about IPAF treatment is limited to case series further research is needed and treatment must be based on an individual case-by-case decision (Fernandes et al. 2019).

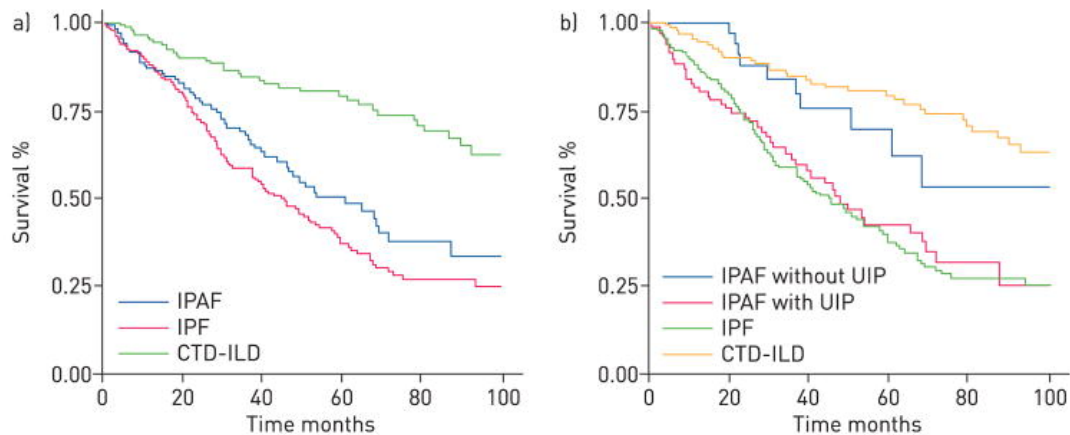


**Figure 8.** Survival of patients with idiopathic pulmonary fibrosis (IPF), interstitial pneumonia with autoimmune features (IPAF) and connective tissue disease related interstitial lung diseases (CTD-ILD). **(a)** Kaplan–Meier survival curves depict a significantly worse survival of patients with IPAF in comparison to patients with CTD-ILD. **(b)** IPAF patients with a UIP pattern (radiological and/or histological) had a similar survival curve to patients with IPF while survival of IPAF patients without UIP appeared to be similar to CTD-ILD. Abbreviations: idiopathic pulmonary fibrosis (IPF), interstitial pneumonia with autoimmune features (IPAF), connective tissue disease related interstitial lung disease (CTD-ILD), usual interstitial pneumonia pattern (UIP). Figure taken and legend adapted from (Oldham et al. 2016)

### 1.3.3 The role of autoimmunity in idiopathic pulmonary fibrosis (IPF)

So far, the importance of the innate and adaptive immune system in the genesis of IPF is unclear and it is focus of controversial discussions. However, recent studies suggest, that innate and adaptive immune cells could play a role in the evolution of IPF or at least promote clinical progression of the disease. In fact, there is data for almost every cell of the immune system to take part in the pathogenesis of IPF including neutrophils, macrophages, monocytes, T lymphocytes and B lymphocytes (Scott et al. 2019). This is especially interesting as new, “patient-individualized therapy strategies” may be found in this context.

Macrophages, representing innate immunity cells, can increase the production and secretion of TGF- $\beta$  and platelet-derived growth factor, which are pro-fibrotic mediators (Kolahian et al. 2016). Neutrophils are known to contribute to the control of ECM homeostasis particularly via the production of pro-fibrotic matrix metalloproteinases, such as matrix metalloproteinase-2, metalloproteinase-8 and metalloproteinase-9 (Henry et al. 2002, Ikezoe et al. 2014). Further, the neutrophil elastase, which is the main component that is produced during proteolysis of alveolar neutrophils, can stimulate the proliferation of fibroblasts and the differentiation of myofibroblasts *in vitro*, promoting ECM deposition (Gregory et al. 2015). Very recently, in a retrospective, multicenter study it has been shown that an increased CD14+ monocyte count is a biomarker for reduced transplant-free survival in IPF (Scott et al. 2019). Another study published in 2021 confirmed that in IPF an increased monocyte count is linked to an increased risk for disease progression and mortality (Kreuter et al. 2021) Moreover, in a post-hoc analysis, that pooled data from the pirfenidone phase III trials *CAPACITY* and *ASCEND*, the cytokine CCL18 which is secreted by cells from the innate immune system (such as dendritic cells, monocytes and



macrophages) was identified as being closely associated with disease progression in IPF (Neighbors et al. 2018). In the past, several potential therapies targeting the innate immune system have been evaluated but did not show the expected effect including the direct inhibition of macrophages via TNF $\alpha$  neutralization by the TNF $\alpha$  receptor etanercept (Raghu et al. 2008), or the therapy with carlumab, a monoclonal antibody against C-C chemokine ligand 2, which is important for recruitment of macrophages (Raghu et al. 2015).

Concerning adaptive immunity, several subpopulations of T lymphocytes were found to be enriched in the lung parenchyma and BAL fluid of patients with IPF (Fireman et al. 1998, Desai et al. 2018). However, T helper cells (e.g. Th2 and Th17 cells) are the subpopulation of T lymphocytes which are best studied in IPF (Desai et al. 2018). A theory that has been studied intensively is the imbalance between Th1 and Th2 cells. While Th1 cells and their secretory products [(IL-12, an inducer of interferon gamma (IFN $\gamma$ ))] are considered to be involved in anti-fibrotic processes, Th2 cells and associated mediators (IL-4 and IL-13) are thought of as pro-fibrotic (Desai et al. 2018). In IPF, IFN $\gamma$  has been reported to be reduced in BAL and blood (Prior and Haslam 1992), while Th2 cells and secreted cytokines were detected as being increased in IPF tissue and blood (Liu et al. 2002, Saito et al. 2003, Kimura et al. 2006). Another cell type, Th17 cells secrete proteins like IL-17, which are on the one hand protective for the host in the context of an infection, but on the other hand can also induce inflammatory processes, like those seen in autoimmune diseases (Onishi and Gaffen 2010). IL-17 is known to promote production and deposition of ECM production but also the TGF- $\beta$  pathway (Wilson et al. 2010). In IPF, IL-17 is increased in lung tissue, BAL and serum (Desai et al. 2018). Different medical treatments targeting T cells were not successful in the past: in a randomized, double-blind, multinational trial the medical treatment with IFN $\gamma$ -1b had no positive effect on progression-free survival and pulmonary function (Raghu et al. 2004). Further, the neutralization of IL-13 via the monoclonal antibodies tralokinumab and lebrikizumab did not affect FVC decline in two phase II studies (Parker et al. 2018, Maher et al. 2021).

In addition to T cells, also B lymphocytes accumulation were found in the lung parenchyma of patients with IPF (Todd et al. 2013, Xue et al. 2013). B cells represent an additional part of the adaptive immune system and are primarily known for their capability to produce antibodies. Increased numbers of CD20+ B cells have been detected in IPF lung tissue (Todd et al. 2013), and in line with this, several studies identified various autoantibodies in patients with IPF which could be an indication of a loss of tolerance in the immune system. These autoantibodies include novel neoepitopes which are mainly structural cell proteins such as annexin-1, cytokeratin 18, cytokeratin 19, desmoplakin, periplakin, and vimentin (Fujita et al. 1999, Dobashi et al. 2000, Yang et al. 2002, Kurosu et al. 2008, Taille et al. 2011, Mathai et al. 2016). Such antibodies, which are directed against self-antigens lead to inflammation with repeated injury and potentially dysregulated wound repair in IPF (Heukels et al. 2019).

Taken together, the data give evidence for B cell accumulation in the lungs of patients with IPF and support the theory of humoral autoimmunity against antigens which can foster and perpetuate inflammation in IPF. However, it remains unclear whether the immune system is already involved in the initiation of IPF or whether it favors the disease progression over time. Concerning therapeutic options, a pilot trial indicated that reduction of autoantibodies using therapeutic plasma exchanges and rituximab, followed by intravenous immunoglobulin therapy might be beneficial in some severely-ill IPF patients with an AE (Donahoe et al. 2015). Though, data from a phase II study evaluating autoantibody reduction therapy in patients with IPF (ART-IPF) (NCT01969409) is still ongoing.

## 2. Objectives

### 2.1 First chapter

Organ fibrosis is an increasing clinical challenge in the developed world and therapeutic options are limited, so far. The origin of fibrosis is, in many cases, not yet known, which is why these entities are called “idiopathic” fibrosis. Reasons for idiopathic fibrosis can be the result of persistent tissue damage, dysregulated regeneration and repair mechanisms, aging or autoimmunity (Schiller et al. 2017). Most data on fibrosis are obtained from gene expression analysis with only limited knowledge on the full-scale quantitative proteome. As the ECM is crucially involved in pathological mechanisms in fibrosis, the proteome of the ECM, the so called matrisome, needs to be further investigated in specific tissues and diseases (Schiller et al. 2017). Analysis of the proteome using mass spectrometry (MS) has been significantly improved in recent years with increasing sensitivity, which allows a reliable identification of peptides even from minimal input material (Aebersold and Mann 2016). Recently, a MS-based, quantitative detergent solubility profiling (QDSP) method was developed, improving previous challenging technical limitations in the analysis of the tissue proteome and matrisome (Schiller et al. 2015).

The aim of the study was to identify common and disease specific features in human tissue fibrosis. Therefore, the specific aims of the first chapter were as follows:

#### 1. *Identification of common and diseases-specific features in human lung and skin fibrosis*

Organ tissue fibrosis can be present not only as an idiopathic form, but also in the context of an underlying autoimmune disease, such as in CTD-ILD. To identify common and disease specific features, the first aim was to match the proteomic data sets from patients with ILD and patients with skin fibrosis due to localized scleroderma, which represents fibrosis in an autoimmune disease (Schiller et al. 2017). Localized scleroderma is a very good model system as involved skin and uninvolved skin can be analyzed in the same patient. Tissue section of patients with different types of ILD and healthy donors were used to extensively study and characterize the nature of the ECM proteome in ILD (Schiller et al. 2017). Findings derived from proteomic analysis in ILD and localized scleroderma were verified using immunostainings and Western blot analysis in larger patient cohorts. Further, lung function and other clinical parameters of patients with ILD were used to correlate MS-based findings with clinical features.

#### 2. *Analysis of IgG subclasses*

The results from the last-mentioned objective revealed the detection of plasma B cells in human ILD and skin fibrosis to an unexpectedly large extent (Schiller et al. 2017). Therefore, the second

part of the first chapter of this thesis aimed to analyze IgG subclasses distribution in patients with ILD using the obtained proteomic data and Western Blot analysis.

## 2.2 Second chapter

The production of autoantibodies might either be the cause of a disease, perpetuate it or solely be the consequence of tissue damage without having feedback effects. To find out more about these different scenarios, first, it is necessary to characterize autoimmune response and analyze the identity and diversity of autoantibodies. As an unbiased and high throughput screening method MS-based proteomic assays can provide such a personalized patient characterization. Given the limited therapy options in IPF, the identification of autoantigens associated with IPF might enable the development of appropriate pre-clinical models to investigate the role of specific antigens in the genesis of idiopathic forms of organ fibrosis. The present study aimed to extend the current knowledge of B cell mediated autoimmunity in ILD using an unbiased MS- driven autoantigen discovery method. Specific aims of the second chapter were as follows:

### 1. *Discovery of autoantigens in ILD*

While in some cases autoantibodies can be used to diagnose a specific disease, they might also be involved in the genesis of the disease. The identification of autoantigens is therefore crucial to learn more about the involvement of autoimmunity in human disease. First, the study aimed for the establishment of a MS-driven autoantigen discovery method to discover novel autoantigens in human ILD. In addition, the method was planned to work objectively and with high through-put. The basis of the assay presented here is immunoprecipitation. Therefore, extracts of human lung proteomes were incubated with serum/plasma from ILD patients to capture potentially pathologic immunoglobulins. Subsequently, quantitative MS was performed. Scl-70 antibodies against topoisomerase is an autoantibody which can be identified in some patients with SSc (Vij and Streck 2013). Patients with CTD-ILD due to SSc served as test subjects for the evaluation of sensitivity and specificity of the method. The findings generated by the assay were compared to previously obtained results from clinically established Scl-70 ELISA tests.

### 2. *Detection of IPF and CTD-ILD specific autoantigens*

As with the Scl-70 antibodies in patients with SSc, other connective tissue diseases can be accompanied by the formation of special auto-antibodies. In contrast to IPF, pulmonary fibrosis in CTD-ILD occurs in the context of a systemic disease with organ involvement of the lungs. Using the MS-assay, the second aim of the study was to identify common and disease specific

autoantibodies in plasma and serum samples from IPF and CTD-ILD from two ILD-centers. Plasma samples from healthy age-matched controls were used as control group.

### *3. Stratification of patient groups based on autoantigen profiles*

Autoimmunity cannot only be presented by one individual autoantigen but also by a signature of several autoantigens. Therefore, the third aim of this study was to identify and stratify patient groups based on autoantigen profiles. In addition, the presence of autoantibody profiles may predict disease progression and therefore be of direct benefit in stratifying patient risk. Therefore, clinical meta-data were integrated to enable the correlation with clinical features such as lung function parameters and transplant-free survival.

### **3. Material and Methods**

#### **3.1 Material and Methods for proteome profiling of human tissue fibrosis project**

##### **3.1.1 Study cohort and human patient material**

Human lung tissue was derived from the BioArchive at the Comprehensive Pneumology Center in Munich (BioArchive CPC-M) (Schiller et al. 2017). Human lung tissue resections were originally obtained from human lung and explant material during lung transplantation at the University Hospital of the Ludwig-Maximilians University in Munich, Germany. For the proteome analysis, tissue of eleven patients with end-stage ILD and three healthy donors was used (Schiller et al. 2017). For the Western blot analysis biopsies from 34 patients with ILD and seven healthy donors were analyzed (Schiller et al. 2017). Clinical data of ILD patients included information about demographics (gender, age) and therapy prior to transplantation (long term oxygen therapy, immunosuppressive therapy, antifibrotic therapy). The most recent pulmonary function test prior to transplantation was collected and included vital capacity (VC) (% pred.), VC (l), total lung capacity (TLC) (% pred.), TLC (l), residual volume (RV) (% pred.), RV (l), forced expiratory volume in 1 second (FEV1) (% pred.), FEV1 (l) and diffusing capacity of the lung for carbon monoxide (DLCo) (SB) (% pred.).

Skin biopsies were obtained from six patients with localized scleroderma (morphea) from the University Hospital of Cologne, Germany (Schiller et al. 2017). From each patient, tissue samples were obtained from regions, which clinically presented with sclerotic and inflammatory lesions (involved area) and also from areas with no signs of tissue fibrosis (uninvolved area) and promptly snap-frozen in liquid nitrogen.

All study participants gave written informed consent. The study was approved by the local ethics committee of the Ludwig-Maximilians University of Munich, Germany (333-10) and the University Hospital of Cologne, Germany (08144) (Schiller et al. 2017).

##### **3.1.2 Sample preparation for proteome analysis**

Approximately 100mg (wet weight) of fresh frozen tissue biopsies (human lung and skin tissue) was put to a mixture of 500 µl phosphate-buffered saline (PBS) with protease inhibitor cocktail and homogenized in an Ultraturrax homogenizer (Schiller et al. 2017). The soluble proteins were collected after centrifugation. Using the QDSP protocol (Schiller et al. 2015), proteins were obtained from the insoluble pellet by using different buffers with increasing stringency. This was

done in three steps with the following buffers: buffer 1: 150 mM NaCl, 50 mM Tris(hydroxymethyl)aminomethane (TRIS)-HCl (pH 7.5), 5% glycerol, 1% IGEPAL<sup>®</sup> CA-630 (Sigma, #I8896), 1 mM MgCl<sub>2</sub>, 1× protease inhibitors [+ ethylenediaminetetraacetic acid (EDTA)], 1% benzonase (Merck, #70746-3), 1× phosphatase inhibitors (Roche, #04906837001); buffer 2: 50 mM TRIS-HCl (pH 7.5), 5% glycerol, 150 mM NaCl, fresh protease inhibitor tablet (+EDTA), 1.0% IGEPAL<sup>®</sup> CA-630, 0.5% sodium deoxycholate, 0.1% sodium dodecyl sulfate (SDS), 1% benzonase (Merck, #70746-3); and buffer 3: 50 mM TRIS-HCl (pH 7.5), 5% glycerol, 500 mM NaCl, protease inhibitor tablet (+EDTA), 1.0% IGEPAL<sup>®</sup> CA-630, 2% sodium deoxycholate, 1% SDS, 1% benzonase (Merck, #70746-3) (Schiller et al. 2015). Separation of the insoluble pellets into soluble and insoluble material was done by resuspension in the respective detergent-containing buffers and incubation for 20 minutes (buffer 1 and 2: on ice, buffer 3: at room temperature) followed by centrifugation for 20 minutes at 16,000 g (Schiller et al. 2017). The soluble fraction from buffer 1 (NP40) was pooled with the earlier obtained PBS from the tissue homogenate. This fraction, the two fractions obtained by using buffer 2 and 3 (ionic detergent extraction) and the insoluble pellet were prepared for LC-MS/MS analysis (Schiller et al. 2017).

Using 80% acetone, precipitation of soluble proteins was carried out and digestion was performed in-solution according to a modified, formerly published protocol (Kulak et al. 2014): First, proteins were reduced in 10mM TCEP and alkylated in 50 mM chloroacetamide simultaneously in 6 M guanidinium hydrochloride (100 mM Tris-HCl pH 8.5) at 99°C for 15 min (Schiller et al. 2015). Afterwards, protein digestion was performed first with LysC (1:50 enzyme to protein ratio) in 10 mM Tris-HCl (pH 8.5) containing 2 M guanidinium hydrochloride (Gdm), 2.7 M urea, and 3% acetonitrile at 37°C for two hours. As second step, fresh LysC (enzyme to protein ratio 1:50) and trypsin (enzyme to protein ratio 1:20) in 600 mM Gdm, 800 mM urea, and 3% acetonitrile were used at 37°C overnight (Schiller et al. 2017). Since insoluble ECM proteins were found to a great extent in the insoluble pellet, an extended protocol including ultrasonication-aided digestion and substantial mechanical disintegration was used to allow an optimized in-solution digestion (Schiller et al. 2015). In order to minimize the size of the particles within the insoluble protein complex, the insoluble pellets were boiled and reduced, followed by an alkylation in 6 M Gdm for 15 minutes followed by insertion into a micro-Dounce device with 200 strokes (Schiller et al. 2017). This was followed by the above explained digestion protocol which contains two digestion steps. In addition, during both digestion steps, the material was exposed to ultrasonication (Bioruptor, Diagenode) for 15 minutes, respectively.

Purification of peptides was done with stage tips comprising a poly(styrene-divinylbenzene) copolymer modified with sulfonic acid groups material (3M, St. Paul, MN, USA) (Schiller et al. 2015). Peptides were divided in two groups for QDSP analysis by using sequential elution from the stage tips (buffer 1:150 mM NH<sub>4</sub>HCO<sub>2</sub>, 60% acetonitrile, 0.5% FA; buffer 2: 5% ammonia and 80% acetonitrile). The peptides of the four different fractions, which were in guanidinium hydrochloride (enzyme/protein ratio 1:50) and derived from LysC and trypsin proteolysis were purified on stage-tips (Schiller et al. 2015).

### 3.1.3 LC-MS/MS analysis

For MS Data acquisition, a Quadrupole/Orbitrap type Mass Spectrometer (Q-Exactive, Thermo Scientific, Waltham, MA) was used as previously described (Schiller et al. 2015, Schiller et al. 2017). Using a four-hour gradient on a 50 cm long column (75- $\mu$ m inner diameter), approximately 2  $\mu$ g of peptides were separated with ReproSil-Pur C18-AQ 1.9  $\mu$ m resin (Dr. Maisch GmbH). Columns were packed in-house beforehand. For reverse-phase chromatography an EASY-nLC 1000 ultra-high pressure system (Thermo Fisher Scientific) was linked to a Q-Exactive Mass Spectrometer (Thermo Scientific) (Schiller et al. 2017). Loading of the peptides was first performed with buffer A (0.1% (v/v) formic acid) and then elution was done with a nonlinear 240 min gradient of 5–60% buffer B (0.1% (v/v) formic acid, 80% (v/v) acetonitrile) using a flow rate of 250 nl/min (Schiller et al. 2017). Washing of the columns after each cycle was done in buffer B (95%) and for reequilibration buffer A was used. An oven with a Peltier element (Thakur et al. 2011), which was constructed in-house, enabled the constant temperature of the column at 50°C degree (Schiller et al. 2017). The SprayQC software was used to control the operational parameters immediately (Scheltema and Mann 2012). Proteomics data were collected using a shotgun proteomics method. A full scan is carried out in each cycle which gives a summary of the complete isotope pattern composition present at that specific moment (Schiller et al. 2017). In the shotgun proteomics protocol (top10 method), a full scan is followed by a maximum of ten MS/MS scans which depend on the generated data on the isotopes that are most abundant not yet sequenced in the respective cycle (Michalski et al. 2011). For the complete scan MS spectra, the value that was targeted was  $3 \times 10^6$  charges in the 300–1,650  $m/z$  range with a maximum time for injection of 20 ms and a resolution of 70,000 at  $m/z$  400 (Schiller et al. 2017). Precursors were isolated with the quadrupole at window of three Thompson (Th) (Schiller et al. 2017). Fragmentation of precursors was performed using higher-energy collisional dissociation (HCD) and a normalized collision energy of 25%. For calculation of an adequate energy, these 25% were taken as well as  $m/z$  and charge state of the precursor (Schiller et al. 2017). MS/MS scans were obtained with an ion target value of  $1 \times 10^5$  charges, a maximum time for injection of 120 ms, a fixed first mass of 100 Th and a resolution of 17,500 at  $m/z$  400 (Schiller et al. 2017). An attempt was made to avoid repetitive peptide sequencing by exclusion of the assorted peptides for 40 seconds.

### 3.1.4 Bioinformatic analysis of MS data

The MaxQuant software (version 1.4.3.20) was used to process MS raw files (Cox and Mann 2008). Using the Andromeda search engine (Cox et al. 2011), the generated peak lists were compared to the human Uniprot FASTA database (version May 2013) as well as a database for frequent contaminants including 247 entries (Schiller et al. 2015, Schiller et al. 2017). Cysteine carbamidomethylation was applied for fixed modification and hydroxylation of proline and



methionine was used for variable modifications. For peptides and proteins with a minimum length of seven amino acids, a reverse database was searched and the false discovery rate (FDR) was set at 10% (Schiller et al. 2017). The specificity of enzymes was determined as C-terminal to arginine and lysine with an allowed maximum of two missed cleavages in the search against the database (Schiller et al. 2017). For the identification of peptides, the mass deviation of the precursor was allowed to have a maximum of 4.5 ppm after time-dependent mass calibration and a fragment mass deviation of 20 ppm was allowed (Schiller et al. 2017). Label-free quantification in MaxQuant was acquired with a minimum ratio count of two. The matching between runs was performed with a retention time alignment window of 30 minute and a match time window of 1 minute (Schiller et al. 2017).

### 3.1.5 Immunohistology stainings

For immunostainings, paraffin embedded lung tissue sections from patients with ILD and controls (tissue tumor-free areas) were obtained from the BioArchive CPC-M. Immunofluorescence staining was performed as described before (Schiller et al. 2015, Strunz et al. 2020). In brief, first, slides were deparaffinized overnight in the incubator at 60°C and then rehydrated by immersion in xylol (twice, each five minutes), followed by 100% ethanol (twice, each for two minutes), 90% ethanol (three minutes), 80% ethanol (three minutes), 70% ethanol (three minutes), and finally ethanol was washed away under running distilled water (30 seconds). As next step, antigen retrieval was done by putting the slides in citrate buffer solution (pH 6.0) in a Decloaking Chamber. The chamber was heated up to 125°C for 30 seconds, then to 90°C for ten seconds followed by slow cooling to room temperature. Afterwards, TRIS buffer was used three times to rinse the slides in (Schiller et al. 2017). To avoid non-specific binding, this was followed by blocking of the slides in 5% bovine serum albumin – TRIS buffer solution for one hour. Staining with the primary antibody was performed by adding the antibody to 1% bovine serum albumin in PBS and placing the slides in a wet chamber at 4°C, overnight. The primary and secondary antibodies used are shown in Table 1. Next, slides were washed twice with PBS (ten minutes, each) which was followed by incubation with the secondary antibody at room temperature for two hours avoiding light. Afterwards, slides were washed twice with PBS (ten minutes, each), followed by the counterstaining with 4',6-diamidino-2-phenylindole (DAPI) (Sigma-Aldrich; St Louis, MO, USA) for 20 minutes. The slides were again washed twice with PBS (ten minutes, each) and covered with Fluorescence Mounting Medium (Dako, Hamburg, Germany). Immunohistology images were taken using the LSM 710 microscope (Zeiss) (Strunz et al. 2020).

<b>Primary anti-human antibody</b>	<b>Biological source</b>	<b>Firm</b>
anti-MZB1	rabbit	Sigma-Aldrich, HPA043745
anti-CD3	rabbit	Abcam, ab16669
anti-CD20	mouse	Dako, MO755
anti-CD27	rabbit	Abcam, ab49518
anti-CD38	mouse	Santa Cruz, sc-374650
anti-CD45	mouse	Sigma-Aldrich, AMAb90518
anti-CD138	mouse	Sigma, SAB4700486
anti-desmin	goat	Santa Cruz, sc-7559
anti-IgG [EPR4421]	rabbit	Abcam, ab109489
<b>Secondary antibody</b>		
anti-goat AF 488	donkey	Invitrogen, A11055
anti-mouse Alexa Fluor (AF) 647	donkey	Invitrogen, A-31571
anti-rabbit AF 568	donkey	Invitrogen, A10042

**Table 1.** Primary and secondary antibodies for immunostaining

### 3.1.6 Protein isolation

Human tissue biopsies (lung and skin) were frozen in liquid nitrogen and homogenized using a microdismembrator (Sartorius, Göttingen, Germany), as described previously (Staab-Weijnitz et al. 2015). Therefore, frozen lung pieces were put in 2 ml tubes (Eppendorf, Hamburg, Germany) together with a cryobead and placed in liquid nitrogen. The tubes were placed in the microdismembrator and after complete pulverization, the cryobeads were removed and the tissues homogenates were lysed in a Radio-Immunoprecipitation Assay buffer (50 mM TRIS HCl pH 7.4, 150 mM NaCl, 1% Triton X100, 0.5% sodium deoxycholate, 1 mM EDTA, 0.1% SDS) including a mixture of phosphatase inhibitor and protease inhibitor (both Roche; Penzberg, Germany) and incubated for 30 minutes (Knuppel et al. 2017). Next, lysates were shortly sonificated and centrifugated for 15 minutes at 13.000 runs per minute (rpm) and 4°C degree for clarification (Staab-Weijnitz et al. 2015). The supernatants were collected thereafter and concentration of the proteins was determined with a Pierce Bicinchoninacid Assay Protein Assay (Thermo Fisher Scientific; Waltham, USA).

### 3.1.7 SDS-Page and Western blot analysis

For Western blot analysis, 20 µg of proteins were used. First, to ensure denaturation, the samples were mixed with Laemmli buffer (65 mM TRIS-HCl pH 6.8, 10% glycerol, 2% SDS, 0.01% bromophenolblue, 100 mM dithiothreitol) and shaken at 99°C degree for 5 minutes (Staab-Weijnitz et al. 2015).

For electrophoretic separation of proteins, protein samples were loaded on 12% sodium dodecyl sulfate polyacrylamide gels (SDS-PAGE) together with a protein marker. Gels were prepared by the PhD student herself by mixing components listed in Table 2 which were then poured into the casting chamber (Bio-Rad, Hercules, USA). To enable the formation of a proper interface, immediately after pouring the resolving gel solution it was overlaid by isopropanol. After full polymerization of the resolving gel, the isopropanol layer was removed using MilliQ® water (Merck Millipore, Darmstadt, Germany). Then, the stacking gel (Table 2) was put into the casting chamber. After loading of the samples and marker, electrophoresis was started with 100 V voltage, which was increased gradually to a maximum of 190 V when samples had passed the stacking gel.

Component	SDS resolving gel 12%	SDS stacking gel 3.6%
	Volume per gel	Volume per gel
4x Resolving buffer	10 ml	---
4x Stacking buffer	---	2 ml
dest. water	13.2 ml	5.04 ml
30% acrylamide	16 ml	960 $\mu$ l
TEMED	60 $\mu$ l	24 $\mu$ l
10% Ammonium persulfate	400 $\mu$ l	100 $\mu$ l

**Table 2.** Composition of 12% SDS polyacrylamide gels

After complete electrophoresis, gels were transferred to polyvinylidene difluoride membranes via immunoblotting. Polyvinylidene difluoride membranes were first activated using methanol and immunoblotting was performed with 360 mA for 90 minutes.

To avoid nonspecific binding, 5% milk in tris-buffered saline-tween (0.1% Tween 20, tris-buffered saline) was used for five minutes to block the membranes which were afterwards incubated in Roti@Block (Carl Roth, Karlsruhe, Germany) for one hour (Staab-Weijnitz et al. 2015). Next, membranes were incubated overnight at 4°C degree with the primary antibody in Roti@Block. Anti-human primary antibodies were used as described in Table 3. Membranes were washed three times for ten minutes with tris-buffered saline-tween and afterwards incubated with anti-rabbit IgG secondary antibody for one hour at room temperature. Finally, tris-buffered saline-tween was again used to wash the blots three times for ten minutes and membranes were then developed with an enhanced chemiluminescence system (Thermo Fisher Scientific, Waltham, MA, USA) and analysis was done with exposing to film (Staab-Weijnitz et al. 2015). For quantification, the ChemiDocXRS+ imaging system (Bio-Rad, Munich, Germany) and the software Image Lab (version 3.0, Bio-Rad, Hercules, CA) was used (Staab-Weijnitz et al. 2015).

<b>Primary anti-human antibody</b>	<b>Biological source</b>	<b>Dilution</b>	<b>Firm</b>
anti-MZB1	rabbit	1:500	Sigma-Aldrich, HPA043745
anti-IgG1	rabbit	1:1000	Abcam, EPR4417
anti-IgG2	rabbit	1:1000	Abcam, EPR4419
anti-IgG3	rabbit	1:1000	Abcam, EPR4419
anti-IgG4	rabbit	1:1000	Abcam, EP4420
<b>Secondary antibody</b>			
anti-rabbit IgG monoclonal (EPR25A)	goat	1:10.000	Abcam, ab199091

**Table 3.** Primary and secondary antibodies for Western blot

### 3.1.8 Statistics

GraphPad Prism software was used for correlation analysis, *t* test statistics and Box plots. The Perseus software package was used to perform statistics and bioinformatics like normalization, pattern recognition, cross-omics comparisons and multiple-hypothesis testing corrections (Tyanova et al. 2016, Schiller et al. 2017). To compare the generated data to a previously published data, microarray data of an independent cohort from the U.S. were used (Gene Expression Omnibus dataset GSE47460) (Bauer et al. 2015). The complete data set is accessible online from the Gene Expression Omnibus with the number GSE47460 (<http://www.ncbi.nlm.nih.gov/geo>) and also on the Lung Tissue Research Consortium website (<http://www.ltrcpublic.com>) (Schiller et al. 2017).

## 3.2 Material and Methods for autoantibody discovery project

### 3.2.1 Study cohorts and clinical data

Human lung tissue material from patients who underwent lung transplantation at the University Hospital of the Ludwig-Maximilians University Munich, was obtained from the BioArchive CPC-M (Leuschner et al. 2021). These tissue samples included both donor tissue (controls) and ILD recipient tissue (patients). Apart from the underlying disease there were no further inclusion criteria. For cohort 1 (Munich) plasma was collected from patients with IPF or CTD-ILD from the in- and out-patient unit of the University Hospital of the Ludwig-Maximilians University Munich via the BioArchive CPC-M (Leuschner et al. 2021). The acquisition of plasma samples was done during routine visits in the ILD out-patient clinic as well as in the in-patient unit while patients underwent evaluation for lung transplantation. Healthy volunteers who were age-matched to the Munich cohort were recruited for control plasma samples and specimen were obtained from the

BioArchive CPC-M. Inclusion criteria for healthy controls were the absence of signs of infection and/or respiratory symptoms (Leuschner et al. 2021). The study was performed and approved in accordance with the local ethics committee of the Ludwig-Maximilian University Munich (approval number 333-10 and 382-10). As part of a cooperation of the German Center for Lung Research (Deutsches Zentrum für Lungenforschung; DZL), serum samples of the study cohort 2 (Hannover) were received from patients with IPF and CTD-ILD seen at the in- and out-patient unit of the University Hospital of the Medizinische Hochschule Hannover (Leuschner et al. 2021). The local ethics committee of the Medizinische Hochschule Hannover approved the study (approval number 2923-2015). All patients/healthy controls were over the age of 18 years and all gave written informed consent to the DZL broad-consent form (Leuschner et al. 2021).

The diagnosis of IPF was established and confirmed in accordance to the official ATS/ERS/JRS/ALAT statement on the diagnosis and management of IPF (Raghu et al.; 2011). This was done either by corresponding findings on high resolution computed tomography, or, if available, a combination of high resolution computed tomography and histopathological findings from surgical lung biopsies (Raghu et al. 2011). A diagnosis of CTD-ILD could be made in patients who had an ILD on imaging and a known diagnosis of an underlying rheumatoid arthritis, SSc, sjogren syndrome polyarthritis or undifferentiated CTD (Leuschner et al. 2021).

Clinical parameters were collected as baseline values at the timepoint when the blood sample was taken. Data comprised information about demographics like gender and age, smoking status, and lung function parameters including forced vital capacity (% pred.) (FVC<sub>%pred.</sub>), FVC (l), and DLCo (SB) (% pred.)). Retrospectively, time to death or lung transplantation (transplant-free survival) after blood sampling was analyzed (Leuschner et al. 2021).

### **3.2.1 Human sample preparation**

For plasma sampling venous blood was freshly collected in tubes coated with ethylenediaminetetraacetate (EDTA) (Sarstedt, Nümbrecht, Germany). Next, samples were centrifugated and supernatant plasma was taken and instantly stored at -80°C degree (BioArchive CPC-M) (Leuschner et al. 2021). The Medizinische Hochschule Hannover provided frozen blood samples as serum.

For the protein extraction of lung tissue explants lung resections of 41 patients with ILD and twelve healthy donor were used (Leuschner et al. 2021). Immediately after lung transplantation the lung tissues were divided into portions of 0.5cm<sup>3</sup>. Liquid nitrogen was used for snap freezing of the pieces and storage was done at -80°C degree in the BioArchive CPC-M in a standardized way (Leuschner et al. 2021). Protein extraction was carried out as already reported in detail in chapter 3.1.6. For the native lung extract pool, all samples were equally pooled.

### 3.2.2 Differential Antigen Capture (DAC) assay

The Differential Antigen Capture (DAC) assay works with the principle of immunoprecipitation, for which specific Protein G agarose beads (Pierce, Thermo Fisher, 20399) were used (Leuschner et al. 2021). These beads can bind 11-15mg human IgG per ml of settled resin (50% of slurry). In comparison to Protein A, these recombinant protein G beads have no affinity for albumin and do almost not bind IgA (according to the manufacturer's information). For every patient, immunoprecipitation was accomplished in triplicates, respectively (Leuschner et al. 2021).

First, plasma or serum samples were gently thawed on ice. As mentioned above, blood samples from Munich were all plasma and blood samples from Hannover were all serum. After thawing, samples were centrifuged at 16.000 g for five minutes at 4°C degree. 15µl of supernatants were mixed with 585µl wash buffer (0.1% IPGAL, 5% Glycerol, 50 mM TRIS pH 7.4, 150 mM NaCl, Roche EDTA free protease inhibitor) representing a pool for triplicate measurements per patient/healthy control (Leuschner et al. 2021). Next, 96 well-filter plates (MultiScreenHTS-BV, 1.2 µm, Millipore) were filled with 20µl of Protein G agarose beads and centrifuged with 200µl wash buffer at 100g for one minute (Leuschner et al. 2021). Afterwards, a mixture of 200µl of plasma or serum and wash buffer (5µl of plasma/serum supernatant and 195µl of wash buffer per well) was placed on beads and incubated at 900 rpm for one hour at room temperature on a shaker (Leuschner et al. 2021). Filter plates were now centrifuged with 100g for one minute at room temperature and three times washed with 200µl wash buffer with 100g for one minute. In the meantime, the native lung tissue extract pool consisting of explants from 41 ILD patients and lung resections from twelve healthy donors was thawed on ice. As a next step, wash buffer was added to this native lung tissue extract pool resulting in a protein concentration of 150µg in 200µl volume per well (Leuschner et al. 2021). The respective 200µl antigen/wash buffer mixture was put on IgG-loaded beads and incubated gently shaking for one hour at room temperature. After this step, no protease inhibitors were included in buffers anymore. Finally, several washing steps were carried out in which the plates were first centrifuged three times at 100g for one minute with wash buffer (without protease inhibitor) followed by three washing steps with PBS (at 100g for one minute) (Leuschner et al. 2021).

### 3.2.3 Mass spectrometry (MS)

In preparation for MS, an on-beat digest was performed with the samples derived from immunoprecipitation. Beads were incubated at 600 rpm for one hour at room temperature with 50 µl 8 M Urea Hepes pH8, 0.5 µg LysC (Wako, #129-02541, 10 AU, in ammonium bicarbonate), 10 mM dithiothreitol (Leuschner et al. 2021). This was followed by an incubation with 0.5µg trypsin (Trypsin from porcine pancreas: Sigma-Aldrich, T6567) in 200 µl 50 mM ammonium bicarbonate (= 50mM NH<sub>4</sub>HCO<sub>3</sub>) with 55 mM chloroacetamide at 600 rpm for one hour at room temperature (Leuschner et al. 2021). Afterwards, plates were centrifuged at 100g for one minute and clean 96

well plates were used to collect the digested peptides which flowed through the filters (Leuschner et al. 2021). Next, 50µl quenching buffer [2M Urea, 50 mM Thiourea, 2mM Hepes in 50 mM ammonium bicarbonate] was used to wash filter plates at 100g for one minute (Leuschner et al. 2021). Overnight, digestion was done on a shaker at 37°C degree with 600 rpm. Thereafter, digestion was discontinued by adding 1% trifluoroacetic acid (TFA) to the samples.

For purification of peptides, stage tipping was performed with poly(styrene-divinylbenzene) copolymer modified with sulfonic acid groups, as described (Schiller et al. 2015). First, activation of stage tips was done with 100 µl acetonitrile. For equilibration, 100 µl 30%MeOH, 1% TFA ran over the stage tips followed by 200 µl 0.2% TFA (Leuschner et al. 2021). Peptide samples (in 1 % TFA) were placed on stage tips which were then washed twice with 100µl isopropanol in 1% TFA, followed by a wash step with 200 µl 0.2% TFA. At last, elution of the samples was done with 60µl of 5% Ammonia and 80% acetonitrile (Leuschner et al. 2021). Finally, samples were evaporated at 30°C degree (Eppendorf Evaporater Plus) and the dissolving of the final eluates was done in 6 µl buffer A\* under sonication. Samples were then put into the -20°C degree freezer until MS-analysis were performed.

For MS-analysis, one hour gradients were used to separate circa 1 µg of peptides on a column with an inner diameter of 75 µm and a length of 50 cm with ReproSil-Pur C18-AQ 1.9 µm resin (by Dr. Maisch GmbH) (Leuschner et al. 2021). Columns were packed in-house. An EASY-nLC 1000 ultra-high pressure system (Thermo Fisher Scientific) connected to a Q-Exactive Mass Spectrometer (Thermo Scientific) was applied for reverse-phase chromatography (Leuschner et al. 2021). First, buffer A (0.1% (v/v) formic acid) was used to load the peptides. Using a flow rate of 250 nl/min, this was followed by elution with a nonlinear 240 min gradient of 5–60% buffer B (0.1% (v/v) formic acid, 80% (v/v) acetonitrile) (Leuschner et al. 2021). 95% buffer B was applied to wash the columns and buffer A was used for re-equilibration after each gradient (Leuschner et al. 2021). An oven (designed in house) with a Peltier element (Thakur et al. 2011) was used to keep the temperature of the column at 50°C degree. Real-time monitoring of the operational parameters was done with the quality monitoring system SprayQC software (Scheltema and Mann 2012). Proteomics data were collected using a shotgun proteomics method, described in detail in chapter 3.1.3 (top10 method) (Michalski et al. 2011, Schiller et al. 2017). The value that was targeted for the complete scan MS spectra was  $3 \times 10^6$  charges in the 300–1,650  $m/z$  range with a maximum injection time of 20 ms and a resolution of 70,000 at  $m/z$  400 (Schiller et al. 2017, Leuschner et al. 2021). The MaxQuant software (Cox and Mann 2008) was used to process the acquired mass spectra raw files enabling for label free protein quantification (Tyanova et al. 2016, Leuschner et al. 2021).

### 3.2.4 Statistics and bioinformatic analysis

Clinical data were analyzed using *t* test statistics, ANOVA tests, Fisher's exact test, Cox multivariate regression analysis and Kaplan-Meier survival analysis with the combined endpoint consisting of death and lung transplantation. Either the GraphPad Prism 5 software (GraphPad Software, San Diego, California) or SPSS version 25.0 (IBM SPSS, Armonk, NY) was used. For the identification of the most commonly identified autoantigens a sum score of Student's *t* test statistics of significantly enriched proteins (FDR<10%) was used (Leuschner et al. 2021). Only antigens were included in further analysis which were (1) identified in a minimum of three patients in one of the four study groups and (2) the sum score was >4 (arbitrary cut-off) (Leuschner et al. 2021). All other bioinformatical and statistical operations were run with the Perseus software package (version 1.5.3.0 and 1.6.1.1.) (Tyanova et al. 2016), including normalization, principal component analysis, hierarchical clustering, annotation enrichment analysis and data integration.



## 4. Results

### 4.1 Characterization of the human proteome in lung and skin fibrosis

Most of the work presented in this chapter has been published as parts of a manuscript in the peer-reviewed scientific journal *American Journal of Respiratory and Critical Care Medicine* (AJRCCM) (Schiller et al. 2017). The AJRCCM is one of the leading journals in the field of pathophysiology and treatment of disease affecting the respiratory system and critically ill patients and publishes data on human biology and disease but also animal and in vitro studies (impact factor 2017: 15.239). The manuscript file is accessible through the AJRCCM website (<https://www.atsjournals.org/journal/ajrccm>) or directly via the digital object identifier (doi): <https://www.atsjournals.org/doi/10.1164/rccm.201611-2263OC>.

The PhD student, as third author of this manuscript, performed all Western Blot analysis and organized and analyzed all clinical and patient data. MS analysis (Figure 9) and writing of the published manuscript was performed by Dr. Herbert Schiller (first author). Dr. Christoph Mayr (second author) performed immunostainings (Figure 10 – Figure 14).

Data on IgG subclasses were not part of the publication and were all performed by the PhD student herself.

#### 4.1.1 Introduction

Fibrotic diseases, including pulmonary fibrosis, are one of the major challenges for health care providers in the developed world, as they account for over 45% of deaths, both directly and indirectly (Cox and Erler 2011). While a dynamic remodeling and reorganization of the ECM is crucial for a regular organ development, wound healing and homeostasis, the uncontrolled or excessive replacement of normal tissue by ECM leads to scarring and fibrosis. Fibrosis can affect different organs including over 200 different types of lung fibrosis in humans (Travis et al. 2013).

While several risk factors have been identified, yet, origin and cause of many fibrotic diseases are still unknown leading to the terminology “idiopathic” or “cryptogenic” (Thannickal et al. 2014). Reasons for the genesis of idiopathic fibrosis which are currently taken into consideration comprise persistent inflammation or injury, impaired repair or regeneration mechanisms, genetic susceptibility, aging, environment and autoimmunity (Thannickal et al. 2014). Autoimmune diseases have been increasingly recognized in the past decades especially in Westernized societies (Lerner and Matthias 2015). CTD-ILD are an excellent example for autoimmune-

mediated fibrosis (Vij and Streck 2013). Although the diagnosis of IPF, as an idiopathic interstitial pneumonia, requires the exclusion of other reasons for ILD such as CTD-ILD (Raghu et al. 2018), autoimmune processes have also been discussed and circulating immune complexes have been described in the past (Dreisin et al. 1978). Still, evidence for that theory is limited.

Besides, impaired regeneration and repair mechanisms which can consequentially lead to fibrosis are commonly associated with the dysregulation of signaling cascades like Wnt, bone morphogenetic protein/TGF- $\beta$ , or sonic hedgehog signaling pathways (Konigshoff et al. 2009, Hogan et al. 2014, Lee et al. 2014, Peng et al. 2015). Secreted morphogens of these pathways can interact with the ECM and impact its function in affecting tissue repair in rodent models (Martino et al. 2014). The structure and function of ECM is therefore of growing interest in translational research also because new technologies open up the possibility of getting a better insight into the field (Hynes 2014). The *in vivo* composition of the ECM proteome, the so called matrisome, in specific tissues and disease including architecture as well as dynamic associations and secreted proteins is still a poorly explored area. Recently, the QDSP method was introduced allowing a profound analysis of the proteome and matrisome in different tissues (Schiller et al. 2015). This QDSP protocol can be used to analyze the proteomes from different types of fibrosis and identify common and disease specific molecular modifications.

The following sections will summarize the results of the herein conducted investigations and analysis. Using mass spectrometry and the QDSP method human lung and skin fibrosis tissue samples were characterized. Localized scleroderma (morphea), which is limited to the skin, is an autoimmune-mediated disease in which chronic inflammatory processes cause the formation of fibrotic plaques (Kreuter et al. 2016). Using localized scleroderma as model for research on fibrosis has numerous advantages, as affected and unaffected areas of the skin can be examined in the same patient. Unexpectedly, plasma B cells positive for the marginal zone B and B1 cell specific protein (MZB1) were detected in large amounts in pulmonary and skin fibrosis. To assess reproducibility of the proteome data immunostaining of human ILD was carried out verifying the increased presence of MZB1 positive plasma B cells in ILD tissue including the coexpression with tissue IgG. To quantify the findings on MZB1, Western blot analysis were performed in a larger cohort of patients with ILD. Furthermore, clinical data were integrated and identified associations between MZB1 levels and lung function parameters.

In addition, given the correlation between MZB1 and tissue IgG in ILD, IgG subclasses distribution was analyzed. Immunoglobulins are produced and secreted by plasma B cells. IgG represents the most common class of antibodies in human serum and can be further subdivided in four subclasses [IgG1 (approx. 61%), IgG2 (approx. 32%), IgG3 (approx. 4%) and IgG4 (approx. 3%)] (Vidarsson et al. 2014). Although over 90% of all IgGs are identical concerning their amino acids, the activation, binding of the antigen and formation of immune complexes differs individually between the subclasses (Vidarsson et al. 2014).

#### 4.1.2 Presence of marginal zone B and B1 cell specific protein (MZB1)-positive tissue resident plasma B cells in lung and skin fibrosis

MS was used to characterize human lung and skin fibrosis tissue biopsies. Human lung tissue resections from three healthy donors and explant tissue from eleven patients with end-stage ILD were derived for proteomic analysis. Further, six patients with localized scleroderma were willing to donate skin biopsies with one biopsy from an involved area and one biopsy from a distant, uninvolved area, respectively (three females, three males; mean age 66 years). Table 4 shows the demographics and clinical characteristics of patients with ILD included in the MS analysis.

##### Patient characteristics

Characteristics	IPF n=2	HP n=3	COP n=1	NSIP n=1	Unclassifiable ILD n=4	All n=11
Male gender, no. (%)	1 (50,0)	1 (33,3)	0 (0)	1 (100,0)	3 (75,0)	8 (72,7)
Age, years, $\pm$ SD	66,0 $\pm$ 4,2	47,3 $\pm$ 13,3	48,0	84,0	54,0 $\pm$ 4,2	58 $\pm$ 13,1
<b>PFT</b>						
VC, l (% pred)	3,41 $\pm$ 0,33 (97,8 $\pm$ 26,6)	1,06 $\pm$ 0,07 (31,7 $\pm$ 4,04)	3,2 (109)	2,32 (69,4)	3,27 $\pm$ 0,62 (81,1 $\pm$ 10,7)	2,72 $\pm$ 1,09 (76,1 $\pm$ 29,9)
TLC, l (% pred)	5,61 $\pm$ 0,70 (95,1 $\pm$ 36,8)	2,23 $\pm$ 0,09 (43,0 $\pm$ 5,2)	4,91 (105,9)	4,25 (66,2)	5,46 $\pm$ 0,28 (86,4 $\pm$ 13,4)	4,62 $\pm$ 1,5 (79,0 $\pm$ 27,1)
RV, l (% pred)	2,20 $\pm$ 1,01 (99,9 $\pm$ 59,2)	1,17 $\pm$ 0,16 (31,7 $\pm$ 27,1)	1,71 (104,9)	1,94 (68,6)	2,09 $\pm$ 0,37 (100,5 $\pm$ 27,0)	1,87 $\pm$ 0,58 (82,3 $\pm$ 41,7)
FEV1, l (% pred)	2,72 $\pm$ 0,73 (97,1 $\pm$ 5,7)	0,93 $\pm$ 0,01 (33,7 $\pm$ 5,77)	2,86 (117,2)	1,79 (75,5)	2,73 $\pm$ 0,59 (86,3 $\pm$ 11,8)	2,25 $\pm$ 0,93 (79,0 $\pm$ 29,8)
DLCO, % pred.	32,8 $\pm$ 6,9	19,0 $\pm$ 5,2	67,9	46,7	56,8 $\pm$ 18,0	40,8 $\pm$ 21,0
pO2 at rest, mmHg	61,25 $\pm$ 22,98	46,67 $\pm$ 9,81	68,7	73,4	75,25 $\pm$ 12,39	63,70 $\pm$ 16,48
<b>Therapy *</b>						
LTOT, no. (%)	1 (50,0)	3 (100,0)	x	x	x	4/5 (80,0)
Steroids, no. (%)	1 (50,0)	3 (100,0)	x	x	x	4/5 (80,0)
Immunosuppressant, no. (%)	1 (50,0)	1 (33,3)	x	x	x	2/5 (40,0)
Antifibrotic drugs, no. (%)	0 (0)	0 (0)	x	x	x	0/5 (0)

**Table 4.** Demographics and clinical characteristics of patients with lung fibrosis included in the proteomic study. Abbreviations: idiopathic pulmonary fibrosis (IPF); hypersensitivity pneumonitis (HP); cryptogenic organizing pneumonia (COP); nonspecific interstitial pneumonia (NSIP); pulmonary function test (PFT); vital capacity (VC); total lung capacity (TLC); residual volume (RV); forced expiratory volume in 1 second (FEV1); diffusing capacity of the lung for carbon monoxide (DLCo); long term oxygen therapy (LTOT). Table taken and legend adapted from (Schiller et al. 2017)

To confirm fibrosis in the respective tissue segments, lung and skin biopsies were first analyzed histologically and only tissue where fibrosis was present was used for MS analysis. In ILD biopsies, 7907 proteins were identified and in morphea 5826 proteins. To identify similarities in the proteome of lung and skin fibrosis all four fractions of the QDSP analysis of both datasets were matched and the fold changes in both disease biopsies were compared. A two-dimensional annotation enrichment analysis identified ECM genes, N-glycan biosynthesis, complement activation, and plasma lipoprotein particles as joint components in lung and skin fibrosis (Figure 9 A). In addition, a significant increment in the number of antibodies was found in ILD as well as localized scleroderma biopsies (Figure 9 A and 9 B). While the analysis of protein outliers with highest fold changes in ILD and localized scleroderma identified several disease specific proteins, the marginal zone B and B1 cell specific protein (MZB1) was the most significant upregulated protein in both diseases (Figure 9 B).

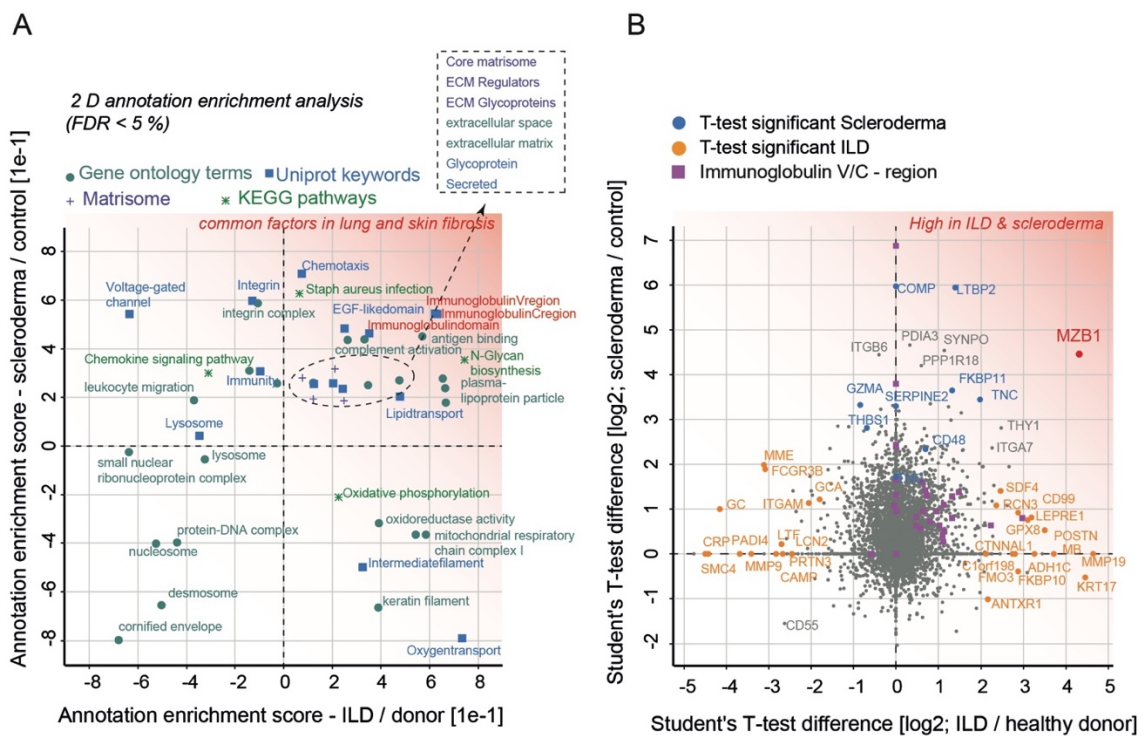


**Figure 9.** Common and disease specific genes enriched in lung and skin fibrosis. (A) A scatterplot displays the annotation enrichment scores of gene groups for patients with interstitial lung disease (ILD) (abscissa) and localized scleroderma (ordinate) in comparison to healthy controls, respectively. Shared gene categories are found in the upper right quadrant, including immunoglobulins (red text). (B) Student's t test differences of proteins in ILD (abscissa) and skin fibrosis (ordinate) in comparison to healthy controls are plotted against each other. While there were proteins enriched exclusively in ILD (orange) or scleroderma (blue), the marginal zone B and B1 cell specific protein (MZB1) was shared between both types of fibrosis. Again, in human lung and skin fibrosis several immunoglobulins were detected (purple squares). Abbreviations: false discovery rate (FDR); Kyoto Encyclopedia of Genes and Genomes. Figure and legend taken and adapted from (Schiller et al. 2017)

MZB1 is localized in the endoplasmic reticulum (ER) and mainly enriched in certain peripheral B cell subsets, which are characterized by their decreased  $\text{Ca}^{2+}$  mobilization, increased integrin activation and fast antibody secretion (Flach et al. 2010). To validate the findings on MZB1, immunostaining of human ILD (Figure 10) was performed. MZB1 was detected in cytoplasm-rich cells, which were rarely detected in controls but more often seen in areas of fibrotic lung tissue, particularly in perivascular regions. Coimmunostaining of different lineage markers identified MZB1-positive cells as CD3 negative (T-lymphocyte lineage marker; Figure 11 A), CD20 negative (B cell lineage marker; Figure 11 B) and CD45 negative (leukocyte lineage marker; Figure 12 A). MZB1-positive cells were unambiguously identified as terminally differentiated plasma B cells in ILD tissue by their co-expression with CD38 (Figure 10 C), CD138 (Figure 12 B) and CD27 (Figure 13 A) (Nutt et al. 2015). In line with the finding that MZB1 is a marker for tissue-resident, antibody-producing plasma B cells, MZB1-positive cells comprised a positive co-staining with human IgG (Figure 13 B). MZB1-positive cells were also found in scleroderma tissue (Figure 14).

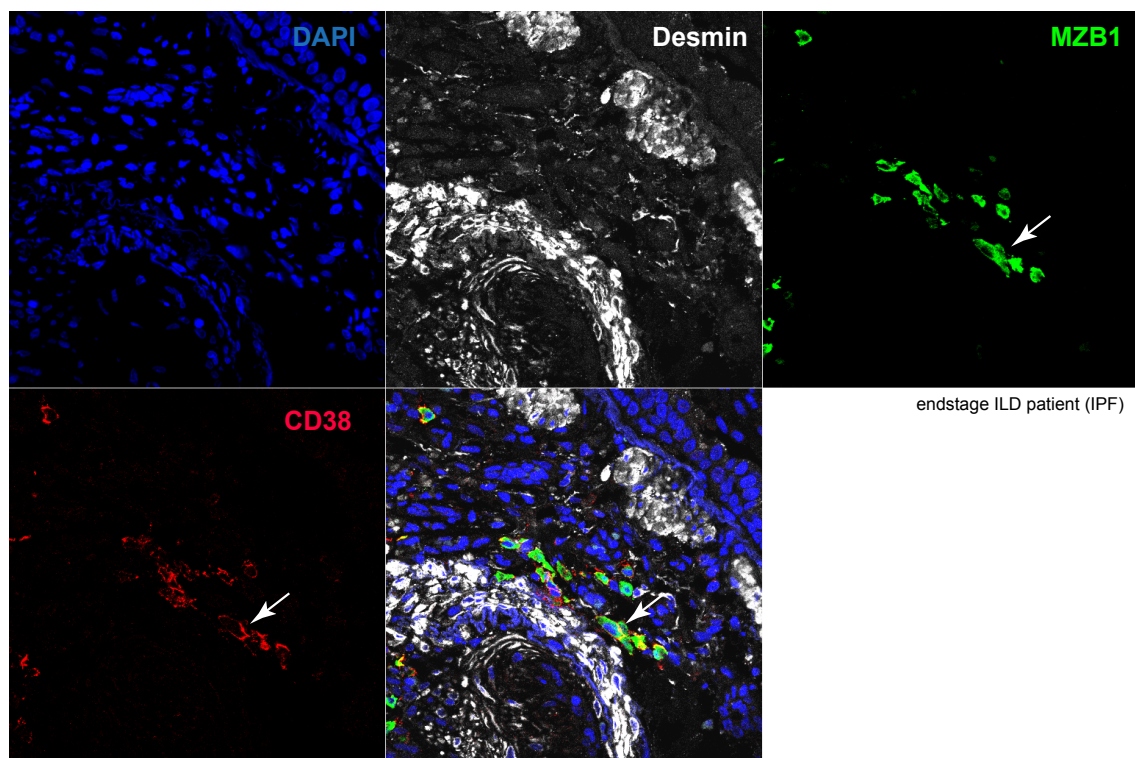


**Figure 10.** Detection of marginal zone B- and B1-cell-specific protein (MZB1) in tissue-resident cells. Immunostainings show distribution of MZB1 in human lung fibrosis of patients with interstitial lung disease (ILD). The co-localization with CD38 characterizes MZB1-positive cells as terminally differentiated plasma B cells (indicated by arrows). Staining with 4',6-diamidino-2-phenylindole (DAPI) indicates nuclei and desmin was used to identify vascular smooth muscle cells and a few mesenchymal cells. Abbreviation: idiopathic pulmonary fibrosis (IPF). Figure and legend taken and adapted from (Schiller et al. 2017)

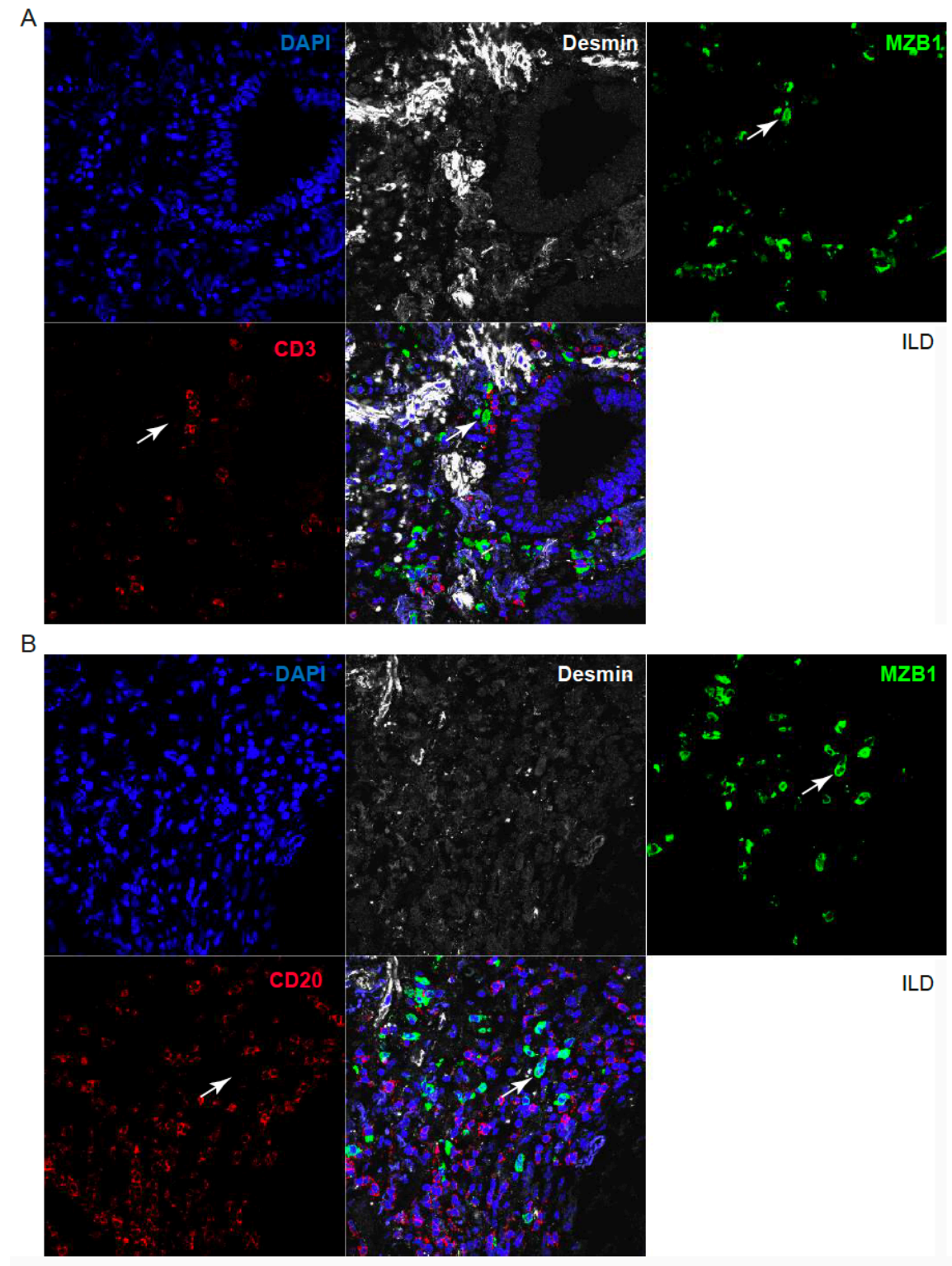


**Figure 11.** Marginal zone B- and B1-cell-specific protein (MZB1) positive cells do not express CD3 or CD20 in lung fibrosis. **(A)** CD3 is a lineage marker for T lymphocytes. **(B)** CD20 is a B cell lineage marker. **(A, B)** Staining with 4',6-diamidino-2-phenylindole (DAPI) indicates nuclei and desmin was used to identify vascular smooth muscle cells and a few mesenchymal cells. MZB1 positive cells are displayed by arrows. Figure taken and legend adapted from (Schiller et al. 2017)

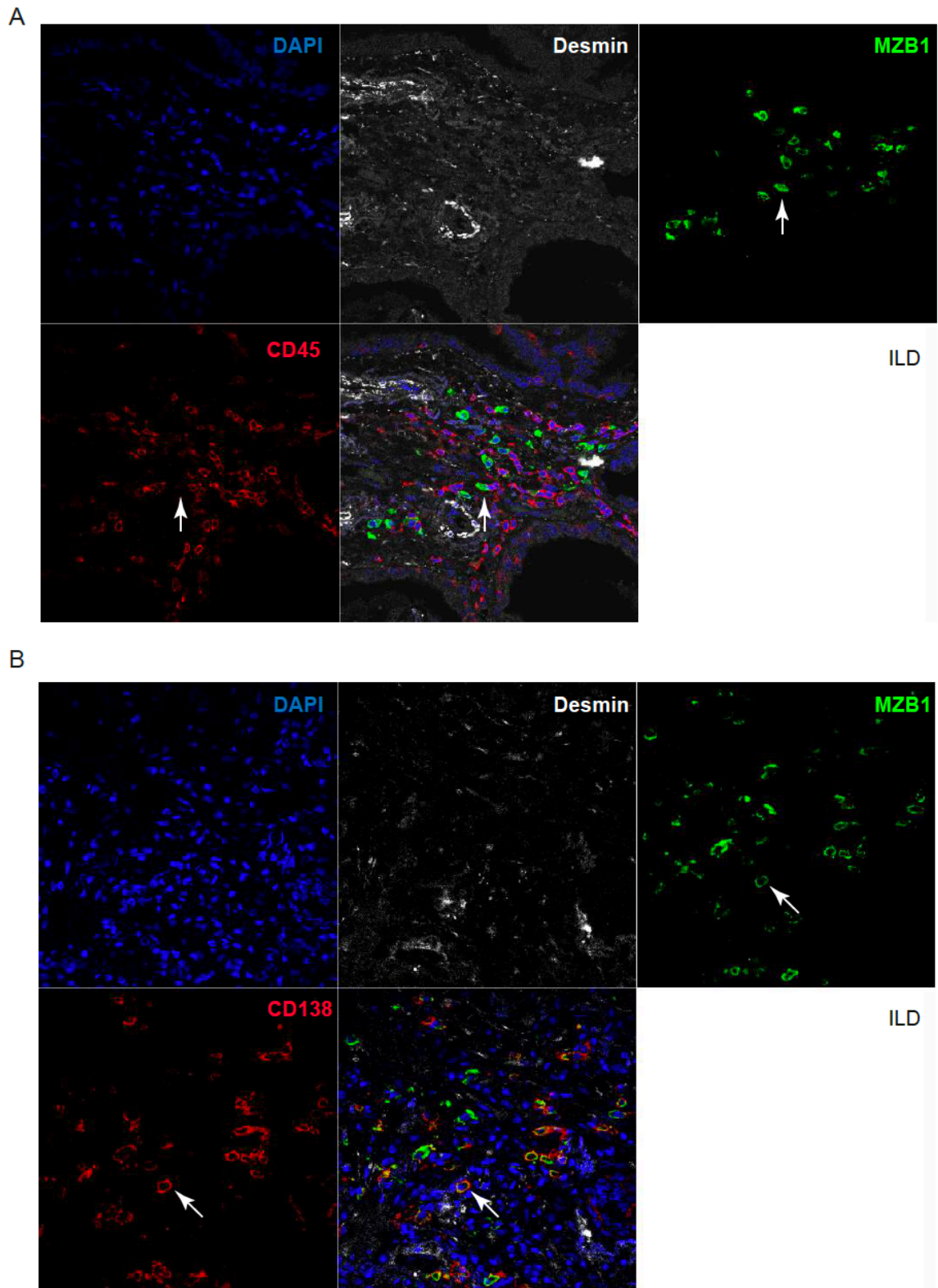


**Figure 12.** Marginal zone B- and B1-cell-specific protein (MZB1) positive do not express CD45 but CD138 in human lung fibrosis. **(A)** CD45 is a leukocyte lineage marker. **(B)** CD138, also known as syndecan 1, is a plasma B cell marker. **(A, B)** Staining with 4',6-diamidino-2-phenylindole (DAPI) indicates nuclei and desmin was used to identify vascular smooth muscle cells and a few mesenchymal cells. MZB1 positive cells and MZB1/CD138 co-expressing cells are displayed by arrows. Figure and legend taken from (Schiller et al. 2017)

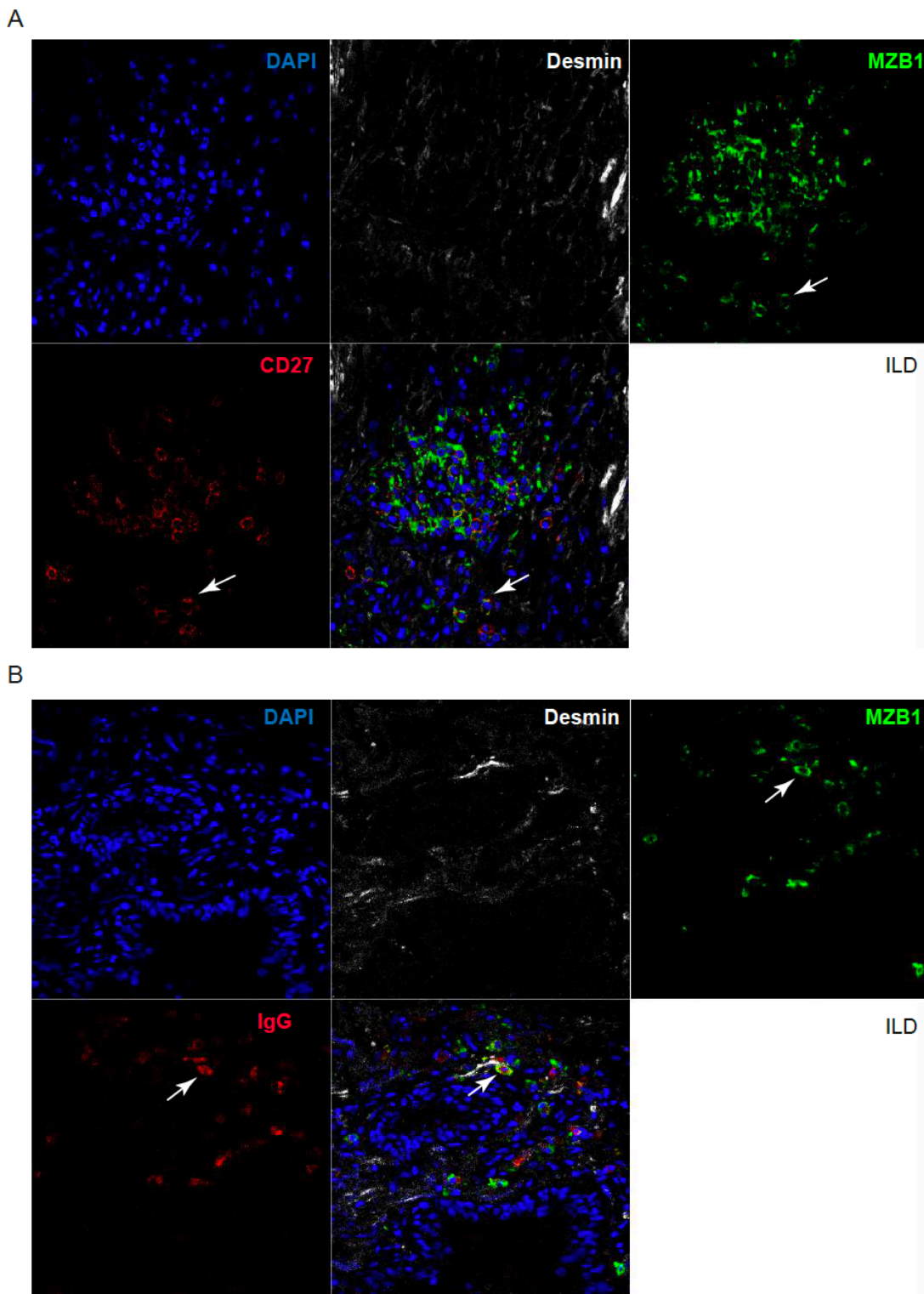


**Figure 13.** Marginal zone B- and B1-cell-specific protein (MZB1) positive cells co-express CD27 and immunoglobulin G (IgG) in human lung fibrosis. **(A)** CD27 is a plasma B cell marker. **(B)** IgGs are produced in plasma B cells **(A, B)** Staining with 4',6-diamidino-2-phenylindole (DAPI) indicates nuclei and desmin was used to identify vascular smooth muscle cells and a few mesenchymal cells. MZB1 positive cells, MZB1/CD27 double positive and MZB1/IgG co-expressing cells are displayed by arrows. Figure and legend taken from (Schiller et al. 2017)



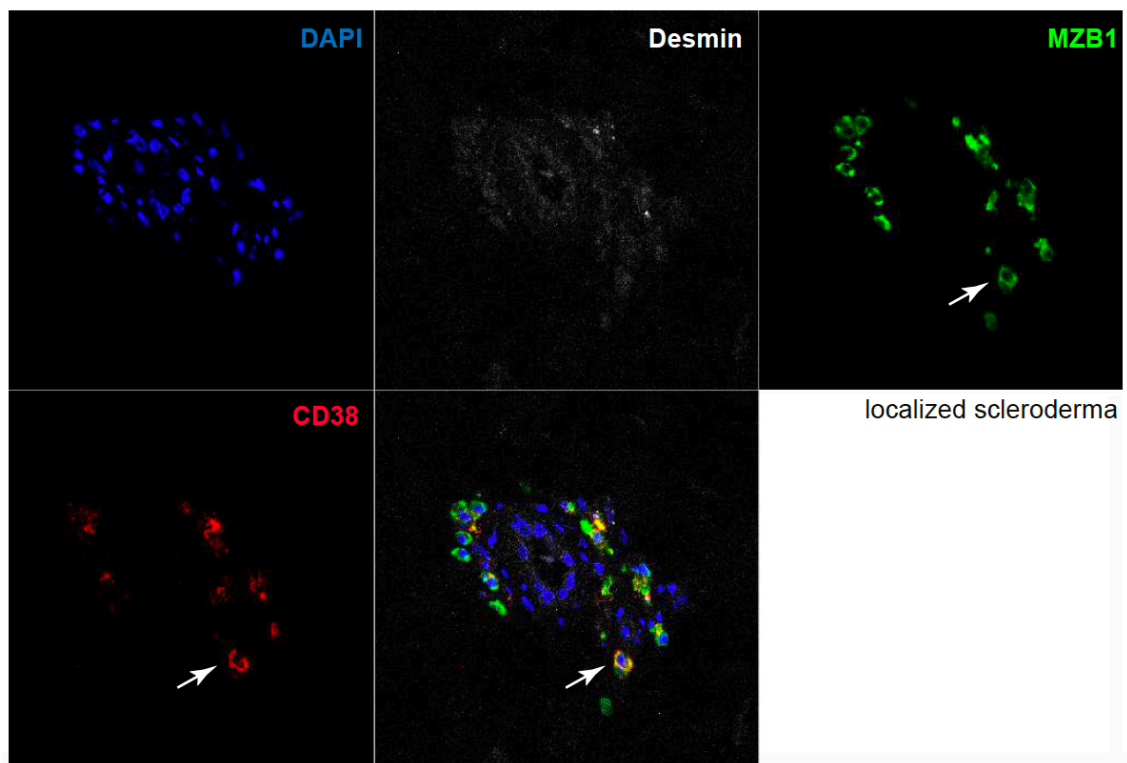


**Figure 14.** Marginal zone B- and B1-cell-specific protein (MZB1) positive do also express CD38 in skin fibrosis of localized scleroderma. CD38 is a surface marker of plasma B cells. Staining with 4',6-diamidino-2-phenylindole (DAPI) indicates nuclei and desmin was used to identify vascular smooth muscle cells and a few mesenchymal cells. MZB1 positive cells and MZB1/CD38 co-expressing cells are displayed by arrows. Figure taken and legend adapted from (Schiller et al. 2017)

In summary, proteomic comparison of ILD and scleroderma revealed significantly enriched antibodies in both diseases and MZB1 as the most significant upregulated protein in both diseases. MZB1+ cells were identified as CD38+/CD138+/CD27+/CD45-/CD20- plasma B cells in pulmonary and skin fibrosis tissue.

#### 4.1.3 Correlation of marginal zone B and B1 cell specific protein (MZB1) with state of diseases and tissue immunoglobulin G (IgG)

To validate the findings on MZB1 in a larger and independent cohort, Western blot analysis was performed with seven healthy donor controls and 34 additional end-stage ILD tissues (IPF: n=14, HP: n=7; CTD-ILD: n=2; NSIP: n=3; unclassifiable ILD: n=12; other ILD: n=3). Demographics and clinical characteristics are shown in Table 5. Western blot analysis showed that compared to healthy donor controls MZB1 was significantly increased in patients with ILD, including IPF and non-IPF ILD (IPF: p=0.0004; non-IPF: p=0.0005; Figure 15 A and 15 B). Similarly, MZB1 was also

found more often in tissue areas with skin fibrosis in comparison to uninvolved tissue in patients with localized scleroderma (n=3; Figure 15 C).

Characteristics	IPF n=14	HP n=7	CTD-ILD n=2	NSIP n=3	Unclassifiable ILD n=12	Other ILD n=3	All n=41
Male gender, no. (%)	12 (85,7)	3 (42,9)	2 (100)	2 (66,7)	7 (58,3)	2 (66,7)	28 (58,3)
Age, years, $\pm$ SD	56,1 $\pm$ 10,0	53,7 $\pm$ 10,5	42,5 $\pm$ 4,9	56,3 $\pm$ 8,1	51,0 $\pm$ 7,0	55,1 $\pm$ 6,9	54,4 $\pm$ 8,8
<b>PFT</b>							
VC, l (% pred)	1,8 $\pm$ 0,2 (38,0 $\pm$ 2,8)	1,5 $\pm$ 0,7 (42,3 $\pm$ 22,5)	2,1 $\pm$ 0,01 (39,5 $\pm$ 9,2)	1,8 $\pm$ 0,2 (38,0 $\pm$ 2,8)	1,5 $\pm$ 0,4 (39,8 $\pm$ 9,3)	1,9 $\pm$ 1,3 (43,7 $\pm$ 28,6)	1,7 $\pm$ 0,6 (40,6 $\pm$ 15,0)
TLC, l (% pred)	3,11 $\pm$ 0,5 (41,5 $\pm$ 0,7)	3,2 $\pm$ 1,2 (54,8 $\pm$ 20,7)	3,1 $\pm$ 0,5 (41,5 $\pm$ 0,7)	2,67 (36) *	2,7 $\pm$ 0,5 (45,7 $\pm$ 6,0)	4,5 $\pm$ 1,7 (63,0 $\pm$ 28,3)	3,2 $\pm$ 1,0 (49,2 $\pm$ 14,2)
RV, l (% pred)	1,06 $\pm$ 0,5 (50,0 $\pm$ 21,2)	1,6 $\pm$ 0,5 (70,2 $\pm$ 32,29)	1,06 $\pm$ 0,5 (50 $\pm$ 21,2)	0,95 (38) *	1,2 $\pm$ 0,3 (59,3 $\pm$ 14,3)	2,3 $\pm$ 0,2 (100,0 $\pm$ 4,2)	1,5 $\pm$ 0,6 (68,5 $\pm$ 35,2)
FEV1, l (% pred)	1,69 $\pm$ 0,3 (40,5 $\pm$ 2,1)	1,2 $\pm$ 0,5 (42,7 $\pm$ 16,5)	1,69 $\pm$ 0,3 (40,5 $\pm$ 2,1)	1,73 $\pm$ 0,1 (46,5 $\pm$ 0,7)	1,3 $\pm$ 0,4 (43,1 $\pm$ 11,6)	1,1 $\pm$ 0,3 (33,3 $\pm$ 9,1)	1,4 $\pm$ 0,5 (42,7 $\pm$ 14,5)
DLCO, % pred.	10 $\pm$ 2,8 n=5	20,5 $\pm$ 10,1 n=4°	10 $\pm$ 2,8	x	22,8 $\pm$ 3,6 n=5°	24 n=1°	19,7 $\pm$ 7,7
pO2 at rest, mmHg	36,0 $\pm$ 7,1	49,2 $\pm$ 8,2]	36 $\pm$ 7,1	x	50,6 $\pm$ 6,8	56 $\pm$ 1,4	48,3 $\pm$ 8,5
<b>Therapy</b>							
LTOT, no. (%)	14 (100)	7 (100)	2 (100)	3 (100)	10 (83,3)	3 (100)	39 (95,1)
Steroids, no. (%)	7 (50,0)	7 (100)	2 (100)	3 (100)	10 (83,3)	3 (100)	32 (78,0)
Immunosuppressant, no. (%)	2 (14,3)	3 (42,9)	1 (50)	0 (0)	2 (16,7)	0 (0)	13 (31,7)
Antifibrotic drugs, no. (%)	7 (50,0)	2 (28,6)	0	1 (33,3)	7 (58,3)	1 (33,3)	13 (31,7)

**Table 5.** Demographics and clinical characteristics of patients with lung fibrosis included in the Western blot analysis. Abbreviations: idiopathic pulmonary fibrosis (IPF); hypersensitivity pneumonitis (HP); cryptogenic organizing pneumonia (COP); nonspecific interstitial pneumonia (NSIP); pulmonary function test (PFT); vital capacity (VC); total lung capacity (TLC); residual volume (RV); forced expiratory volume in 1 second (FEV1); diffusing capacity of the lung for carbon monoxide (DLCo); long term oxygen therapy (LTOT). \* n=1; ° not all patients were able to perform a DLCo. Table taken and legend adapted from (Schiller et al. 2017)

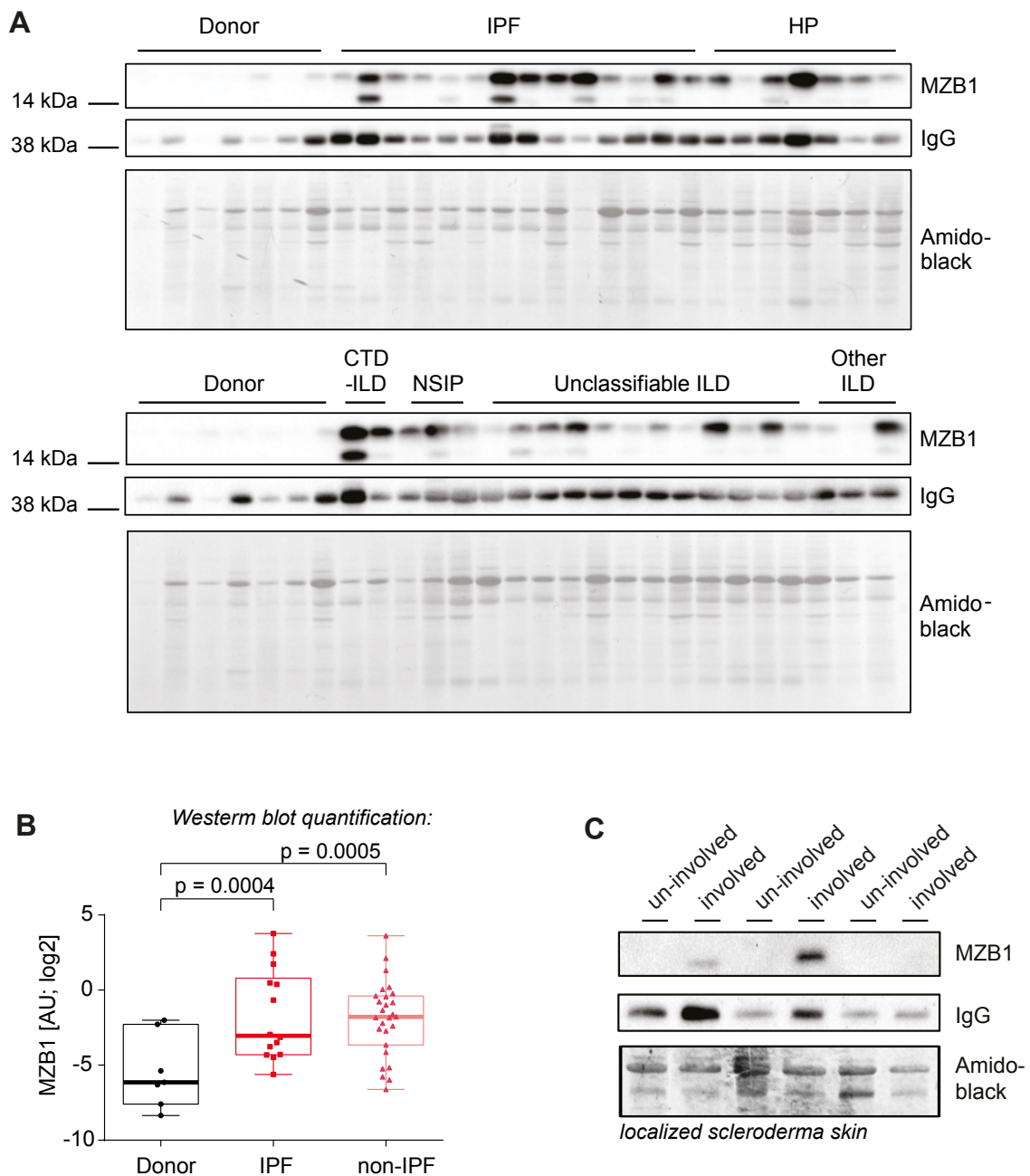


**Figure 15.** Identification of marginal zone B- and B1-cell-specific protein (MZB1)-positive cells in interstitial lung disease (ILD) and localized scleroderma using Western blot analysis. **(A)** Antibodies against MZB1 were used to perform Western blot and analyze homogenated tissues of different types of lung fibrosis due to ILD. To uncover the relationship between MZB1 positive cells and immunoglobulin G (IgG), additionally, antibodies against IgG were used. Amido black served as loading control and displayed the total protein loading of each sample. **(B)** *Box-and-whisker* plot is used to depict Western blot quantification of healthy donor tissue, idiopathic pulmonary fibrosis (IPF) and non-IPF ILD [raw data from (A); results are normalized to amido black] and indicates significantly more MZB1 in ILD compared to donor tissue. **(C)** Homogenated tissues of un-involved and involved skin from patients with localized scleroderma were subjected to Western blot analysis. Antibodies against MZB1 and IgG were used and amido black served as loading control and displayed the total protein loading of each sample. Figure and legend taken and adapted from (Schiller et al. 2017)

The amount of MZB1 in ILD correlated significantly with the tissue IgG ( $r=0.48$ ;  $p=0.0005$ ; Figure 16 A). Analyzing microarray data of an independent cohort from the U.S. with over 400 patients (Gene Expression Omnibus dataset GSE47460)(Bauer et al. 2015), MZB1 expression was also significantly increased in ILD in comparison to healthy donors (Figure 16 B). There was a significant negative correlation between MZB1 and DLCo (%) in both, the proteomic ILD cohort ( $r=-0.76$ ;  $p=0.006$ ; Figure 16 C) and the Western blot ILD cohort ( $r=-0.787$ ;  $p=0.0002$ ; Figure 16 D).

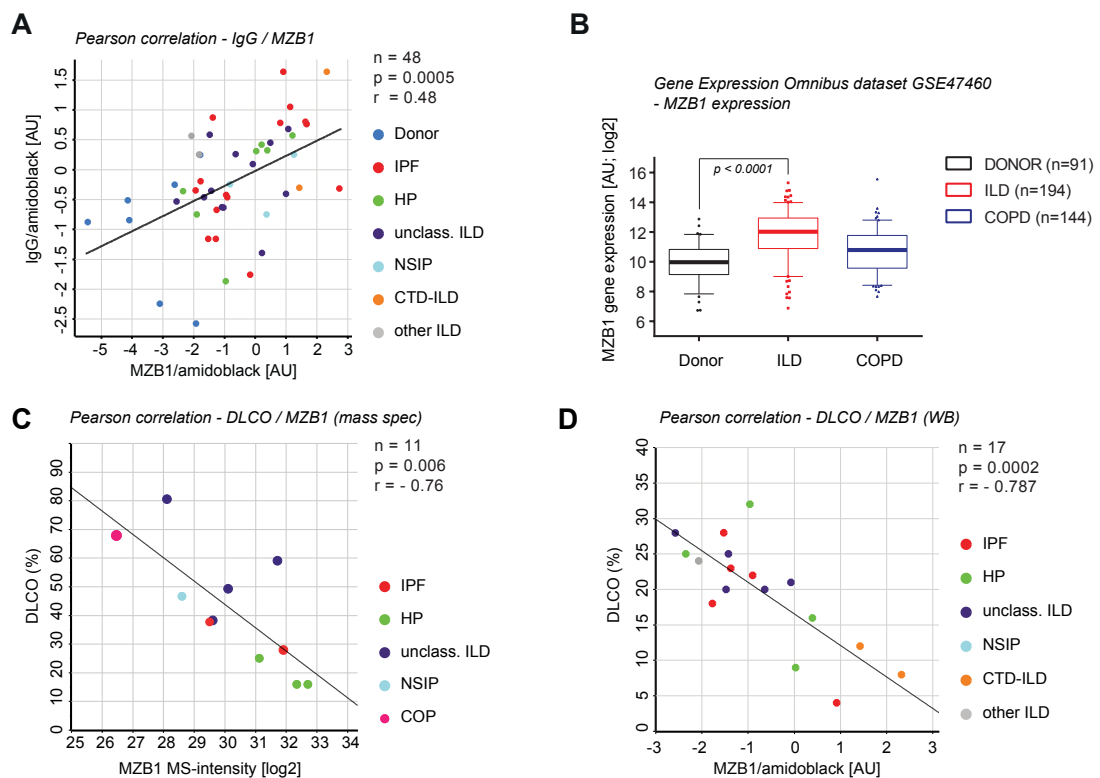


**Figure 16.** Marginal zone B- and B1-cell-specific protein (MZB1)-positive cells correlate positively with tissue immunoglobulin G (IgG) and negatively with diffusing capacity of the lung for carbon monoxide (DLCo). **(A)** Linear regression analysis of MZB1 and IgG shows a moderate, positive correlation. **(B)** *Box-and-whisker* of MZB1 expression in a large U.S. microarray cohort (Gene Expression Omnibus dataset GSE47460 published by the Lung Tissue Research Consortium) (Bauer et al. 2015). MZB1 is significantly higher in ILD than in healthy donor tissue. **(C)** Pearson correlation of mass spectrometry data (Figure 9) shows a strong, negative correlation of MZB1 and DLCo (%). **(D)** Pearson correlation of Western blot data depicts a strong, negative correlation of MZB1 and DLCo (%). **(A, C, D)** Color code shows distribution of different forms of ILD. For MZB1 raw data see Figure 15A. Abbreviations: arbitrary units (AU); chronic obstructive pulmonary disease (COPD); connective tissue disease (CTD); hypersensitivity pneumonitis (HP); interstitial lung disease (ILD); idiopathic pulmonary fibrosis (IPF); nonspecific interstitial pneumonia (NSIP); unclassifiable ILD (unclass. ILD); Western blot (WB). Figure and legend taken and adapted from (Schiller et al. 2017)

Apart from the DLCo, however, no associations were found between MZB1 and other clinical parameters. MZB1 expression was independent of age ( $r=0.063$ ;  $p=0.694$ ; Figure 17 A), VC (%) ( $r=-0.128$ ;  $p=0.433$ ; Figure 17 B), treatment with steroids (Figure 17 C) or antifibrotic therapy (Figure 17 D) and sex (Figure 17 E).

In summary, MZB1 was found to be significantly increased in ILD tissue in comparison to healthy donors. MZB1 correlates not only with tissue IgG but is also associated with worse lung function.

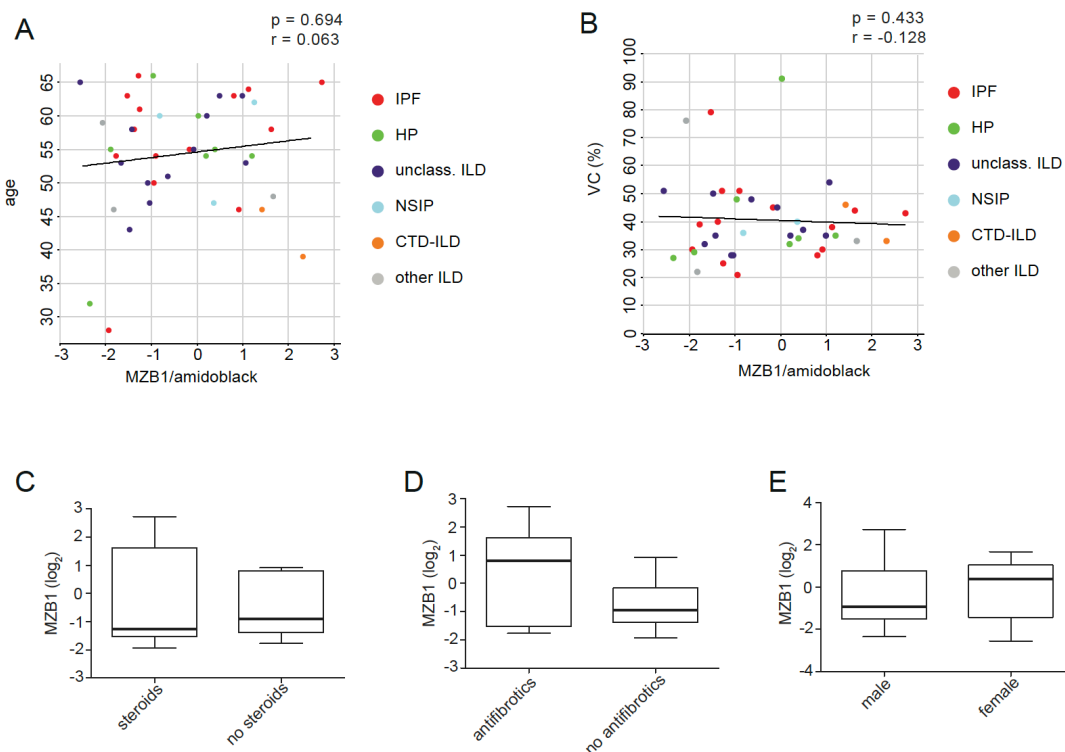


**Figure 17.** The amount of marginal zone B- and B1-cell-specific protein (MZB1) is independent of demographic and therapeutic factors in human lung fibrosis. **(A)** Linear regression analysis shows no correlation between MZB1 and age. **(B)** Linear regression analysis shows no correlation between MZB1 and vital capacity (VC) in %. **(C – E)** *Box-and-whisker* identifies no relationship between MZB1 tissue level and steroids, antifibrotic therapy and gender, respectively. **(A, B)** Color code shows distribution of different forms of ILD. **(A – E)** For MZB1 raw data see Figure 15A. Figure taken and legend adapted from (Schiller et al. 2017)

#### 4.1.4 IgG subclasses in ILD

As mentioned above, the level of tissue IgG correlated significantly with MZB1 in ILD (Figure 16 A). Like MZB1, the quantification of IgG from the Western blot analysis revealed a significantly greater amount of IgG in ILD tissue than in healthy donor tissue (Figure 18 A). A re-analysis of

IgG subclasses of the published MS data (Schiller et al. 2017) identified a significantly increased expression of IgG4 in ILD tissue in comparison to healthy controls (Figure 18 B).

The production of IgG4 is mainly induced by repeated or long-term exposure to a non-infectious antigen or allergen (Vidarsson et al. 2014). In general, IgG4 is associated with anti-inflammatory processes. An increase of IgG4 can be observed, for example, in IgE-mediated allergic diseases under allergen-specific immunotherapy (Jutel and Akdis 2011). Nevertheless, IgG4 seems to be also involved in pathological processes. While isolated IgG4 deficiency syndromes are rare and the clinical relevance remains unclear (Vidarsson et al. 2014), increased levels of IgG4 can, for example, be observed in autoimmune dermatosis pemphigus and there are so-called IgG4-related diseases (Sitaru et al. 2007, Aalberse et al. 2009). In IgG4-related diseases, lymphocytes and IgG4-producing plasma cells are deposited in the tissue leading to increased plasma levels of IgG4 (Campbell et al. 2014, Vidarsson et al. 2014). Clinically, IgG4-related diseases can vary highly, however, cases of ILD have been described in association with IgG4-related diseases (Campbell et al. 2014, Schneider et al. 2016). Based on the findings from the re-analysis of the MZB1 datasets (Figure 18) distribution of IgG subclasses and especially expression of IgG4 in ILD were further studied using Western blot analysis (Figure 19 A-D).

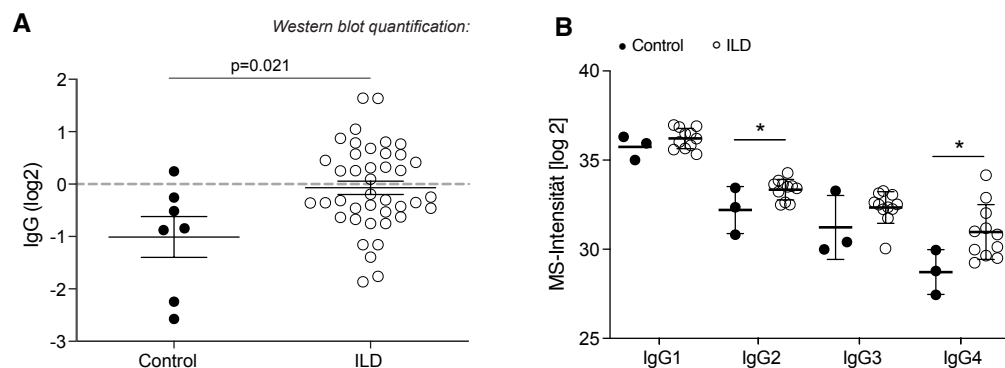


**Figure 18.** Immunoglobulin G (IgG) and IgG subclasses distribution in the proteome profiling datasets. Raw data was taken from (Schiller et al. 2017). **(A)** Western blot analysis identified significantly more tissue IgG in interstitial lung disease (ILD) than in controls. **(B)** Quantification of IgG subclasses in proteomics data.

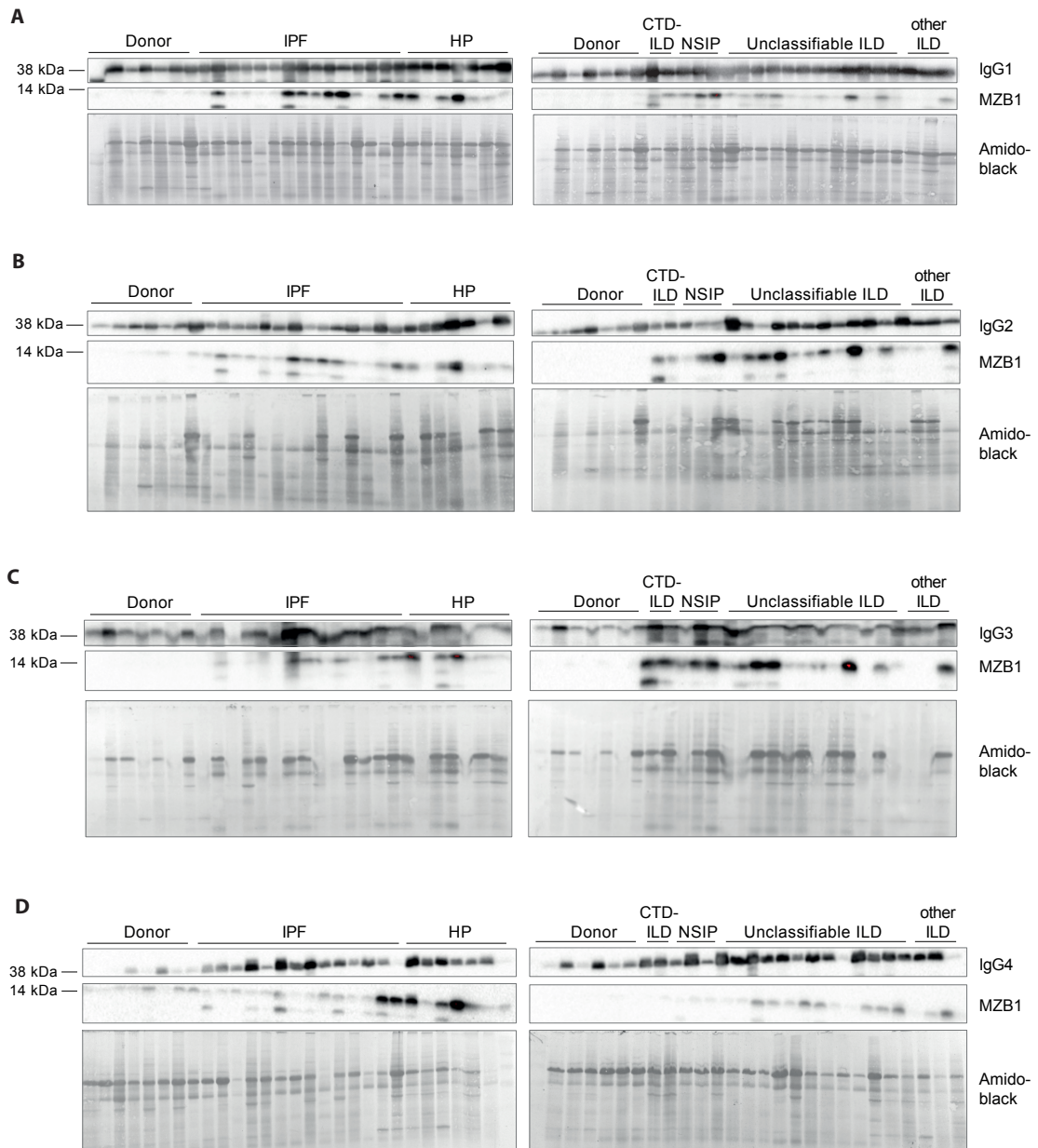


**Figure 19.** Immunoglobulin G (IgG) subclasses in interstitial lung disease (ILD) tissue. **(A-D)** Tissue homogenates of healthy donors and different ILD entities were analysed by Western blot with antibodies against marginal zone B and B1 specific protein (MZB1) and IgG1 (A), IgG2 (B), IgG3 (C) and IgG4 (D). For quantification of the total protein loading blots were also stained with amido black.

Tissue homogenates were derived from seven donors who served as healthy controls and 34 end-stage ILD tissues as described in 4.1.3. Clinical characteristics have been described in Table 5 (4.1.3). Antibodies against IgG1, IgG2, IgG3, IgG4 and MZB1 were used for staining. For the further quantification of the total protein loading blots were also stained with amido black (Figure 19 A-D).

Western blot quantification showed a significantly lower amount of IgG3 in ILD tissue (Figure 20 A). Although tissue IgG4 was elevated in ILD, neither the difference (Figure 20 A) nor the IgG1 to IgG4 ratio (Figure 20 B) did reach statistical significance when compared to healthy donors. Still, levels of MZB1 correlated weak but significantly with IgG2 and IgG4 (Figure 21 A-D), hinting towards a potential association between plasma cells and IgG4 in ILD tissue.

In summary, IgG subclasses were characterized in ILD tissue. While the proteome data indicated an increased proportion of IgG4 in ILD tissue, Western blot analysis could not definitely validate this finding in general. Although the trend of a higher IgG4 expression and a higher IgG4 to IgG1 ratio was seen, no statistical significance was reached. However, MZB1 levels correlated significantly with IgG4 expression. Additional efforts are needed to uncover the role of IgG4 in the pathogenesis of ILD.

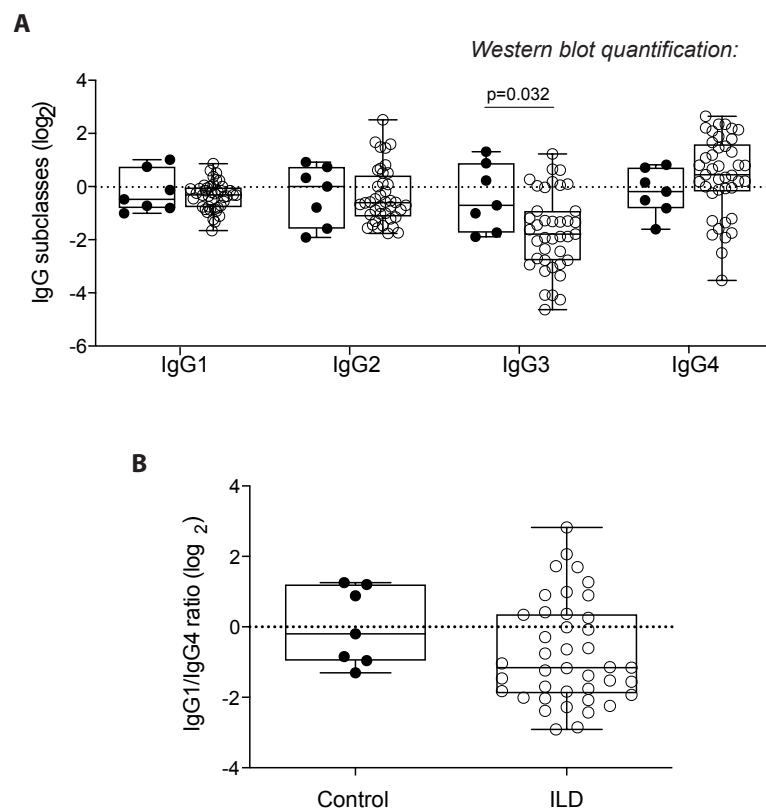


**Figure 20.** Quantification of Western blot analysis of immunoglobulin G (IgG) subclasses. (A, B) Box-and-whisker of the respective IgG subclass in the Western blot analysis, see Figure 22 A-D and the IgG1 to IgG4 ratio.



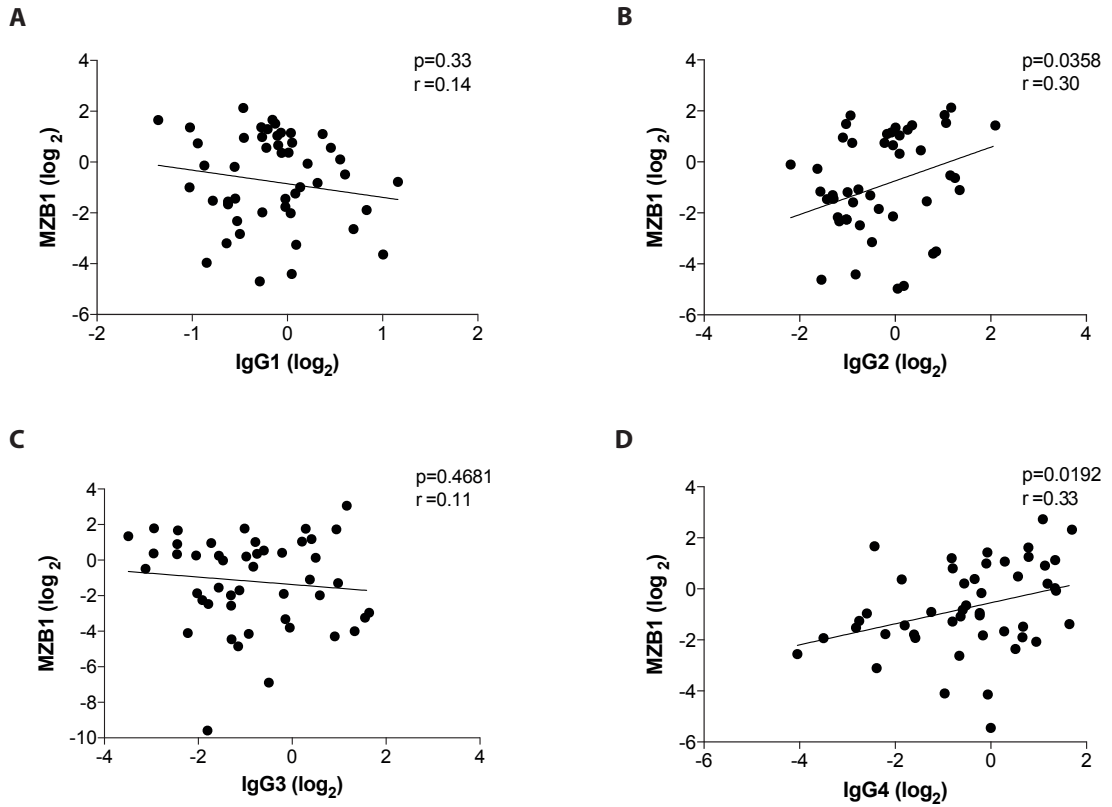


**Figure 21.** Correlation of marginal zone B- and B1-cell-specific protein (MZB1) and IgG subclasses in interstitial lung disease (ILD) tissue. **(A-D)** Correlation of IgG1 (A), IgG2 (B), IgG3 (C) and IgG4 (D) and MZB1 levels identifies a positive correlation for IgG2 (B) and IgG4 (D).

### 4.1.5 Discussion

Recent advances in MS-driven proteomics enable the exact detection and quantification of numerous proteins (Aebersold and Mann 2016). Given the remaining lack of knowledge of the genesis of idiopathic fibrosis, this method may provide important information to gain better understanding of the diseases and possibly find therapeutic targets. In the presented work biopsies of human lung and skin fibrosis tissue were analyzed and over 7.900 proteins were quantified (Schiller et al. 2017). Up to this point of time, this was the most extensive study on proteomics in human tissue fibrosis and also the first comparison of tissue fibrosis in different organ systems. Protein profiling of various forms of human ILD and localized skin fibrosis (morphea) revealed common and disease-specific protein regulations in different forms of fibrotic diseases. Surprisingly, a large number of MZB1-positive plasma B cells were present in human lung and skin fibrosis (Schiller et al. 2017).

Since the ILD cohort of this work was heterogenous, it is not surprising, that the samples differed highly on the molecular level. In the future, recently developed high-throughput methods such as single-cell mRNA sequencing (Macosko et al. 2015) might be helpful to find out more about the heterogeneity of cell populations in chronic lung disease. Nevertheless, given the heterogenic patient cohort, it is of even more interest, that an essential amount of proteins were commonly enriched in all specimen. The most important shared protein in human lung and skin fibrosis was MZB1, which was characterized as being expressed in plasma B cells positive for CD38/CD13/CD27 and negative for CD20/CD45 (Schiller et al. 2017). Studies have shown that in respiratory immunity, B cells can be found in bronchus-associated lymphoid tissue, where distinct B cell follicles are present (Moyron-Quiroz et al. 2004, John-Schuster et al. 2014). Plasma cells were also found to be among the most common cells present in mural fibrosis and honeycombing areas of patients with IPF (Parra et al. 2007).

In the present work MZB1-positive B cells were detected as scattered over the entire lung tissue with a rather predominantly perivascular localization and not primarily associated to tertiary lymphoid organs (Schiller et al. 2017). It has been shown that MZB1 plays an important role in the ER of plasma B cells, which experience ER stress, when antibody secretion is highly activated (Flach et al. 2010, Rosenbaum et al. 2014). MZB1 seems to be especially needed for the proper biosynthesis of immunoglobulin  $\mu$  heavy chains under conditions of ER stress (Rosenbaum et al. 2014). Interestingly, the results from immunostainings in the presented work revealed B cells with high and B cells with low expression of MZB1 hinting towards a tight regulation. Cells with high MZB1 expression were characterized by a large cytoplasm and co-expression of a several established markers for mature plasma B cells verifying these cells as tissue-resident, terminally differentiated antibody-producing plasma cells (Schiller et al. 2017). Besides, MZB1 levels correlated significantly with lung function parameters which implicates that antibody-mediated autoimmunity might be involved in ILD and it is associated with worse respiratory status of the patient. In line with this finding a previous study identified plasma B cells to be more prevalent in

explanted lungs in rapidly progressing patients with IPF than in slowly progressing IPF (Balestro et al. 2016).

Further, MZB1 levels correlated strongly with tissue IgG. Although in the proteomic data the IgG subclass IgG4 was significantly upregulated in comparison to healthy donors, this finding could not be validated in Western blot analysis in a larger ILD cohort. Still, MZB1 levels correlated rather with IgG4 and IgG2 than with IgG1 levels, which is the most prevalent IgG subclass and also the IgG4 to IgG1 ratio was higher in ILD, not significant though. Since it has been described that IgG4 related disease can cause cases of ILD (Campbell et al. 2014, Schneider et al. 2016), a higher secretion of this subclass in patients with ILD would be logical. In IgG4 related disease, lung manifestation mainly shows interstitial pneumonitis, inflammatory pseudotumor, lymphomatoid granulomatosis and organizing pneumonia (Morales et al. 2019). However, so far, from the data shown in this work, no conclusions can be drawn if there are IgG subclasses that are more present in lung fibrosis. Further work is needed to identify the role of IgG subclasses distribution in ILD.

It needs to be acknowledged that tissue biopsies analyzed in this work were to a large extent derived from patients with idiopathic interstitial pneumonia, such as IPF, idiopathic NSIP and unclassifiable ILD. Therefore, future studies are needed to further clarify the role of antibody-mediated autoimmunity in idiopathic forms of fibrosis. There is increasing evidence that a lot of patients with idiopathic interstitial pneumonia, including IPF, may demonstrate clinical characteristics which would fit to an underlying autoimmune process. However, since these cases do not qualify for the diagnosis of CTD-ILD, the term “IPAF” has recently been proposed by a European Respiratory Society/American Thoracic Society task force (Fischer et al. 2015) (see 1.3.2).

In IPF, the presence of circulating autoantibodies has first been described in 1978 (Dreisin et al. 1978) and more recently there is also data suggesting that B cell mediated autoimmunity might also be one of the causal factors which leads to the genesis of IPF (Xue et al. 2013, Donahoe et al. 2015). While patients with SSc usually present with positive autoantibody testing, the role of circulating autoantibodies in localized scleroderma is not clear yet (Fleischmajer and Nedwich 1972). Nevertheless, fibrotic lesions in these patients histologically reassemble fibrotic reactions in SSc including strong inflammatory processes surrounding the vessels (Fleischmajer and Nedwich 1972).

As mentioned earlier, recently, autoantibodies targeting the lung specific protein BPI fold containing family B member 1 were found in 12% of patients with idiopathic interstitial pneumonia (Shum et al. 2013). The study further demonstrated that in mice, T cells specific for BPI fold containing family B member 1 can induce pulmonary fibrosis (Shum et al. 2013). Therefore, first, it is possible that autoantibodies and autoreactive T cells which target previously unidentified antigens could trigger or at least favor some of the idiopathic forms of ILD. Second, identifying

formerly unidentified autoantigens might be used to improve patient stratification and or new treatment strategies in the future (Schiller et al. 2017).

However, future immunotherapies require the identification auf disease-specific autoantigens specific for the respective disease. Further, preclinical models are needed for the evaluation of a causal role of specific antigens for certain forms of idiopathic fibrosis.

## 4.2 Autoantigen discovery in interstitial lung disease (ILD)

The work presented in the following chapter was largely included into a manuscript which was prepared for submission to a scientific journal. The manuscript has not been peer-reviewed yet. However, a preprint version of the manuscript has been published on *medRxiv*. *medRxiv*, which is a spin-off of the more commonly known *bioRxiv*, is a server and online archive which enables authors to publish their scientific work as complete but previously unpublished manuscripts (preprints) with free access to readers. It covers science from the medical, clinical, and related health sciences field. Both, *bioRxiv* and *medRxiv*, are run by Cold Spring Harbor Laboratory, as a not-for-profit research and educational institution. The file of the manuscript can be found on the *medRxiv* website (<https://www.medrxiv.org>) or directly via the digital object identifier (doi): (<https://doi.org/10.1101/2021.02.17.21251826>). The citation of this preprint manuscript in this thesis will be: (Leuschner et al. 2021).

The PhD student is the first author of this manuscript and was involved in all parts of this study and performed most of the practical work. All human samples from Munich were organized and clinical data were analyzed by the PhD student. Credit goes to Dr. Christoph Mayr, for the organization and performance of MS runs, assistance in setting up the Differential Antigen Capture assay and help with analysis of the proteomics data, and Prof. Antje Prasse for supply of human serum and clinical data from Hannover.

### 4.2.1 Introduction

Among idiopathic interstitial pneumonias, IPF is the most commonly diagnosed form. As described before (chapter 1.1.3), so far, the disease is considered incurable and as the prognosis is estimated to be two to five years after diagnosis, survival is limited (Bjoraker et al. 1998). Yet, the only definite therapy for IPF is lung transplantation (Noble et al. 2011, King et al. 2014, Richeldi et al. 2014). Therefore, it is crucial to further explore the pathogenesis of IPF to identify other targets for future therapies.

In clinical practice, to rule out the differential diagnosis of a CTD-ILD, the clinical presentation and a panel of autoantibodies are evaluated. Usually and in contrast to a typical patient with IPF, in patients with CTD-ILD antinuclear antibodies (e.g. Scl-70 antibody against topoisomerase-I in SSc) can be detected in the laboratory test. Such autoantibodies can help to classify patients and possibly also guide clinicians to a proper diagnosis. Nevertheless, there is an increasing number of data that many idiopathic interstitial pneumonias, including IPF, may have clinical features fitting to autoimmune processes. In fact, various studies have shown that positive circulating autoantibodies are found in up to 30% of IPF patients (Lee et al. 2013, Moua et al. 2014, Leuschner et al. 2018), without fulfilling the criteria which need to be present for the diagnosis of

CTD-ILD and IPAF (Fischer et al. 2015). Very recently, it has been shown that an antioxidant therapy with N-acetylcysteine is more effective in patients with IPF and positive antinuclear antibodies (Oldham et al. 2018). Since there are very different clinical courses in IPF, this may indicate that clinical phenotyping needs to be more individual in order to be able to pursue a more personalized therapy strategy in IPF. As shown in detail in the *proteome profiling of human lung and skin fibrosis* project (see chapters 4.1.2 – 4.1.3), recently, plasma B cells which are positive for MZB1 and produce and secrete antibodies were identified in tissues of patients with ILD (Schiller et al. 2017). MZB1 is a protein located at the ER that is increasingly expressed in B cells with high antibody secretion (Flach et al. 2010). Since in the study by Schiller et al. MZB1 levels were associated with higher tissue IgGs and worse lung function parameters, the question arises whether some of the detected IgGs are autoreactive. In the genesis of IPF, in addition to the data shown above, there are increasing indications for a B cell-mediated autoimmunity with repetitive damage to the lung parenchyma (Dreisin et al. 1978, Xue et al. 2013). In comparison to healthy controls and patients with COPD, higher plasma levels of factors essential for B cell function have been identified in patients with IPF in the past: One is B lymphocyte stimulating factor, also known as B cell activating factor, that is needed for the proper differentiation and survival of B cells (Xue et al. 2013), and another factor is C-X-C motif chemokine 13, that is important for the migration of B-cells to foci of inflammation in the tissue (Vuga et al. 2014, DePianto et al. 2015). For both, C-X-C motif chemokine 13 and B lymphocyte stimulating factor, an increased concentration in the lung tissue appears to be associated with poorer survival (Xue et al. 2013, Vuga et al. 2014, DePianto et al. 2015). A possible mode of action of B lymphocyte stimulating factor might be the rescue of auto-reactive B cells (Thien et al. 2004).

Former studies have already reported that the presence or high levels of certain autoantibodies could be linked to poorer survival in IPF, for example in patients positive for anti-vimentin antibodies (Li et al. 2017) or anti-heat-shock protein 70 antibodies (Kahloon et al. 2013). In IPF, autoantibodies against periplakin as well as anti-parietal cell antibodies also appear to be linked with a more severe course of the disease (Taille et al. 2011, Beltramo et al. 2018). Experimental evidence in mice suggests that T cells targeting a sole lung specific autoantigen have the ability to cause pronounced and irreparable lung fibrosis (Shum et al. 2013). One could therefore think that there are certain autoantibodies and, accordingly, autoreactive T cells that can trigger or at least preserve many IPF cases and that identification of unknown autoantigens can be used to stratify patients and to possibly develop immunotherapy options in the future for IPF. So far, studies about autoantibodies in IPF have only focused on specific antigens. The following sections will summarize the results of the investigations conducted in the discovery of unknown autoantibodies with regard to both disease specificity and prognosis for IPF and CTD-ILD. Therefore, a proteomics workflow for the exact and precise detection of autoantigens associated with lung diseases was established in ILD patient material from Munich. The MS-based autoantigen discovery platform is based on patient plasma antibody capture and immunoprecipitation of a pooled protein extract derived from lung explants of end stage ILD patients. Using this unbiased approach, a broader spectrum of autoimmunity in the individual

patient could be identified including the identification of common and disease-specific patterns of autoimmunity in patients with CTD-ILD and IPF. To assess reproducibility across patient cohorts, a second cohort from Hannover was analyzed and uncovered cohort-specific as well as robustly detected autoantigens across cohorts. The integration of clinical meta-data and autoantibody profiles identified novel autoantigens in IPF and CTD-ILD associated with transplant-free survival.

#### **4.2.2 Identification of lung specific autoantigens in interstitial lung disease (ILD) using a proteomic workflow**

For the identification of autoantigens with large-scale turnover methods, protein microarrays (Rosenberg and Utz 2015), or phage display libraries which represent a synthetic human peptidome (Larman et al. 2011), have recently been used (Leuschner et al. 2021). Nevertheless, for such assays synthetic antigens are needed. To discover autoantigens that are associated with specific lung diseases an unbiased and high throughput method, the Differential Antigen Capture assay (DAC), was developed. The DAC consists of immunoprecipitation of proteome extracts from ILD and healthy donor lung tissue and plasma IgGs. Afterwards, quantitative shotgun proteomics follows, which is analogical to affinity purification MS (Figure 22) (Leuschner et al. 2021).

The DAC protocol is described in detail in 3.2.2. In brief, plasma of IPF, CTD-ILD and age-matched healthy controls was incubated with protein G beads which allow binding of plasma immunoglobulins. Unbound plasma components were washed off thoroughly (Leuschner et al. 2021). Afterwards, the beads were incubated with a pooled protein extract derived from lung explants of ILD patients and excess tissue from healthy lungs of transplant donors representing an average ILD lung proteome and putative autoantigens. Specific autoantigens from native lung extracts can bind to the protein G-coupled immunoglobulins and form antibody-antigen-complexes. After on bead-digest and purification, proteins were then identified and quantified using the latest technique and equipment of MS.

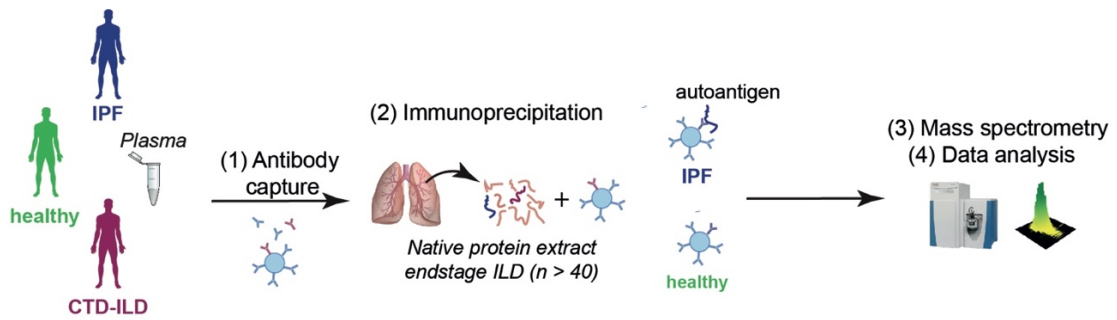


**Figure 22.** Experimental workflow of the Differential Antigen Capture assay (DAC). Immunoprecipitation was used to generate and enrich autoantibody-antigen complexes out of patients' plasma and native extracts from end stage interstitial lung disease (ILD). Shotgun proteomics was used to quantify differential protein detection in diseased patients versus healthy age matched controls. Figure and legend taken and adapted from (Leuschner et al. 2021)

Plasma samples of patients with SSc and CTD-ILD, who were clinically characterized by ELISA tests positive for antibodies against the antigen topoisomerase I (TOP1; specific antibody Scl-70), were analyzed to evaluate sensitivity and specificity of the DAC (Figure 23 A) (Leuschner et al. 2021). Each patient sample was measured in triplicates and proteins were counted as putative autoantigens in the respective ILD patient if they were significantly enriched (FDR <10%) on beads in comparison to plasma from healthy and age matched controls (Figure 23 B). The DAC assay identified clinically verified Scl-70-positive patients (n=8) and Scl-70-negative patients (n=7) with very good specificity and sensitivity. Further, the informative value compared to the clinically approved ELISA test was similarly meaningful: While there was no evidence of TOP1 in Scl-70 negative patients, in seven Scl-70 positive patients TOP1 was identified in all three triplicates and one SCL-70 positive patient had evidence of TOP1 in two out of three samples (Figure 23 A, C, D) (Leuschner et al. 2021). In addition to the identification of TOP1, the DAC assay simultaneously identified a plethora of other enriched putative autoantigens (Figure 23B) (Leuschner et al. 2021).

In summary, the DAC assay was developed to allow a multiplexed and unbiased approach to the identification of a broad spectrum of autoimmunity in patients with IPF and CTD-ILD. Human plasma antibodies were captured on Protein-G beads and used for immunoprecipitation of potential autoantigens from lung tissue homogenates of end stage ILDs. Using clinically approved ELISA test results for TOP1 revealed an exceptionally good specificity and sensitivity of the DAC assay.



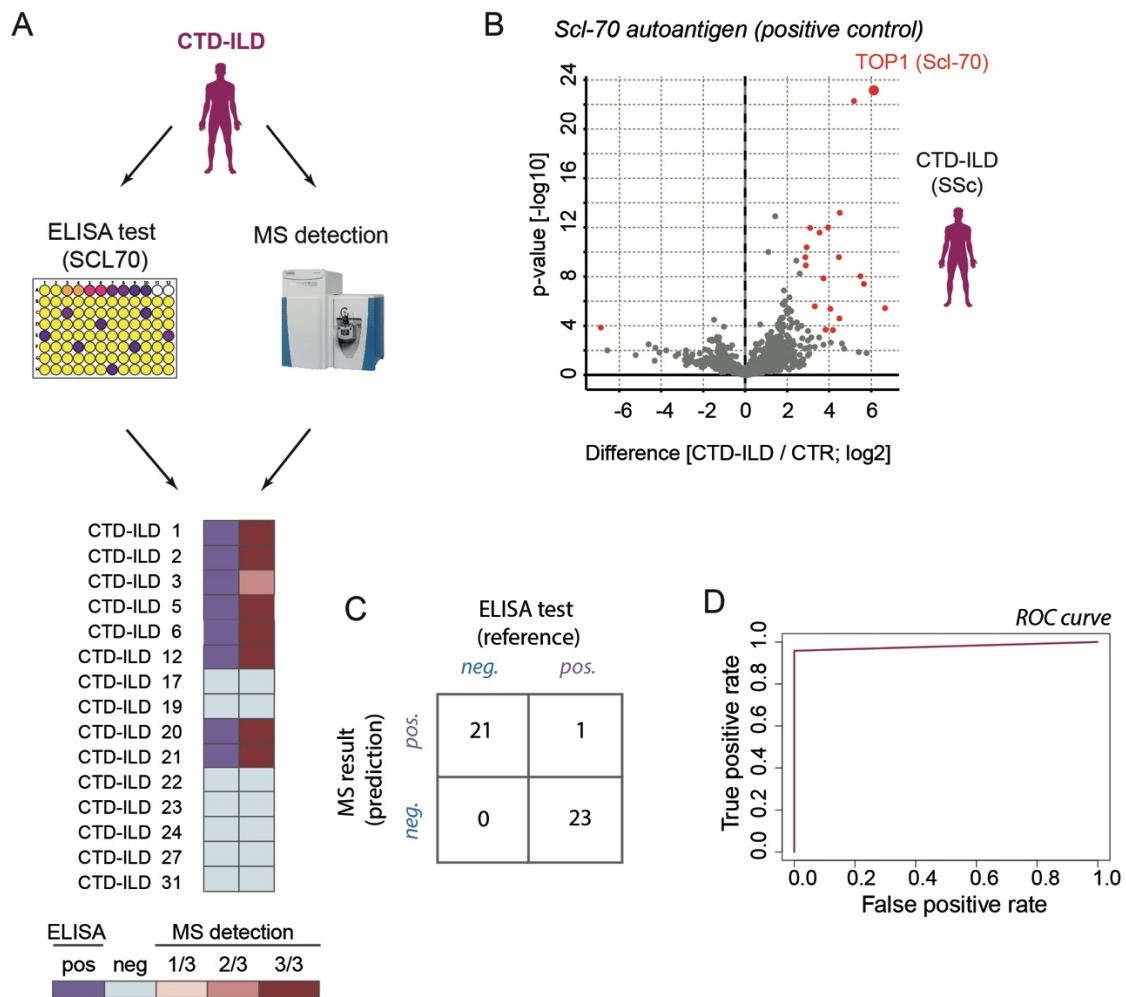


**Figure 23.** A proteomic workflow detects autoantigens in patients with interstitial lung disease (ILD) with high sensitivity and specificity. **(A)** Proof of concept was successfully reached with plasma from patients with systemic sclerosis (SSc) and connective-tissue related interstitial lung disease (CTD-ILD), who were clinically characterized by Scl-70 antibodies (antigen topoisomerase I; TOP1) using an approved ELISA test. The different coloring shows the number of significant enrichments for Scl-70/TOP1 in the three replicates in the mass spectrometry (MS)-analysis. **(B)** The volcano plot is an example of a patient with SSc, in whom TOP1 was detected. Red colored points depict significantly enriched proteins (FDR <10%) in comparison to healthy age matched controls. Abscissa: x-fold difference to control-values (log<sub>2</sub>); ordinate: p-value (-log<sub>10</sub>). **(C, D)** Each patient sample in the proof of concept pilot experiment was processed and analyzed three times (panel B). The four-field table indicates the amount of true and false positive measurements. The ROC analysis shows that the sensitivity of significantly enriched TOP1 (detected by MS-analysis) in SSc-patients in comparison to healthy controls was 96% and the specificity 100%. Figure and legend taken and adapted from (Leuschner et al. 2021)

### 4.2.3 Study cohorts and patient characteristics

For the systematic identification of potential autoantigens in IPF and CTD-ILD, the DAC assay was used in two independent cohorts (Munich and Hannover). Figure 24 shows a scheme of the two cohorts and the accessibility of data about lung function and/or survival.

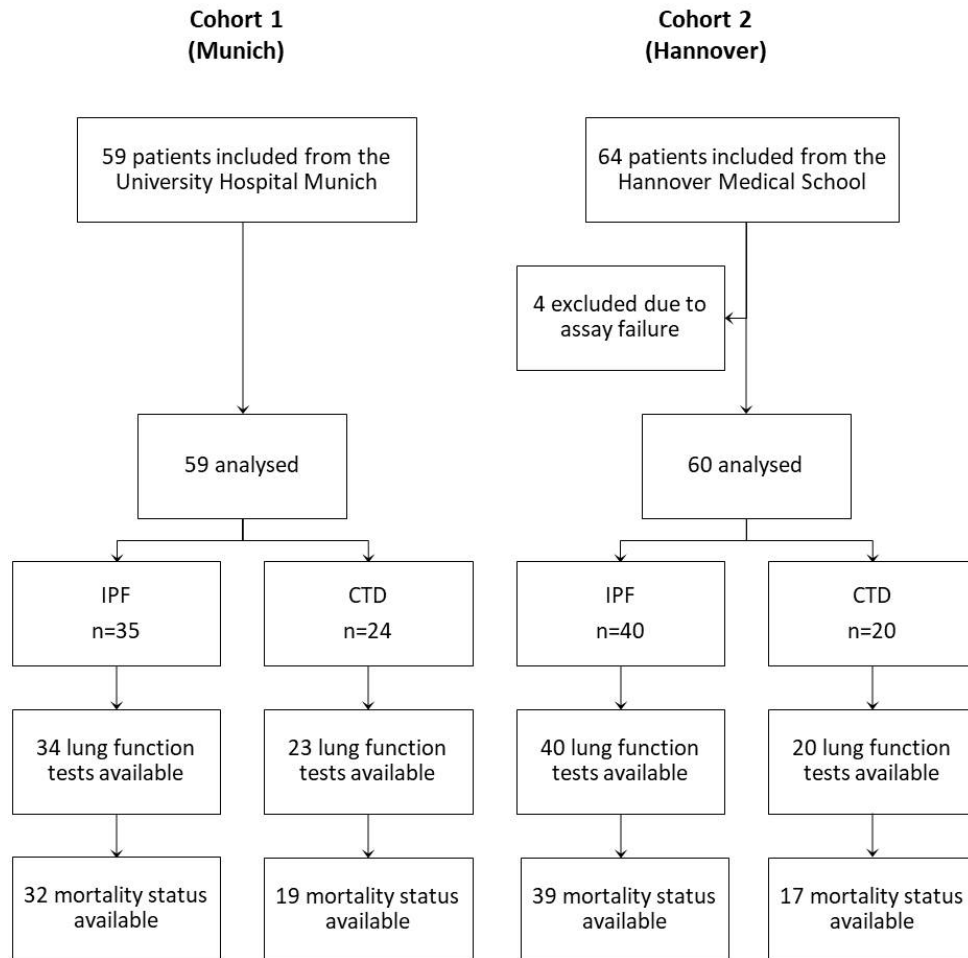


**Figure 24.** Investigation of autoantibody profiling in one cohort from Munich (cohort 1) and a second cohort from Hannover (cohort 2). Figure taken and legend adapted from (Leuschner et al. 2021)

Study cohort 1 (Munich; Table 6) consisted of IPF (n=35), CTD-ILD (n=24) and age-matched healthy controls (n=32; mean±SD 58.8±11.1 years, range 40-82 years) (Leuschner et al. 2021). The CTD-ILD patients had SSc (n=15), unspecific CTD (n=5), rheumatoid arthritis (n=4), and mixed connective tissue disease (n=1) (Leuschner et al. 2021). The mean±SD age of the study cohort was 63.0±9.1 years (IPF: 63.3±8.4 years; CTD-ILD 62.7±10.2 years). The FVC % pred. was significantly lower in patients with IPF than in patients with CTD-ILD (54.5±15.8 vs. 65.7±18.9; p=0.025) (Leuschner et al. 2021). Study cohort 2 (Hannover; Table 7) also comprised IPF (n=40) and CTD-ILD patients (n=20; sjogren's syndrome n=6; SSc n=5; rheumatoid arthritis n=5; CREST syndrome n=3; antisynthetase syndrome n=1) (Leuschner et al. 2021). The age of IPF patients from cohort 2 (mean±SD age 70.4±8.1 years) was significantly higher than the age of any of the other patient groups (p=0.003). Furthermore, in comparison to cohort 1, patients from cohort 2 had a significantly better lung function. Combining both cohorts, patients with CTD-ILD had a significantly worse transplant-free survival in comparison to patients with IPF (p=0.009; Figure 25) (Leuschner et al. 2021).

	All (n=59)	IPF (n=35)	CTD (n=24)
Age, years	63.0 ± 9.1	63.3 ± 8.4	62.7 ± 10.2
Sex			
Female	26 (42.6)	8 (22.9)	18 (69.2)
Male	35 (57.4)	27 (77.1)	8 (30.8)
Ever smoker	28 (66.7) <sup>1</sup>	22 (73.3) <sup>2</sup>	6 (50) <sup>3</sup>
Baseline lung function			
FVC% <sub>pred</sub>	59.3 ± 17.9 <sup>4</sup>	54.5 ± 15.8	65.7 ± 18.9
DlCO% <sub>pred</sub>	28.3 ± 13.0 <sup>5</sup>	25.6 ± 10.1	29.0 ± 17.8

**Table 6.** Demographics and clinical characteristics of patients with idiopathic pulmonary fibrosis (IPF) and connective tissue disease related interstitial lung diseases (CTD-ILD) from Munich (cohort 1). Data is given as mean (±SD) or n (%). Abbreviations: percentage of forced vital capacity (FVC%<sub>pred</sub>), percentage of diffusion capacity of carbon monoxide (DlCO%<sub>pred</sub>). <sup>1</sup> smoking status of n=42, <sup>2</sup>smoking status of n=30, <sup>3</sup> smoking status of n=12, <sup>4</sup> FVC of n=59 (IPF n=34, CTD-ILD n=25), <sup>5</sup> DlCo of n=49 (IPF n=28, CTD-ILD n=21). Table and legend taken and adapted from (Leuschner et al. 2021).

	All (n=60)	IPF (n=40)	CTD (n=20)
Age, years	62.7 ± 10.2	70.4 ± 8.1	62.8 ± 11.4
Sex			
Female	24 (40.0)	8 (20)	16 (80)
Male	36 (60.0)	32 (80)	4 (20)
Ever smoker	38 (65.5) <sup>1</sup>	30 (78.9) <sup>2</sup>	8 (40)
Baseline lung function			
FVC% <sub>pred</sub>	70.5 ± 16.6	72.1 ± 15.8	67.3 ± 18.1
DlCO% <sub>pred</sub>	54.9 ± 16.7 <sup>3</sup>	54.0 ± 15.3	56.9 ± 20.1

**Table 7.** Demographics and clinical characteristics of patients with idiopathic pulmonary fibrosis (IPF) and connective tissue disease related interstitial lung diseases (CTD-ILD) from Hannover (cohort 2). Data is given as mean (±SD) or n (%). Abbreviations: percentage of forced vital capacity (FVC%<sub>pred</sub>), percentage of diffusion capacity of carbon monoxide (DlCO%<sub>pred</sub>). <sup>1</sup> smoking status of n=58, <sup>2</sup> smoking status of n=38, <sup>3</sup> DlCo of n=54 (IPF n=38, CTD-ILD n=16). Table and legend taken and adapted from (Leuschner et al. 2021).

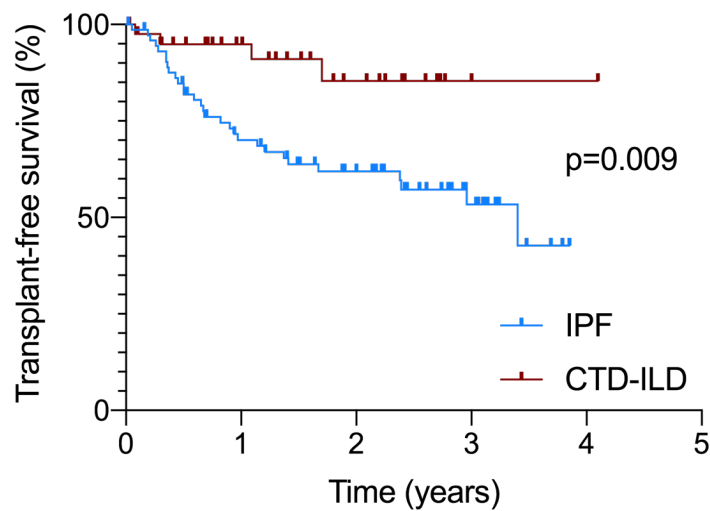


**Figure 25.** Kaplan-Meier survival analysis shows a significantly better transplant-free survival in patients with connective tissue related interstitial lung disease (CTD-ILD) in comparison to patients with idiopathic pulmonary fibrosis (IPF).

In summary, two clinical cohorts including patients with IPF and CTD-ILD were used to identify autoimmune profiles. Overall, cohort 1 was already in a more advanced stage of disease in comparison to cohort 2 with both cohorts together representing a broad spectrum of the respective diseases.

#### 4.2.4 Discovery of unknown autoantibodies in idiopathic pulmonary fibrosis (IPF)

The DAC assay identified >500 proteins per patient in the respective patient groups in cohort 1 and 2 (Leuschner et al. 2021). In cohort 1, on average, 586 proteins per patients were quantified in patients with IPF (mean±SD 633±97), CTD-ILD (mean±SD 561±150) and healthy controls (mean±SD 577±139; Figure 26 A) (Leuschner et al. 2021). Interestingly, gene categories did not show great differences between IPF and CTD-ILD with mostly cytoplasmic, nuclear and cytoskeletal components (Figure 26 B) (Leuschner et al. 2021). A *t* test comparing IPF and CTD-ILD was performed and identified 209 regulated autoantigens (FDR <10%), seven of which were enriched in CTD and 202 in IPF (Figure 26 C). In CTD-ILD, the mostly enriched antigens were TOP1 and the POTE ankyrin domain family member E. So far, the POTE ankyrin domain family member E has been recognized as cancer antigen in multiple, different types of human cancers

such as non-small-cell lung cancer, where it has been shown to be linked to worse survival (Wang et al. 2015). Recently, a study on immune cells identified POTE ankyrin domain family member E expression specifically in macrophages (Vekariya et al. 2019). In IPF, the greatest differences to CTD-ILD were observed for Alpha-centractin, the Ras-related protein Rab-1B and the Protein disulfide-isomerase A6 (PDIA6). Alpha-centractin, an actin-related protein and subunit of the dynactin complex, was recently found to be involved in toll-like receptor 2-mediated immune signaling (Kamal et al. 2019). Ras-related protein Rab-1B, a member of the RAS oncogene family, might be involved in antiviral innate immunity (Beachboard et al. 2019). Protein disulfide-isomerase A6 might be essential for hematopoiesis (Choi et al. 2020). In cohort 2, the mean $\pm$ SD amount of identified proteins was 535 $\pm$ 88 in IPF and 544 $\pm$ 72 in CTD-ILD (Figure 26 D) (Leuschner et al. 2021).

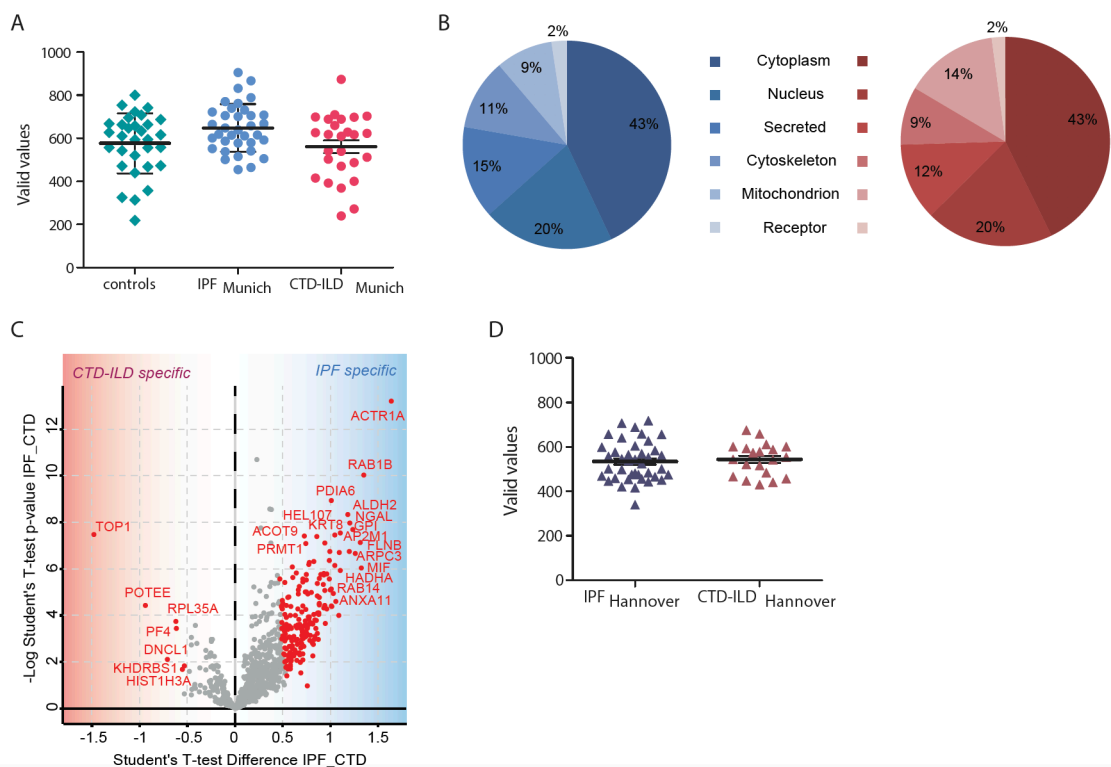


**Figure 26.** Protein quantification and identification of interstitial lung disease (ILD) associated autoantigens. **(A)** Number of quantified proteins in controls, idiopathic pulmonary fibrosis (IPF) and connective tissue disease related interstitial lung disease (CTD-ILD) (cohort 1). **(B)** Categories of proteins detected in IPF (left, blue colors) and CTD-ILD (right, red colors) from cohort 1 hardly differed in both diseases. **(C)** Volcano plot showing significantly different expressed genes in IPF and CTD-ILD without accounting for differences to healthy controls. Red colored points depict significantly enriched proteins (FDR <10%). **(D)** Number of quantified proteins in patients with IPF and CTD-ILD from cohort 2. Panel A, B and D taken and adapted from (Leuschner et al. 2021).

Consideration of only significantly enriched proteins (compared to controls), revealed a mean $\pm$ SD of 29 $\pm$ 56 antigens (ranging from 0 to 279) per patient in IPF and a mean $\pm$ SD of 12 $\pm$ 19 antigens (ranging from 0 to 101) in CTD-ILD in cohort 1 (Leuschner et al. 2021). On average, fewer autoantigens were detected in cohort 2 (IPF: 6 $\pm$ 5 antigens per patient; CTD-ILD: 6 $\pm$ 5 antigens per patient). The prevalence of autoantigens in IPF was not inferior than the prevalence in CTD-ILD: while all patients with IPF (from cohort 1 and cohort 2) had a mean $\pm$ SD number of autoantigens of 16 $\pm$ 40 per patient, patients with CTD-ILD (cohort 1 and 2) had a mean $\pm$ SD number of autoantigens of 9 $\pm$ 15 per patient (Figure 27 A) (Leuschner et al. 2021). A wide range of different autoantigens was found in IPF across both of the two cohorts: while the majority of antigens were solely detected in one or two patients, only a very small proportion of the identified antigens (<10%) were found in more than four patients (Figure 27 B) (Leuschner et al. 2021).

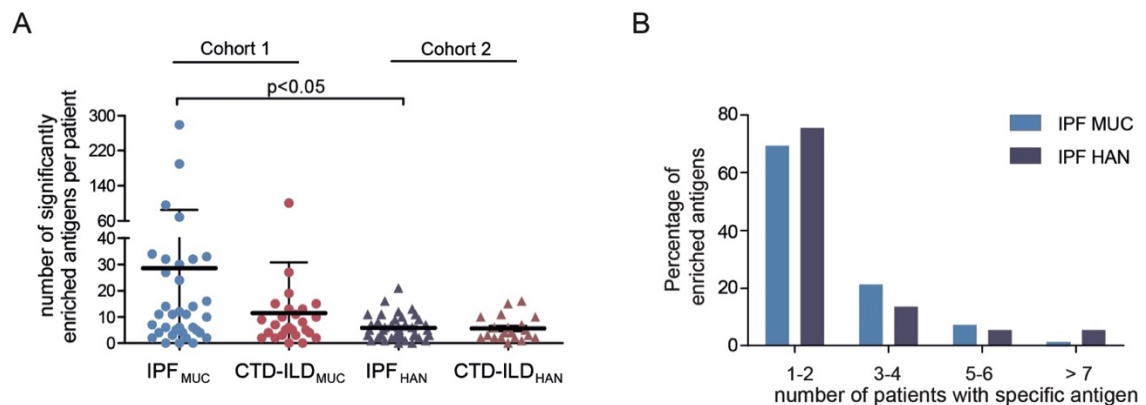


**Figure 27.** Significantly enriched antigens in patients from two independent cohorts. **(A)** The amount of identified potential autoantigens (significantly enriched) in patients with idiopathic pulmonary fibrosis (IPF) and connective tissue diseases related interstitial lung disease (CTD-ILD) from the Munich (cohort 1) and Hannover (cohort 2). Patients with IPF from Munich had the highest number of autoantigens. **(B)** The bar graph shows that in IPF most antigens were only detected in 1-2 patients, while only a small number of antigens were found in more than 7 patients. This distribution pattern was similar in Munich and Hannover. Figure and legend taken and adapted from (Leuschner et al. 2021)

Antigens that were most frequently identified in IPF patients from cohort 1 were RuvB-like 2 (28.6%;  $n=10$ ), Histone H3 (25.7%;  $n=9$ ) and Tubulin beta-8 chain (TUBB8; 25.7%;  $n=9$ ) (Leuschner et al. 2021). So far, anti-RuvB-like 1/2 antibodies were detected as novel biomarkers related to SSc with association to male gender, older age at disease onset, myositis overlap and diffuse cutaneous involvement (Kaji et al. 2014). Additionally, anti-RuvB-like 1/2 antibodies were also identified in SSc patients negative for anti-nuclear antibodies (Pauling et al. 2018). Yet, the role of anti-RuvB-like 2 in IPF is unknown as there are no data on it. Patients with RuvB-like 2 in this analysis were mainly male (70%) and were not characterized by clinical signs for SSc or autoimmune features. While no differences in FVC were observed in IPF patients from cohort 1 with and without antibodies against RuvB-like 2 and Histone H3, (Figure 28 A, B), antibodies against TUBB8 were associated with significantly higher FVC (Figure 28 C) (Leuschner et al.

2021). Concerning survival data, IPF patients from cohort 1 with the detection of RuvB-like 2 had a trend for a superior survival ( $p=0.052$ ; Figure 28 D) and patients with TUBB8 had in fact a significantly better transplant-free survival (Figure 28 E) (Leuschner et al. 2021). In patients with IPF from cohort 2, the most frequently identified autoantigens were Ficolin-3 (FCN3; 32.5%;  $n=13$ ), 60S ribosomal protein L35 (RPL35; 25%;  $n=10$ ) and Alpha-1-antitrypsin (SERPINA1; 22.5%;  $n=9$ ) (Leuschner et al. 2021). The presence of none of the antigens just listed was linked to differences in FVC (Figure 28 F - 28 H) (Leuschner et al. 2021). FCN3, which is found in lung and liver, is a protein which can activate the lectin pathway of the complement system (Endo et al. 2007, Munthe-Fog et al. 2009). Recently, it has been shown in humans, that an acute pulmonary inflammation caused by lipopolysaccharide leads to an increase of alveolar FCN3 (Plovsing et al. 2016).

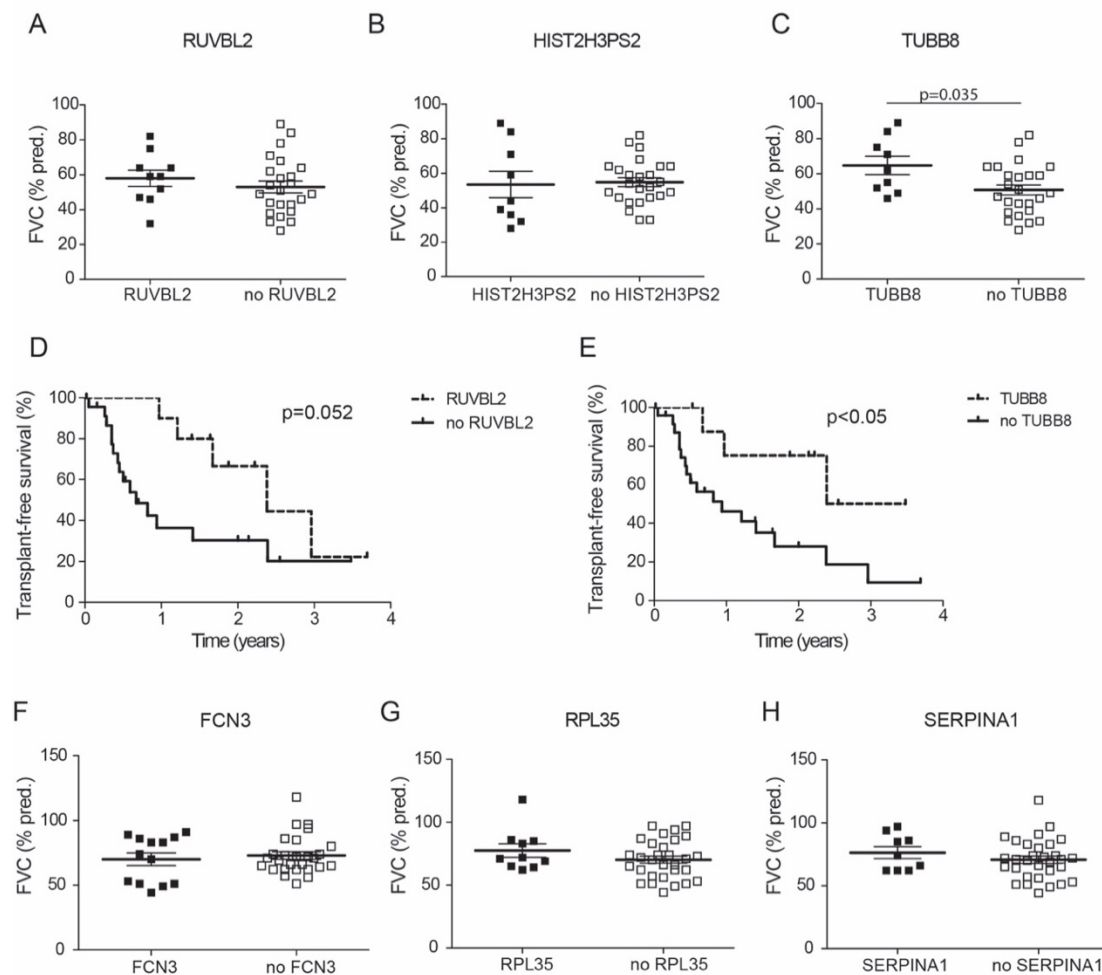


**Figure 28.** Most frequently identified autoantigens in idiopathic pulmonary fibrosis (IPF) from both cohorts. **(A-C)** In patients with IPF from the Munich cohort, RuvB-like 2 (RUVBL2) (A), Histone H3 (HIST2H3PS2) (B) and Tubulin beta-8 chain (TUBB8) (C) were the autoantigens which were most frequently detected. Differences in forced vital capacity (FVC) were only found in TUBB8 positive versus TUBB8 negative patients. **(D-E)** While the benefit for transplant-free survival for patients with RuvB-like autoantigens did not reach significance (D), the Kaplan-Meier survival showed a significantly longer time to death or transplantation for patients positive for TUBB8 (E). **(F-H)** In the Hannover IPF cohort, Ficolin-3 (FCN3) (F), 60S ribosomal protein L35 (RPL35) (G) and Alpha-1-antitrypsin (SERPINA1) (H) were most frequently detected but the FVC values were similar in patients positive and negative for the respective autoantigens. Figure taken and legend taken and adapted from (Leuschner et al. 2021).

There were essential variations across diagnoses and cohorts concerning the significantly increased autoantigens as the majority of autoantigens (66.6%) were either specifically found in IPF or CTD-ILD or in only one of the two cohorts (Figure 29): we identified 279 cohort- and ILD entity-specific autoantigens in IPF from cohort 1, 26 in IPF from cohort 2, 49 in CTD-ILD from cohort 1 and 13 in CTD-ILD from cohort 2, respectively (Leuschner et al. 2021).

The high number of individually identified autoantigens in patients with IPF from cohort 1 (50.6% of all identified antigens) was partially driven by four patients with a very high autoimmune signature (range 69 to 279 autoantigens per patient). Although these four patients had 240 antigens, which were significantly enriched in comparison to the other IPF patients from cohort 1 (Figure 30 A), clinically, they showed no signs for CTD-ILD or IPAF. Furthermore, FVC (Figure 30 B) and transplant-free survival (Figure 30 C) were similar to the other IPF patients from cohort 1.

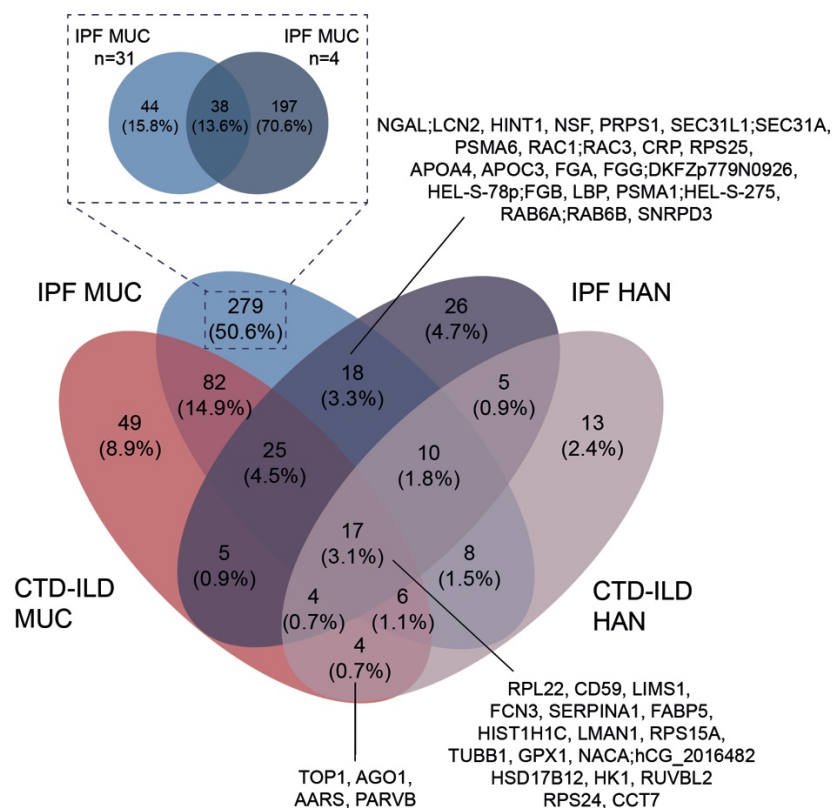


**Figure 29.** Common and individual autoantigens in idiopathic pulmonary fibrosis (IPF) and connective tissue diseases-related interstitial lung diseases (CTD-ILD). Individual and common autoantigens in IPF and CTD-ILD in the Munich and Hannover cohort are displayed in a Venn diagram. The dashed rectangle provides information about the composition of IPF-specific autoantigens (n=279) of cohort 1. The majority (70.6%) of autoantigens were exclusively derived from four patients with high autoimmune signature. Figure and legend taken and adapted from (Leuschner et al. 2021).



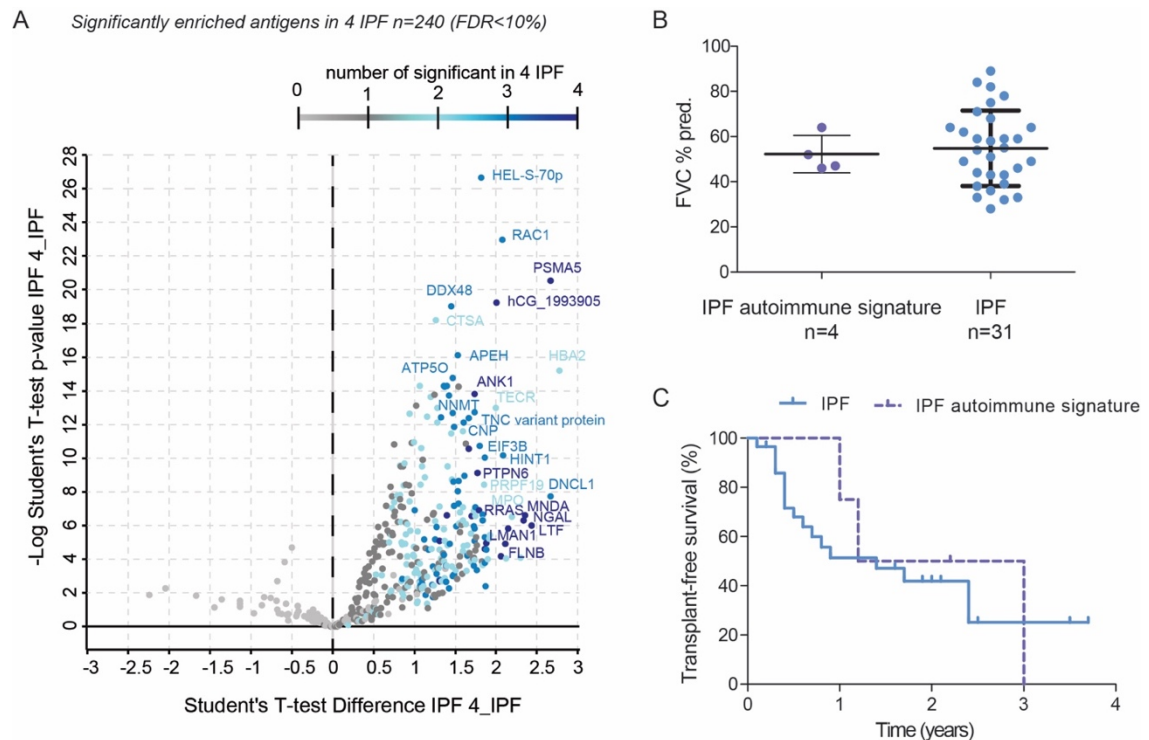


**Figure 30.** Subgroup of patients with idiopathic pulmonary fibrosis (IPF) from Munich and high autoimmune signature. **(A)** Volcano plot showing enriched antigens in four individual IPF patients in comparison to the other IPF patients from cohort 1. The color code indicates the number of patients (out of four) with significantly enriched antigen. **(B)** The forced vital capacity ( $FVC_{\%pred.}$ ) did not differ between the four IPF patients with high autoimmune signature and other IPF patients. **(C)** Transplant-free survival was similar between both IPF groups.

A subanalysis of IPF from cohort 1 showed that the four IPF patients with high autoimmune signature (see Figure 27 A and Figure 30) accounted for the majority (70.6%) of IPF-specific autoantigens (Figure 29, dashed rectangle). However, there were 18 (3.3%) autoantigens, which were shared and exclusively found in both IPF cohorts and 4 (0.7%) autoantigens, including TOP1, which were identified only in the two CTD-ILD cohorts (Figure 29) (Leuschner et al. 2021). Analyzing the distribution of the 18 IPF-specific autoantigens across patients with IPF from both cohorts, the least frequently detected autoantigens were present in two (2.7%) and the most frequently detected autoantigen was found in 9 patients (12.0%; Figure 31 A) (Leuschner et al. 2021). The most commonly identified autoantigen in IPF was Apolipoprotein A-IV (APOA4;  $n=9$ ), and in comparison to patients without APOA4 its detection was connected to a significantly better FVC ( $p=0.016$ ; Figure 31 B). None of the other IPF-specific autoantigens was associated with an elevated or reduced FVC in IPF patients (Figure 31 C - 31 Q) (Leuschner et al. 2021).

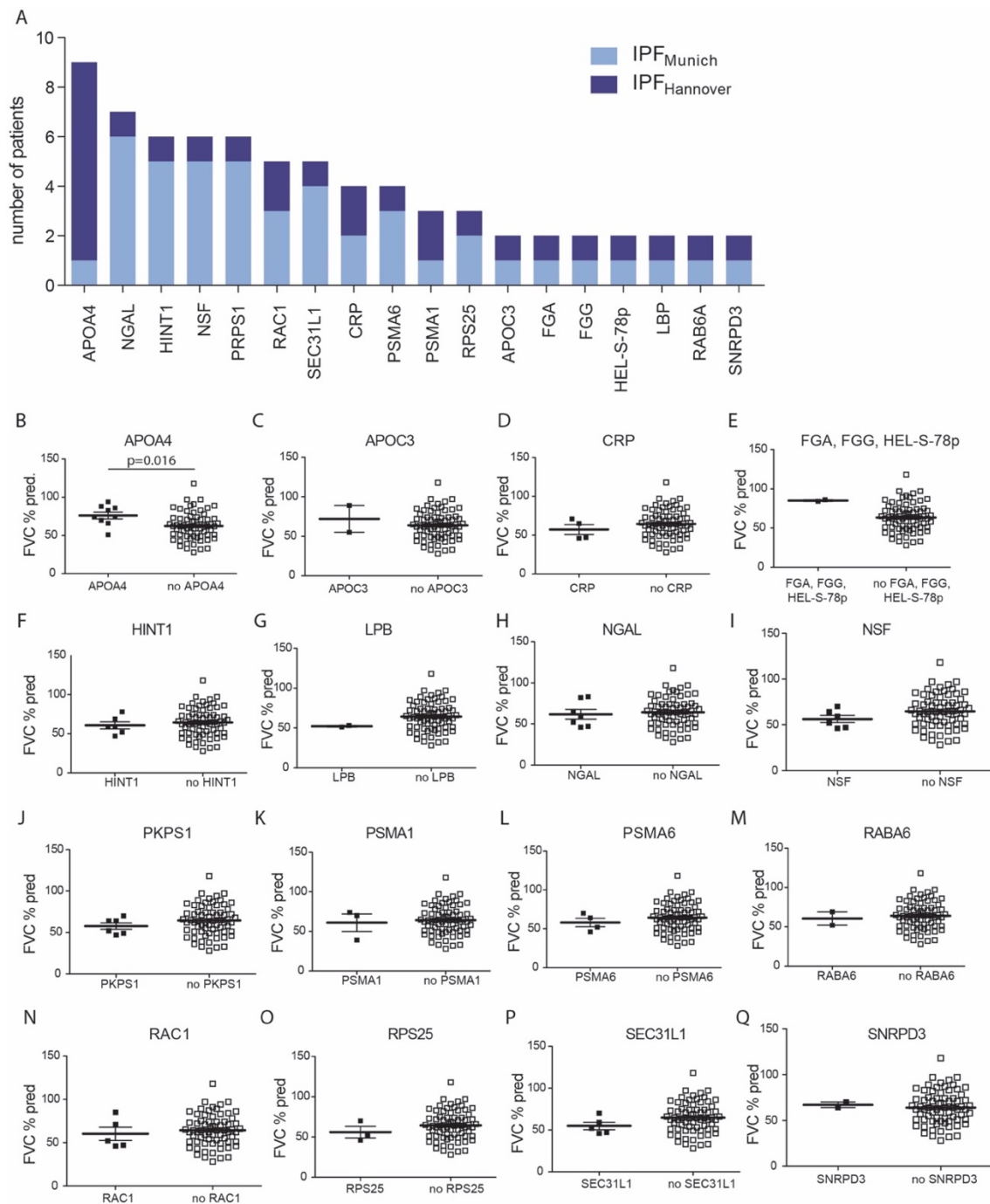


**Figure 31.** Identified autoantigens specific for idiopathic pulmonary fibrosis (IPF). **(A)** The bar graph shows all autoantigens specifically and exclusively detected in patients with IPF in two independent cohorts. The color code displays the distribution between Munich and Hannover. **(B)** Patients positive for Apolipoprotein A-IV (APOA4) had a higher forced vital capacity (FVC) than patients in whom APOA4 was not detected as autoantigen. **(C-Q)** The FVC showed no differences in patients with the respective autoantigen compared to all other IPF patients. Figure and legend taken and adapted from (Leuschner et al. 2021).

In addition to cohort- and entity-specific autoantigens, we also identified 17 shared autoantigens in all four groups (Figure 29). The most frequently shared and detected autoantigens were epidermal fatty acid-binding protein, FCN3 and SERPINA1 (Figure 32 A) (Leuschner et al. 2021).

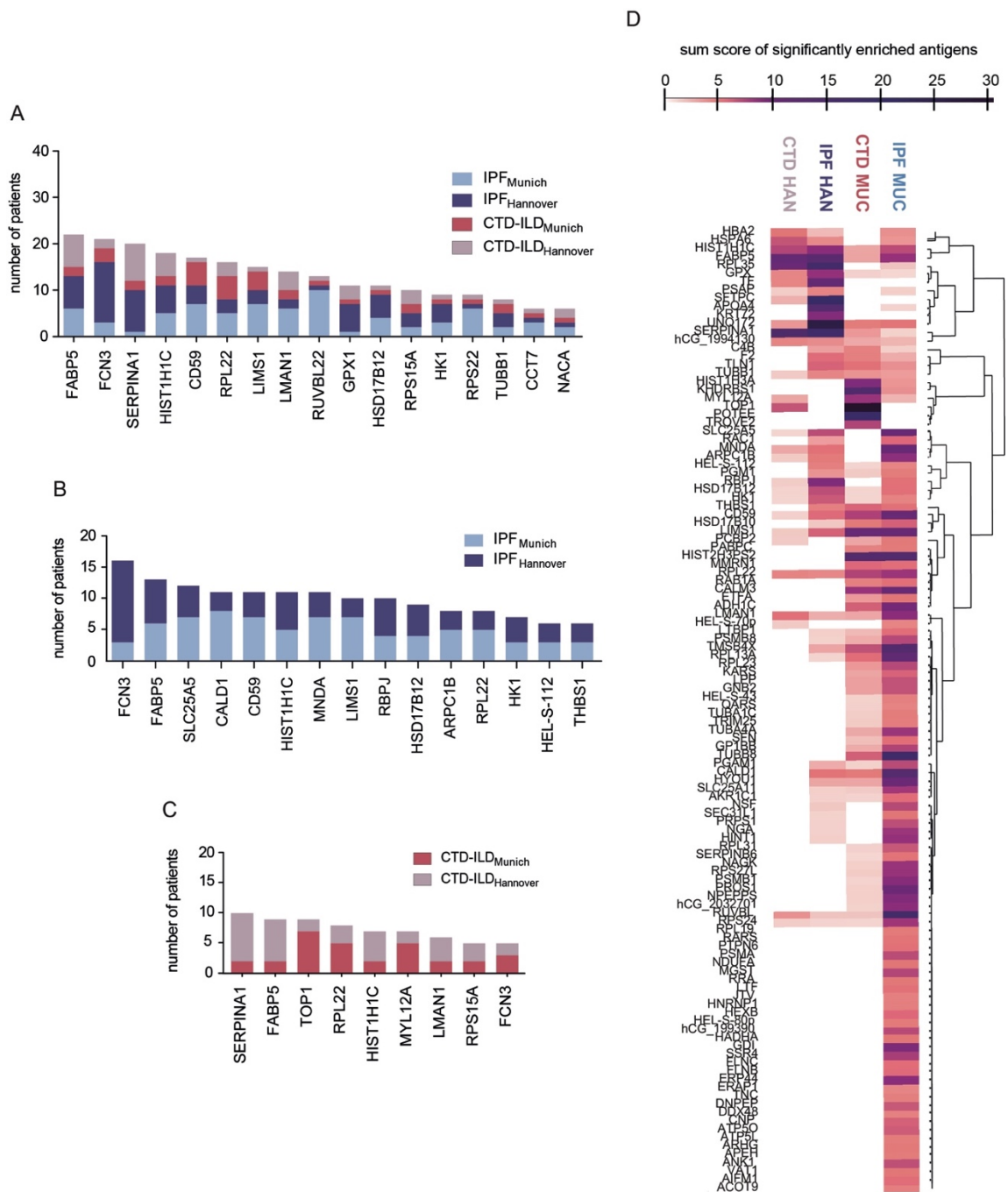


**Figure 32.** Most commonly identified autoantigens in idiopathic pulmonary fibrosis (IPF) and connective tissue disease related interstitial lung disease (CTD-ILD). **(A)** The bar graph pictures autoantigens which were shared between all patient groups from Munich and Hannover. The color code provides information about the frequency distribution within the groups. **(B)** Bar graph shows autoantigens that were found in at least three patients in both IPF groups and were therefore the most frequently identified autoantigens in IPF. **(C)** Bar graph shows autoantigens that were found in at least two patients in both CTD-ILD groups and were therefore the most frequently identified autoantigens in CTD-ILD. **(D)** All antigens which were detected in a minimum of three patients in one of the four groups are displayed in a heat map. The color code of these most commonly identified autoantigens gives information about the so called “sum score” which was derived from the Student’s *t* test statistics of significant proteins with FDR <10%. Arbitrarily, a minimum value of >4 was chosen which resulted in a number of 116 most frequently identified autoantigens. Figure and legend taken and adapted from (Leuschner et al. 2021).

To find out more about reproducibly occurring antigens in IPF, a threshold was now set that required an antigen being found in a minimum of three patients in both respective IPF cohorts. Using this threshold detected 15 autoantigens of which FCN3 was the most frequently identified (Figure 32 B) (Leuschner et al. 2021). Interestingly, none of these was exclusively found in IPF. Given the lower number of identified autoantigens, to repeat this approach for CTD-ILD, a threshold was set requiring an antigen being detected in a minimum of two patients in both respective CTD-ILD cohorts. Hereby, 9 autoantigens were found, whereby one of them was TOP1, which is CTD-ILD specific (Figure 32 C) (Leuschner et al. 2021). SERPINA1 was the most commonly present autoantigen in CTD-ILD.

Next, a sum score of Student's *t* test statistics of significantly enriched proteins (FDR<10%) was used for all antigens, that were found in a minimum of three patients in one of the four patient groups. Using an arbitrary limit of >4 for the sum score, 116 top autoantigens were detected with IPF patients from cohort 1 presenting the greatest autoantibody repertoire (Figure 32 D) (Leuschner et al. 2021).

In summary, using the DAC assay, a wide range of autoreactivity was identified in patients with IPF and CTD-ILD from two independent ILD-cohorts. Compared to CTD-ILD, the amount of autoreactive antibodies was not lower in IPF and detected autoantigens were common, disease- and cohort-specific. Yet, the burden of autoimmunity was very individual for each patient.

#### **4.2.5 Association between novel autoantigens and transplant free survival**

The generated autoantibody data were linked to clinical meta-data to determine a predictive potential and clinical relevance of detected autoantigens in IPF. In further analyses, only autoantigens were considered which were present in both IPF cohorts. Further, autoantigens had to be found in a minimum of three IPF patients to enable a statistical evaluation, requiring presence in at least two patients in one of the two cohorts. Following these requirements, 58 autoantigens were detected (Leuschner et al. 2021). Of note, in eleven patients (cohort 1: n=8; cohort 2: n=3) none of these autoantigens were identified. Kaplan-Meier survival analysis was individually performed for each of the respective 58 autoantigens, grouping patients in antigen positive or antigen negative. Combining cohort 1 and 2, the mean±SD follow-up was 1.7±1.1 years. During the follow-up, four patients from cohort 1 and ten patients from cohort 2 died. While 17 patients from cohort 1 underwent lung transplantation, no patient from cohort 2 underwent lung transplantation (Leuschner et al. 2021).

Combining IPF patients from both cohorts, detection of APOA4 or Glutathione peroxidase 1 (GPX1), a downstream antioxidant factor of the oxidative stress-related factors Nrf2/Bach1 (Liu

et al. 2017), was associated with a significantly better transplant-free survival (Leuschner et al. 2021). In contrast, patients who were positive for thrombospondin-1 (THBS1; n=6; 8.0%; p=0.002; Figure 33 A), tubulin beta-1 chain (TUBB1; n=5; 6.7%; p=0.019; Figure 36 B) and CD5L (n=3; 4.0%; p=0.0015; Figure 36 C) had significantly reduced transplant-free survival time compared to patients who had no evidence for the respective autoantigen (Leuschner et al. 2021). The glycoprotein THBS1 plays a role in matrix interactions and cell-to-cell communication (Lee et al. 2014). TUBB1 encodes the tubulin  $\beta$ -1 chain, which is one of nine beta-tubulin isotypes in mammals and majorly expressed in megakaryocytes and platelets (Burley et al. 2018). Along with alpha tubulins, beta tubulins are main components of microtubules, that are important elements of the eukaryotic cytoskeleton. Concerning the lung, beta tubulins are targets of a number of chemotherapeutic agents, including paclitaxel and vinca alkaloids (Zhou and Giannakakou 2005). CD5L, also known as apoptosis inhibitor of macrophage has been found in macrophages and inhibits apoptosis (Amezaga et al. 2014).

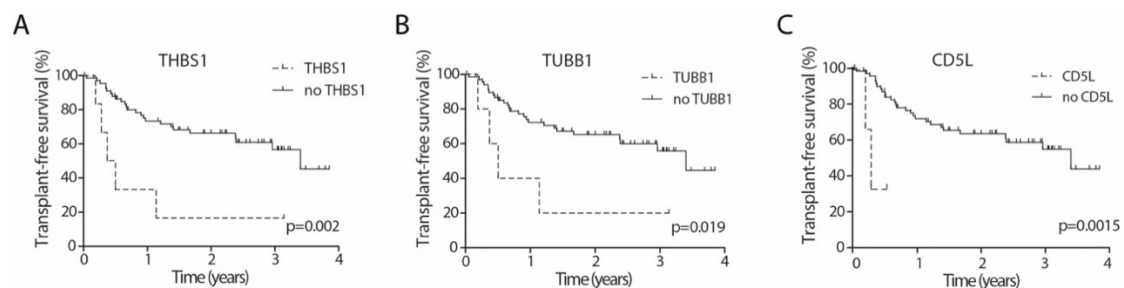


**Figure 33.** Kaplan-Meier curves for survival in patients with idiopathic pulmonary fibrosis (IPF) and specific autoantigens. **(A-C)** The presence of autoantibodies against thrombospondin-1 (THBS1) (A), tubulin beta-1 chain (TUBB1) (B), or CD5L (C) was associated with a shorter transplant-free survival. Figure and legend taken and adapted from (Leuschner et al. 2021).

Interestingly, while THBS1 was detected in six patients (cohort 1: n=3; cohort 2: n=3), five of these patients were concurrently positive for TUBB1 (cohort 1: n=2; cohort 2: n=3). In the multiple regression analysis THBS1 was an independent predictor for transplant-free survival when controlling for the cofounders age, FVC and gender (HR: 3.98; 95%-CI: 1.432-11.074; p=0.008; Table 8) (Leuschner et al. 2021). Separate Kaplan-Maier analysis of the two cohorts showed that patients positive for THBS1 had significantly shorter transplant-free survival in cohort 1 (p=0.0016) and cohort 2 (p=0.0319), respectively (Figure 34) (Leuschner et al. 2021). Controlling for the same cofounders (age, FVC and gender), corresponding results were seen for TUBB1 in the multiple regression analysis, as TUBB1 was also an independent predictor for mortality/lung transplantation (HR 3.469; 95%-CI: 1.150 - 10.464; p=0.027) (Leuschner et al. 2021). Since TUBB1 was indeed detected in three patients from cohort 2 but, in contrast to THBS1 only in two patients from cohort 1, no separate Kaplan-Meier analysis was carried out for both cohorts.

variable	HR	95%-CI	p-value
FVC	0.959	0.939 – 0.981	<0.001
Age	0.621	0.952 – 1.030	0.621
Gender	1.603	0.554 – 4.639	0.384
THBS1	3.98	1.432-11.074	<b>0.008</b>

**Table 8.** Multiple regression analysis in idiopathic pulmonary fibrosis (IPF) for transplant-free survival. Autoantibodies against thrombospondin-1 (THBS1) are an independent predictor for transplant-free survival. Table taken and legend taken and adapted from (Leuschner et al. 2021).

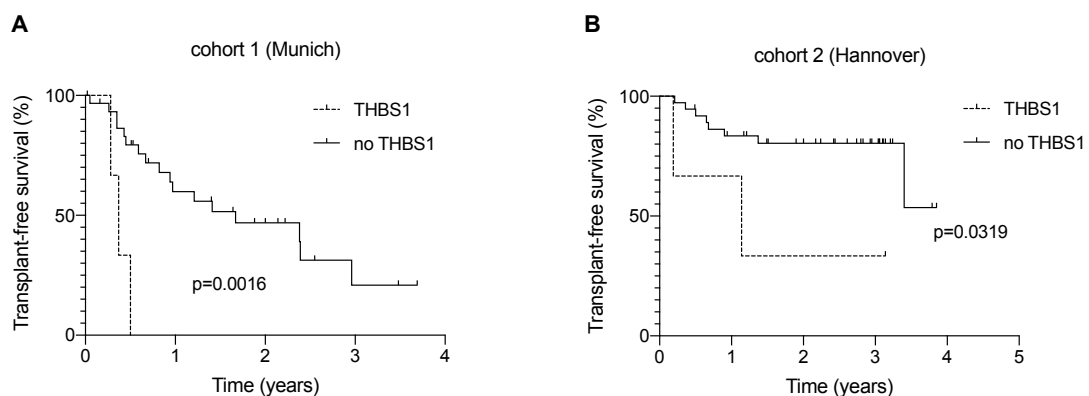


**Figure 34.** Kaplan-Meier curves for transplant-free survival in patients with idiopathic pulmonary fibrosis (IPF) either positive or negative for thrombospondin-1 (THBS1) autoantibodies. In patients with autoantibodies against THBS1, survival was shorter in both the Munich (A) and the Hannover cohort (B), respectively. Figure and legend taken and adapted from (Leuschner et al. 2021).

Next, given the co-expression of THBS1 and TUBB1 associated with a greater risk for mortality/lung transplantation, autoimmune profiles and shared autoantigen repertoires should be identified. Hierarchical clustering was used to display IPF patients from cohort 1 and cohort 2 which uncovered again the broad, individual heterogeneity of autoantigens (Figure 35) (Leuschner et al. 2021). Two major gene clusters dominated in the depiction, one of which comprised 20 distinct autoantigens (cluster 1) depicting 13 patients (cohort 1: n=11; cohort 2: n=2) and one of which was based on six autoantigens (cluster 2) depicting a group of six patients (cohort 1: n=3; cohort 2: n=3). The six genes from cluster 2 were Zyxin (ZYG), epididymis secretory protein Li 112 (HEL-S-112), Latent-transforming growth factor beta-binding protein 1

(LTBP1), TUBB1, THBS1 and Talin 1 (TLN1) (Leuschner et al. 2021). LTBP1 plays a role in the TGF- $\beta$  signalling (Miyazono et al. 1991). TLN1 is a cytoplasmic protein that participates in the conformation of the integrin lymphocyte function-associated antigen-1, which in turn induces slow rolling and arrest of neutrophils (Lefort et al. 2012).

Patients were now grouped using a principal component analysis (PCA) of the values of the Z-scored Student's *t* test statistics of the 58 autoantigens. The PCA separated one patient group (PCA group 1) in component 1, that explains 21.3% variability of the data. A second patient group (PCA group 2), that is responsible for 7.8% variability of the data, was separated in component 2 (Figure 36 A) (Leuschner et al. 2021). Of note, the patients in the PCA group 1 (cohort 1: n=8; cohort 2: n=3) were all included in cluster 1 in der hierarchical clustering (Figure 35). Similarly, six of the nine (66.7%) patients from PCA group 2 (cohort 1: n=4; cohort 2: n=5) were from cluster 2 in the hierarchical clustering (Figure 35). With the help of a scatter plot which displays the loading proteins of the respective PCA component it could be shown that component 1 was mainly driven by T-complex protein 1 subunit eta (CCT7), histidine triad nucleotide-binding protein 1 (HINT1), myeloid cell nuclear differentiation antigen (MNDA), vesicle-fusing ATPase (NSF), proteasome subunit alpha type-6 (PSMA6), Ras-related protein Rac1 (RAC1), 40S ribosomal protein S25 (RPS25), protein transport protein Sec31A (SEC31L1) and signal transducer and activator of transcription 3 (STAT3), which were all part of the heat map cluster 1 except for Ras-related protein Rac1 (Figure 36 B) (Leuschner et al. 2021). Component 2 was enriched for TUBB1, THBS1, TLN1, LTBP1, ZYX, epididymis secretory protein Li 112 (HEL-S-112), the LIM and senescent cell antigen-like-containing domain protein 1 (LIMS1) and caldesmon, which were all part of cluster 2 of the hierarchical cluster except for the last two mentioned autoantigens (Figure 35). Kaplan-Meier analysis showed similar transplant-free survival curves for patients from PCA-group 1 and all other IPF patients from the two cohorts (Figure 36 C) (Leuschner et al. 2021). In contrast, the transplant-free survival of patients included in PCA-group 2 was significantly shorter compared to other IPF patients (median survival 0.9 years versus 3.4 years;  $p=0.046$ ; Figure 35 D) (Leuschner et al. 2021). There were neither significant differences in terms of age ( $p=0.282$ ) nor in FVC ( $p=0.155$ ) between patients from PCA group 2 and all the other IPF patients.

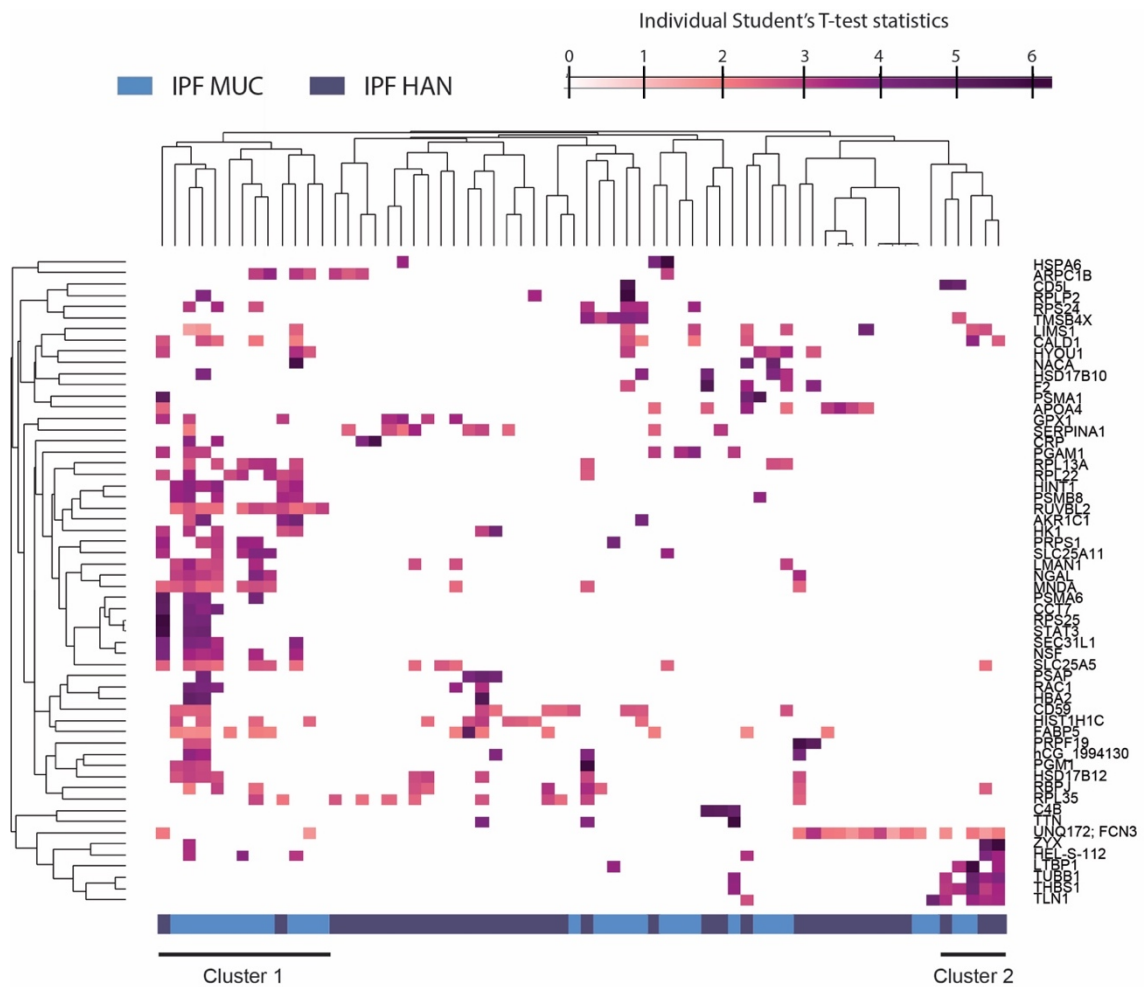


**Figure 35.** Hierarchical clustering of potential autoantigens in idiopathic pulmonary fibrosis (IPF). Hierarchical clustering displays 58 genes. These had to be (1) present in IPF patients from Munich and Hannover and (2) detected in a minimum of two patients in one of the two groups. Two autoantigen clusters were identified (cluster 1 and cluster 2). Figure and legend taken and adapted from (Leuschner et al. 2021).



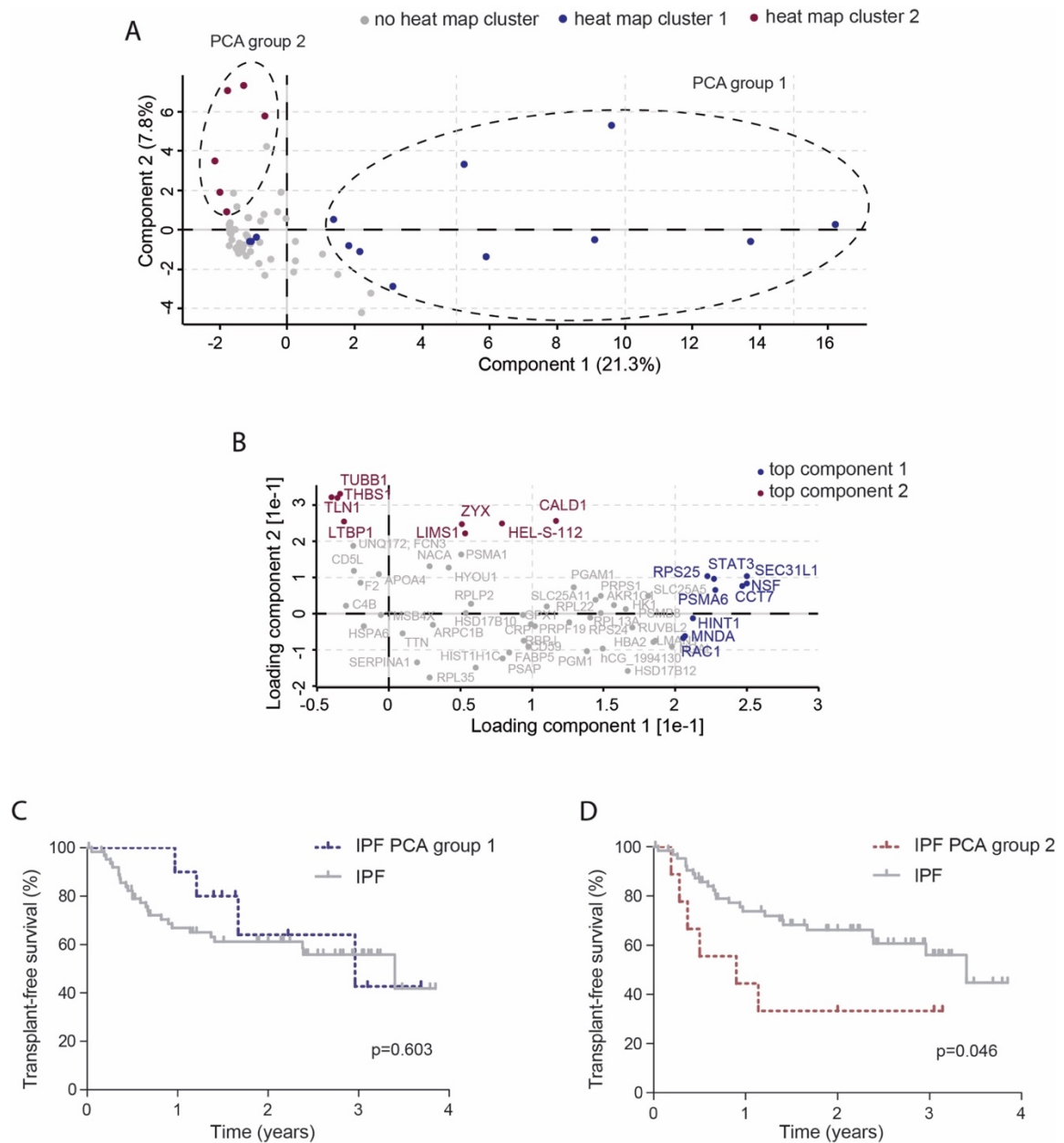


**Figure 36.** Potential predictive autoantigens in idiopathic pulmonary fibrosis (IPF). **(A)** Grouping of patients based on the same 58 proteins as used in Figure 35 by a principal component analysis (PCA). **(B)** The loadings of component 1 and 2 of the PCA from panel A are displayed with a color code for the top antigens of component 1 (blue) and component 2 (purple). **(C)** The survival curve of patients from PCA group 1 is similar to all other IPF patients. **(D)** Kaplan-Meier curve identifies IPF patients from PCA group 2 as having a significantly reduced transplant-free survival. Figure and legend taken and adapted from (Leuschner et al. 2021).

To assess if similar to the IPF cohort associations between autoimmune profiles and survival can be found for CTD-ILD, the data from patients with CTD-ILD from both cohorts were integrated with clinical meta-data. Likewise, autoantigens were only included in this analysis, if they were found in both CTD-ILD cohorts and in one of the both cohorts the respective antigen had to be present in at least two patients. Using this approach, in total, 19 autoantigens were identified. Seven patients had none of these 19 autoantigens. The mean $\pm$ SD follow-up of CTD-ILD patients was 4.2 $\pm$ 6.6 years. During the follow-up two patients from cohort 1 underwent lung transplantation and two patients from cohort 2 died. Performing Kaplan-Meier analysis for transplant-free survival, the presence of Protein argonaute-1 (AGO1) and FCN3 was linked to a significantly worse transplant-free survival in CTD-ILD ( $p=0.022$  and  $p=0.037$ , respectively; Figure 37 A and 37 B). A heat map of the 19 autoantigens identified four clusters of patients (Figure 38). Cluster 1 (cohort 1:  $n=4$ ; cohort 2:  $n=4$ ) was mainly based on Apolipoprotein E, cytoplasmatic Alanine-tRNA ligase, and Histone H1.2, cluster 2 (cohort 1:  $n=2$ ; cohort 2:  $n=3$ ) was primarily driven by SERPINA1, Interferon alpha-inducible protein 6, Nascent polypeptide-associated complex subunit alpha (NACA) and FCN3, cluster 3 (cohort 1:  $n=1$ ; cohort 2:  $n=5$ ) consisted of poly(rC)-binding protein 2, HCG1994130, isoform CRA\_a (hCG\_1994130), Protein ERGIC-53 (LMAN1), 60S ribosomal protein L22 and epidermal fatty acid-binding protein and cluster 4 (cohort 1:  $n=5$ ; cohort 2:  $n=1$ ) was related to AGO1, TOP1, myosin regulatory light chain 12A (MYL12A), TUBB1 and GPX1.

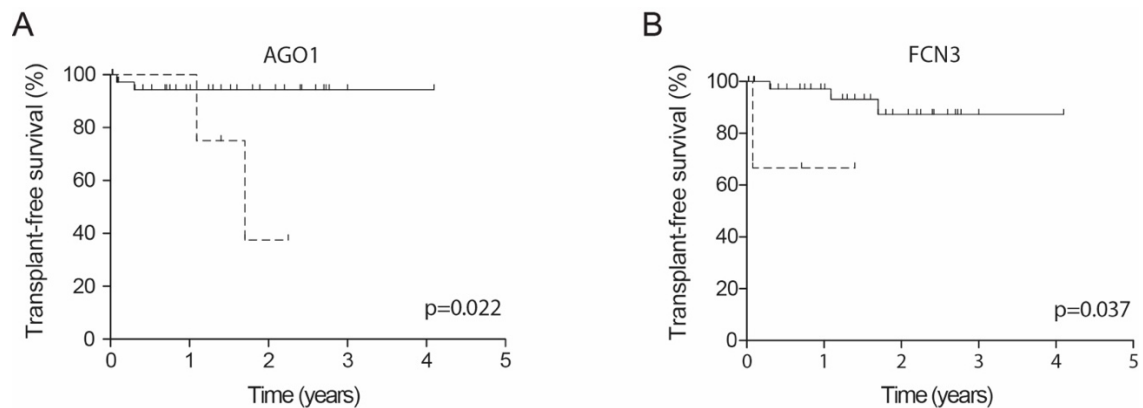


**Figure 37.** Kaplan-Meier curves for survival in patients with connective tissue disease related interstitial lung disease (CTD-ILD) and specific autoantigens. **(A-B)** The presence of autoantibodies against Protein argonaute-1 (AGO1) (A) and Ficolin-3 (FCN3) (B) was associated with a shorter transplant-free survival. Patients with the respective autoantigen are shown with dashed line.

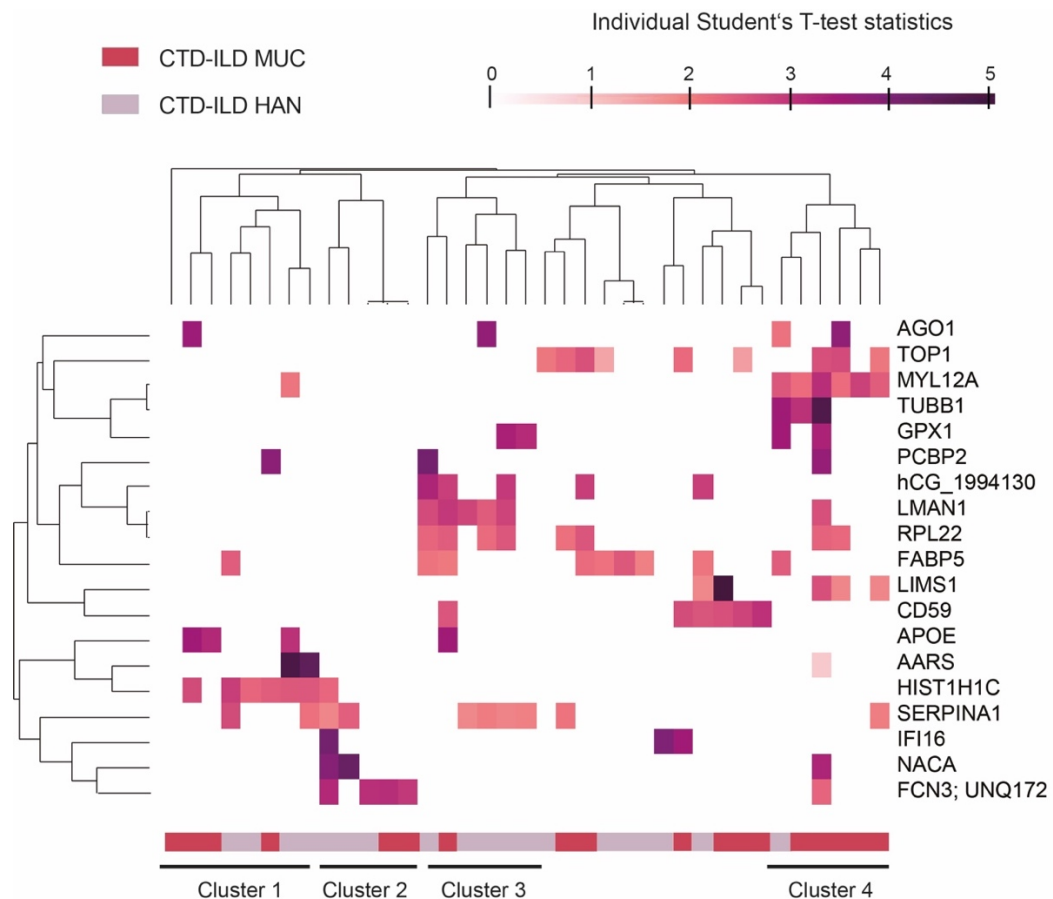


**Figure 38.** Hierarchical clustering of 19 potential autoantigens in patients with connective tissue disease related interstitial lung disease (CTD-ILD). The autoantigens had to be (1) present in CTD-ILD patients from Munich and Hannover and (2) detected in a minimum of two patients in one of the two groups. The clustering depicts four distinct autoantigen-cluster (cluster 1-4).

The Z-scored Student's *t* test statistics were used to generate a PCA of the 19 identified autoantigens. The analysis revealed three distinct patient groups in component 1, which was responsible for 17.2% of the variability of data and component 4, which explained 9.3% of the data variability (Figure 39 A). The PCA group 1 identified 4 patients, all from heat map cluster 4, the PCA group 2 consisted of five patients, all from heat map cluster 3 and the PCA group 3 depicted eight patients, of which five were from heat map cluster 2. The loadings are displayed using a scatter plot (Figure 39 B) and showed that component 1 was mainly enriched for genes from heat map cluster 3 and 4, namely HCG1994130, isoform CRA\_a (hCG\_1994130), Protein ERGIC-53 (LMAN1), poly(rC)-binding protein 2, 60S ribosomal protein L22, GPX1, TOP1, TUBB1, LIMS1 and myosin regulatory light chain 12A (MYL12A). Component 2 was enriched for IFI16, SERPINA1, FCN3 and nascent polypeptide-associated complex subunit alpha, all of which corresponded to the genes from the heat map cluster 2. Kaplan-Meier analysis identified patients from the PCA group 1 and 3 as having significantly worse transplant-free survival ( $p=0.013$  and  $p=0.001$ , respectively; Figure 39 C and 39 E), whereas the PCA group 2 showed no significantly different time to death or transplantation in comparison to the remaining CTD-ILD patients (Figure 39 D).

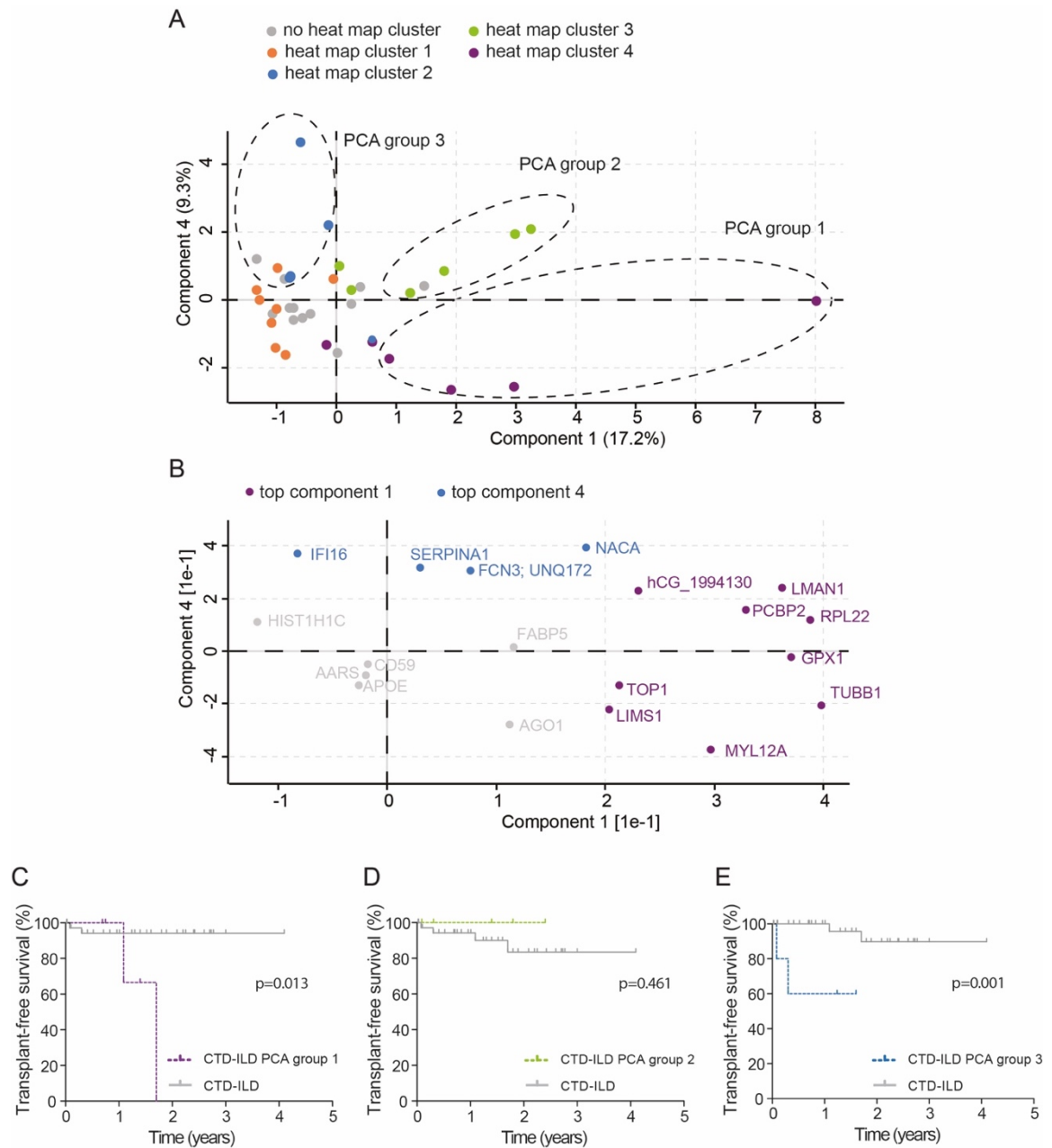


**Figure 39.** Identification of predictive autoantigens in connective tissue disease related interstitial lung disease (CTD-ILD). **(A)** Based on component 1 and component 4, a principal component analysis (PCA) of the same 19 proteins as used in Figure 38 distinguishes three different groups of patients. **(B)** The loadings of component 1 and 4 of the PCA from panel A are displayed with a color code for the top antigens of component 1 (purple) and component 4 (blue). **(C)** Kaplan-Meier curve depicts CTD-ILD patients from PCA group 1 as having a significantly worse transplant-free survival. **(D)** Survival of CTD-ILD patients from PCA cluster 2 is similar to all other CTD-ILD patients. **(E)** Patients from PCA cluster 3 have a significantly shorter time to death or transplantation according to Kaplan-Meier curves.

In addition to the identification of potential autoantigens, a significant number of V-segments derived from immunoglobulin variable regions were identified in the study population. Using an ANOVA test, in cohort 1, 39 V-segments (Figure 40 A), and in cohort 2, 47 V-segments (Figure 40 B) were identified as significantly different in IPF in comparison to CTD-ILD. Of these, the V2-15 protein was identified in both cohorts and showed a high specificity for IPF: V2-15 was only identified in IPF patients in cohort 1 ( $n=5$ ; 14.3%) and in cohort 2, it was only identified in IPF ( $n=9$ ; 22.5%) but one CTD-ILD, where it was found in 2/3 measurements. While the Kaplan-Meier survival analysis revealed a significantly shortened time interval to death or transplantation in V2-15 protein positive IPF patients from Munich, there were no significant differences observed in patients from Hannover (Figure 40 C).

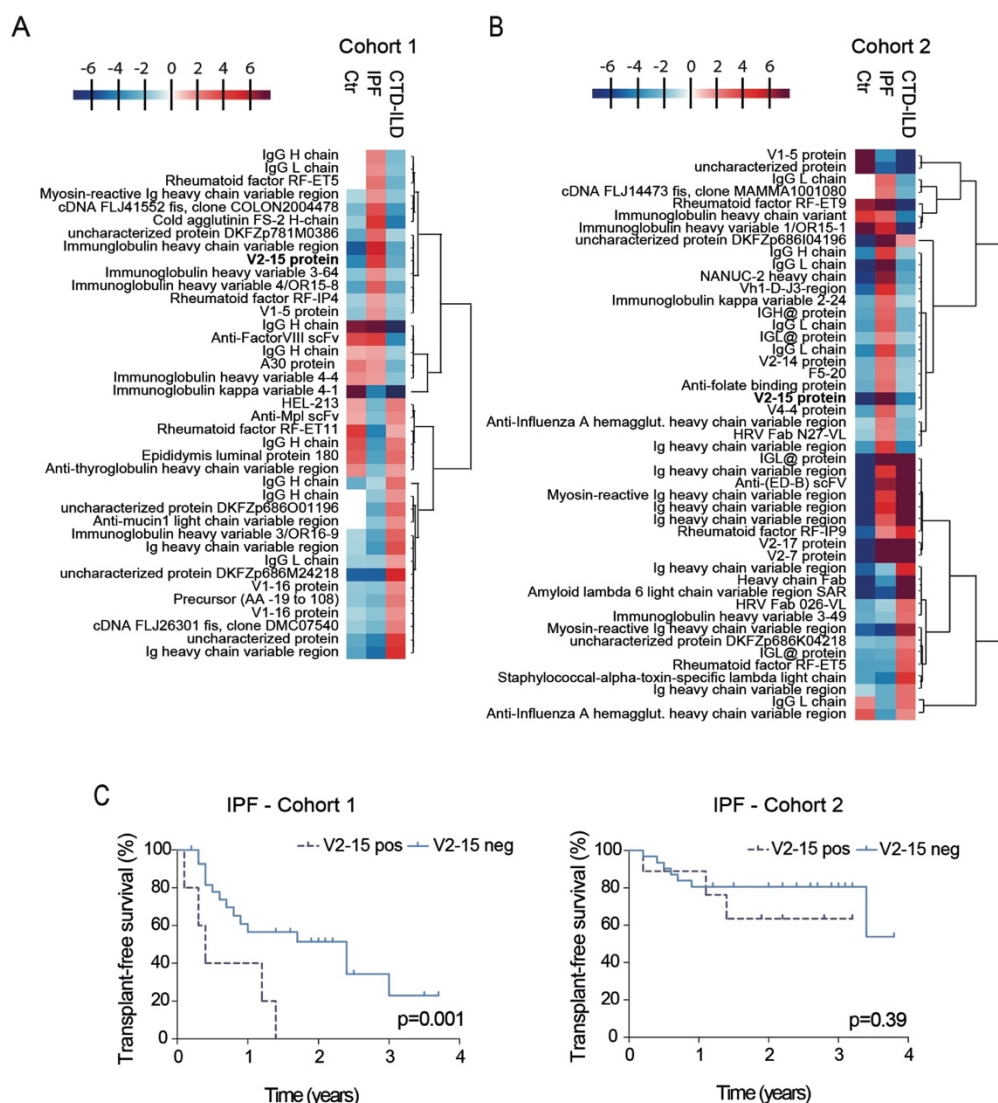


**Figure 40.** Analysis of autoantibodies reveals differential V-segment usage in idiopathic pulmonary fibrosis (IPF) and connective tissue disease related interstitial lung disease (CTD-ILD). **(A-B)** Hierarchical clustering of ANOVA-significant V-segments in patients with IPF and CTD-ILD from Munich (A) and Hannover (B). The color code depicts ANOVA significance. **(C)** Survival in cohort 1 and 2 in V2-15 protein positive and negative IPF patients.

In summary, integrating clinical data to findings from the DAC assay identified 58 autoantigens that were robustly found in IPF patients from Munich and Hannover. The merger of cohort 1 and cohort 2 identified two antigens, which were predictors of transplant-free survival in multiple regression analysis: THBS1 and TUBB1. Additionally, patients positive for THBS1 were found to have significantly shorter survival when analyzing cohort 1 and cohort 2 separately indicating reproducible predictive results. Moreover, an autoimmune signature consisting of several genes was found to be linked to a significantly reduced survival in IPF. Using the same approach for CTD-ILD, 19 autoantigens were robustly detected in both cohorts. Similar to the findings in IPF, two autoimmune signatures were linked to significantly shorter time to death or lung transplantation in CTD-ILD. Furthermore, a high number of V-segments were found in the analysis in IPF and CTD-ILD revealing differential V-segment usage in both diseases.

### 4.2.6 Discussion

Until now the exact genesis of IPF is not completely enlightened but the diagnosis requires the exclusion of other ILDs such as autoimmunity-related, CTD-ILD (Raghu et al. 2018). Still, we and others have shown that there might be B cell mediated autoimmunity involved in IPF (Xue et al. 2013, Vuga et al. 2014, Schiller et al. 2017). To learn more about immune tolerance break our work intended to utilize an unbiased approach for the analysis of antibody mediated autoimmunity in ILD. Therefore, a DAC assay was established, which enables the identification of a wide range of autoreactivity in both, CTD-ILD and IPF. Surprisingly, patients with CTD-ILD did not show a higher prevalence of autoreactive antibodies (Leuschner et al. 2021). Further, a broad number of the identified autoantigens were not disease specific but shared between IPF and CTD-ILD. The analysis detected new autoantigens in patients with IPF and CTD-ILD. Interestingly, these included autoantigens that were found robustly in two independent cohorts and were associated with a shorter transplant-free survival (Leuschner et al. 2021).

Type 2 immunity, which is primarily observed in inflammation caused by allergic reactions or infections with parasites, can contribute to pathological fibrosing processes in many different organ systems including the lung (Gieseck et al. 2018). Characteristic of type 2 immunity is the generation and secretion of the interleukins IL-4, IL-5, IL-9 and IL-13 and accompanying cells including B cells, T helper 2 cells, basophils, mast cells, eosinophils, group 2 innate lymphoid cells and macrophages which can be activated by IL-4 and IL-13 (Nakayama et al. 2017, Gieseck et al. 2018). Type 2 immunity plays a role in regular repair mechanisms in human tissues and if these become dysregulated, exaggerated or chronic this can potentially lead to organ fibrosis such as ILD (Gieseck et al. 2018). A central feature of type 2 immunity is the B cell-mediated production of antibodies (Allen and Sutherland 2014). This is not only essential for host defense (as needed in a (re-) infection with parasites) but may also play a role in tissue repair processes (Esser-von Bieren et al. 2013, Leuschner et al. 2021). The continuous damage of the tissue and the resulting activation of cytokines profiles in chronic organ injury could induce a duplication of autoreactive germinal centers, which additionally intensifies the autoimmune reaction and ultimately causes tissue fibrosis which is irreversible (Degn et al. 2017). So far, neither is there data on such a scenario in patients with ILD nor is it known if there are other ILD entities than CTD-ILD which have an association with the production of antibodies. Compared to other currently used workflows the DAC developed in this project is highly competitive and can contribute important new findings in many ways: First, a big advantage is the fact that for the workflow only little amounts of plasma or serum is needed (20-50  $\mu$ l per patient) (Leuschner et al. 2021). Second, an unbiased approach was pursued using MS technology, and the complete proteome of diseased and healthy lung tissue from which autoantigens could be identified by immunoprecipitation. Compared to targeted assays this allowed a more comprehensive and higher throughput screening. Third, autoantigens can result from diseases associated posttranslational protein modifications, which are difficult to approach using methods based on recombinant proteins such as in targeted assays. Therefore, the MS data of this project were

checked for posttranslational protein modifications in the identified autoantigens (Leuschner et al. 2021).

A major finding of this study was the wide range of different autoantigens in IPF and CTD-ILD including shared, disease specific, cohort specific and individually expressed autoantigens (Leuschner et al. 2021). In IPF, while 12% of the patients had only one or none autoantibodies, another 12% had more than 30 different autoantigens. Most of these autoantigens were only detected in one or two patients which emphasizes the great individuality among patients. That in turn showed that most of the autoantigens were only found in IPF or CTD-ILD of one cohort with almost 200 autoantigens being exclusively expressed in four individual IPF patients. Only 18 autoantigens were robustly detected as “IPF-specific” since they were identified in IPF patients from Munich and Hannover but not in any of the patients with CTD-ILD in either cohort. Interestingly, of these, only APOA4 was associated with differences in FVC. APOA4 was found in 12% of IPF patients and these patients had a significantly better FVC in comparison to the remaining IPF patients. Although, so far, no link between APOA4 and lung fibrosis has been made, there is data that plasma APOA4 is elevated in early liver fibrosis (Wang et al. 2017).

Interestingly, 58 autoantigens were robustly identified by the DAC assay in patients with IPF in two independent clinical cohorts. It should be noted that these included both, IPF-specific and non-IPF-specific antigens. Of these, autoantibodies against CD5L, THBS1 and TUBB1 were associated with significantly worse survival. TUBB1 showed a co-expression with THBS1 of 100% and both were independent predictors for survival (adjusted for gender, age and FVC). THBS1 was present in 8% of IPF patients but not IPF-exclusive, since it was also found in 7% of CTD-ILD (Leuschner et al. 2021). THBS1 is present in different cells including platelets, endothelial cells, vascular smooth muscle cells, fibroblasts and macrophages (Ide et al. 2008). The glycoprotein has various properties which include a role in wound healing as well as stimulation and inhibition of angiogenesis and tumor growth (Bornstein 1995). Apart from that THBS1 appears to have significant activating properties for the TGF- $\beta$ 1 pathway (Crawford et al. 1998, Murphy-Ullrich and Poczatek 2000, Leuschner et al. 2021). Furthermore, THBS1 seems to be involved in epithelial regeneration in lung injury as THBS-1 deficient mice lack sufficient repair mechanisms in case of alveolar injury (Lee et al. 2014). Hence, it should be discussed whether THBS1 plays a key role in the development of fibrotic diseases. There is even evidence that THBS1 might be of predictive value in IPF. First, compared to controls and patients with sarcoidosis, THBS1 plasma levels are not only significantly elevated in patients with idiopathic interstitial pneumonia, including IPF, but also correlate inversely with FVC (Ide et al. 2008). The finding of elevated THBS1 plasma levels in IPF in comparison to controls was validated very recently in samples from patients included in the Idiopathic Pulmonary Fibrosis Prospective Outcomes (IPFPRO) Registry using aptamer-based proteomics (Todd et al. 2019). Furthermore, THBS1 was found to be significantly reduced in lung tissue of IPF patients in comparison to healthy controls (Murray et al. 2017). The results from this project are supporting the theory of a role of THBS1 in IPF, as autoantibodies against THBS1 were robustly found in two independent IPF cohorts. Further, THBS1 was an independent predictor for transplant-free survival in this



study. The coexpression of THBS1 and TUBB1 autoimmunity was unambiguously. Clustering of genes further identified a group of autoantigens associated with the THBS1/TUBB1 profile, including TLN-1, LTBP1, epididymis secretory protein Li 112 (HEL-S-112), ZYX, LIMS1 and caldesmon. Like THBS1, some of these proteins seem to have associations to fibrotic diseases (Leuschner et al. 2021). LTBP1 is crucial for the correct creation and release of TGF- $\beta$ 1, which in turn appears to affect the occurrence of LTBP1 (Miyazono et al. 1991, Taipale et al. 1994, Koski et al. 1999). While the relationship between THBS1 and TGF $\beta$  has been discussed above, it is unclear if THBS1 interacts directly with LTBPs. Interestingly, TLN-1 and ZYX have both been characterized as focal adhesion markers, which are reduced on the protein level in primary human fibroblasts that were cultured on 3D-lung tissue cultures compared to 2D plastic dishes (Burgstaller et al. 2018). In addition to autoantigens associated with worse survival, using clinical meta-data, APOA4 and GPX1 were characterized as autoantigens with a beneficial predictive capability in IPF. APOA4, which was one of the IPF-specific autoantigens, was not only associated with better lung function but also with a more favorable survival in IPF. As mentioned above, so far, there is no evidence of a connection between lung fibrosis and APOA4. GPX1, which is among others a downstream antioxidant factor of the oxidative stress-related factors Nrf2/Bach1, has recently been shown to be decreased in mouse lung fibroblasts after treatment with pirfenidone on mRNA and protein level (Liu et al. 2017).

In CTD-ILD, only four robustly detected “CTD-ILD specific” autoantigens were identified, including TOP1. Of the 19 autoantigens, that were detected in both CTD-ILD cohorts regardless of the entity specificity, AGO1 and FCN3 were associated with a significantly worse survival. AGOs have been studied in mammals mainly for their cytoplasmic role in the biogenesis of small RNA (Muller et al. 2019). AGO1 is a major component of the RNA induced silencing complex (MacRae et al. 2008), which can be programmed to target nucleic acid sequences and regulate gene expression (Pratt and MacRae 2009). A study on miRNA expression patterns in IPF revealed that in human lung biopsies of slow and rapidly progressing IPF, AGO1 was significantly reduced in comparison to healthy controls (Oak et al. 2011). In our study, AGO1 was exclusively detected as significant autoantigen in CTD-ILD of both cohorts and no IPF patient. In contrast, FCN3 was not CTD-ILD specific but also expressed in several IPF patients. Nevertheless, in IPF, there was no survival difference in FCN3 positive and FCN3 negative patients. FCN3, also called Hakata antigen, has the ability to activate the complement system via the lectin signaling (Endo et al. 2007). Together with the classical and the alternative pathway, the lectin pathway is one of the three pathways that can activate the complement system, which has a crucial role in the innate immune system. FCN3 is present in the human lung and liver (Akaiwa et al. 1999), with the highest expression pattern in the lung in comparison to other ficolins (Hummelshoj et al. 2008). In the lung, FCN3 is produced in ciliated bronchial epithelial cells and alveolar epithelial cells type II, from where it is secreted into the bronchus and alveolus (Akaiwa et al. 1999). It has a high potential to activate the complement pathway (Hummelshoj et al. 2008). A case report of homozygote FCN3-deficiency characterized a 32-year old man with, among other conditions, recurrent severe pulmonary infections developing severe bronchiectasis and pulmonary fibrosis

(Munthe-Fog et al. 2009). Further, Miyagawa et al. found that although serum levels of FCN3 did not differ in control subjects and patients with SSc, decreased levels of FCN3 were linked to a greater prevalence of ILD (Miyagawa et al. 2017). As FCN3 serum levels correlated inversely with ground glass opacity in SSc, the authors assumed a role of FCN3-related innate immunity in the development of ILD in patients with SSc. Interestingly, Using the DAC assay in this study, FCN3 was not only detected in SSc but also patients with rheumatoid arthritis and CREST syndrome. Further, using the CTD-ILD cohorts from Munich and Hannover, FCN3 was associated with IFI16, SERPINA1, and nascent polypeptide-associated complex subunit alpha. A second autoimmune signature was based on GPX1, TUBB1, TOP1, myosin regulatory light chain 12A (MYL12A) and LIMS1. CTD-ILD patients from one of these autoimmune profile groups had a significantly worse survival. As an association of TUBB1 and LIMS1 with worse survival was already seen in IPF patients, but GPX1 was rather associated with better survival in IPF, this displays again common and diverse roles of autoimmunity in both diseases.

In addition to many advantages of this project, there are also limitations, which need to be acknowledged. First, the study included two independent ILD cohorts, which showed clear differences in clinical characteristics and patient samples including markedly differences in age and lung function parameters (Leuschner et al. 2021). Additionally, some of the heterogeneity between cohorts might be caused by the fact that blood samples from cohort 1 were plasma samples but cohort 2 were all serum samples. Several parameters can have an influence on the sensitivity of the DAC assay and these might differ between the various pairs of antibodies and antigens autoantigen/antibody pairs. The enrichment and consequently the detection of autoantigens can depend on (1) the titer of autoantigens in plasma/serum, (2) concentration of autoantigens in the native tissue extract, (3) antibody-antigen affinity, (4) other unknown factors (Leuschner et al. 2021). Since for the DAC assay one defined condition and protocol had to be established it was to be expected that some possible autoantigens would be missed. Actually, some autoantibodies/antigens which were previously identified and showed associations with severity of IPF or prognosis, were not detected by the MS-workflow, including antibodies against parietal cells, heat-shock protein 70 or vimentin (Taille et al. 2011, Kahloon et al. 2013, Li et al. 2017, Beltramo et al. 2018).

Finally, the data of the project show that there is a great heterogeneity of B cell driven autoimmune profiles in IPF and CTD-ILD with shared, disease specific, cohort specific and individually expressed autoantigens. In IPF, autoantibodies against THBS1 were predictors for transplant-free survival. Moreover, in CTD-ILD and IPF, respectively, autoimmune profiles were identified consisting of several co-expressed genes, which were associated with worse survival. Although our data does not give evidence for a disease-causing IPF-specific autoantigen, autoimmune response seems to have an impact on a selected number of patients with IPF.

## 5. Conclusion and future directions

IPF is a chronic disease in which the excessive deposition of ECM subsequently leads to organ malfunction and reduced gas exchange. The pathogenesis is still not completely clear and treatment options are limited, despite the two antifibrotic drugs pirfenidone and nintedanib, that can slow the progression of the disease. Hence, there is an urgent need to clarify the exact processes involved in the genesis of IPF and identify possible cellular or molecular targets for future effective therapies.

In our first study presented here, using an unbiased proteomics approach, we identified a large extent of MZB1-positive B cells in different types of ILD and also in skin tissue of localized scleroderma (Schiller et al. 2017). MZB1 is a plasma B cell marker and it is assumed to be essential for the proper biosynthesis of immunoglobulin  $\mu$  heavy chains under conditions of ER stress (Flach et al. 2010, Rosenbaum et al. 2014). Immunostainings identified MZB1-positive cells as tissue-resident, terminally differentiated antibody-producing plasma cells (Schiller et al. 2017). The significantly higher expression of MZB1 in ILD tissue in comparison to healthy donors could be validated in a second, larger ILD cohort. Interestingly, MZB1 levels correlated significantly and negatively with lung function parameters suggesting the involvement of humoral autoimmunity in ILD. Furthermore, we observed a strong correlation with the total tissue IgG (Schiller et al. 2017). While proteomic data identified an upregulation of the IgG4 subclass, this could not be verified in further analysis using Western blot. Therefore, further work is needed to identify the role auf IgG subclasses and the distribution in different types of ILD.

Given the poor prognosis and limited treatment options, the immune system should be further investigated as a potential therapeutic target for IPF. In this regard, a therapeutic attempt with recombinant pentraxin, which inhibits the differentiation of monocytes into proinflammatory macrophages, appears promising. In a phase II study, compared to placebo, patients under such a therapy showed a significantly lower decline of FVC (Raghu et al. 2018). The open-label extension study showed persistent results on continuation over time and positive effects on FVC loss in patients who crossed over from placebo (Raghu et al. 2019). Another new therapeutic option might be PBI-4050, which is an orally active small-molecule compound that can bind the two G-protein coupled receptors GPR40 and GPR84 and either activate or antagonize them (Gagnon et al. 2018). Treatment with PBI-4050 can reduce or even reverse fibrotic processes by regulation of not only epithelial cells, fibroblasts and myofibroblasts but also macrophages (Gagnon et al. 2018). A 12-week open-label study including patients with IPF showed promising results for treatment with only PBI-4050 and also the combination of PBI-4050 and nintedanib (Khalil et al. 2019).

Based on our results on tissue IgG, another approach would be, for example, the identification of a damaging antigen followed by an immunotherapy specifically targeting this antigen, which has already been successfully investigated in other diseases and is now being used experimentally.

Recently, chimeric autoantibody receptor T cells (CAAR-T cells) have been found to serve as valuable and specific therapy eliminating autoreactive plasma B cell clones while preserving the protective immunity (Ellebrecht et al. 2016). As already mentioned, the feasibility of such therapies in the future depends on the presence and detection of autoantigens which are disease specific and pathogenic. In the second chapter of this work, we aimed to learn more about immune tolerance break and identify potential autoantigens in IPF. To enable an unbiased approach the DAC assay was established (Leuschner et al. 2021). We analyzed the autoantigen repertoire not only in IPF and healthy controls but also in patients with CTD-ILD from two independent ILD cohorts. Of note, the number of potential autoantigens was not higher in patients with CTD-ILD and a wide range of autoantigens were not diseases specific but commonly found in IPF and CTD-ILD (Leuschner et al. 2021). We were able to identify novel autoantigens and autoimmune signatures consisting of several co-expressed genes in IPF and CTD-ILD, which were detected in both cohorts and were associated with worse transplant-free survival. Autoantibodies against THBS1 were identified as independent predictor for mortality/lung transplantation in IPF patients (Leuschner et al. 2021). THBS1 was detected by the DAC assay in 8% of patients with IPF and 7% of CTD-ILD, respectively.

However, based on our data it cannot be determined if the identified autoantigens are disease-causing. Nevertheless, humoral autoimmunity seems to impact a selected number of patients with IPF. At the experimental level, our work could benefit from further validation using sequential plasma samples from the same patients correlated with clinical data. This could help to determine if autoantibodies are present in a distinct subpopulation of patients from early stages of the disease or if they occur later. Though, it is difficult to collect such samples in a standardized way in clinical practice. Another approach would definitely be to use the DAC assay in IPF-like mouse models such as the bleomycin model (Moeller et al. 2008). The advantage of a mouse model would be that repetitive blood sampling would be more standardized and easier to obtain than in humans. To further study the role of THBS1 in IPF a knock-out model might also be of interest in the future.

Taken together, the existing literature and our work show that there is an urgent need for a better understanding of the pathogenesis in IPF including autoimmune processes. Overall, the herein presented data provide new insights into the role of B cell-mediated autoimmunity in IPF. Given the highly diverse clinical courses in IPF, personalized therapy options that are directed against autoimmune processes could be of decisive relevance in the future.

## References

- Aalberse, R. C., S. O. Stapel, J. Schuurman and T. Rispens (2009). "Immunoglobulin G4: an odd antibody." *Clin Exp Allergy* **39**(4): 469-477.
- Aebersold, R. and M. Mann (2016). "Mass-spectrometric exploration of proteome structure and function." *Nature* **537**(7620): 347-355.
- Ahmad, K., T. Barba, D. Gamondes, M. Ginoux, C. Khouatra, P. Spagnolo, M. Streck, F. Thivolet-Bejui, J. Traclet and V. Cottin (2017). "Interstitial pneumonia with autoimmune features: Clinical, radiologic, and histological characteristics and outcome in a series of 57 patients." *Respir Med* **123**: 56-62.
- Akaiwa, M., Y. Yae, R. Sugimoto, S. O. Suzuki, T. Iwaki, K. Izuhara and N. Hamasaki (1999). "Hakata antigen, a new member of the ficolin/opsin p35 family, is a novel human lectin secreted into bronchus/alveolus and bile." *J Histochem Cytochem* **47**(6): 777-786.
- Allen, C. D. and J. G. Cyster (2008). "Follicular dendritic cell networks of primary follicles and germinal centers: phenotype and function." *Semin Immunol* **20**(1): 14-25.
- Allen, J. E. and T. E. Sutherland (2014). "Host protective roles of type 2 immunity: parasite killing and tissue repair, flip sides of the same coin." *Semin Immunol* **26**(4): 329-340.
- American Thoracic, S. and S. European Respiratory (2002). "American Thoracic Society/European Respiratory Society International Multidisciplinary Consensus Classification of the Idiopathic Interstitial Pneumonias. This joint statement of the American Thoracic Society (ATS), and the European Respiratory Society (ERS) was adopted by the ATS board of directors, June 2001 and by the ERS Executive Committee, June 2001." *Am J Respir Crit Care Med* **165**(2): 277-304.
- Amezaga, N., L. Sanjurjo, J. Julve, G. Aran, B. Perez-Cabezas, P. Bastos-Amador, C. Armengol, R. Vilella, J. C. Escola-Gil, F. Blanco-Vaca, F. E. Borrás, A. F. Valledor and M. R. Sarrias (2014). "Human scavenger protein AIM increases foam cell formation and CD36-mediated oxLDL uptake." *J Leukoc Biol* **95**(3): 509-520.
- Avrameas, S. and C. Selmi (2013). "Natural autoantibodies in the physiology and pathophysiology of the immune system." *J Autoimmun* **41**: 46-49.
- Balestro, E., F. Calabrese, G. Turato, F. Lunardi, E. Bazzan, G. Marulli, D. Biondini, E. Rossi, A. Sanduzzi, F. Rea, C. Rigobello, D. Gregori, S. Baraldo, P. Spagnolo, M. G. Cosio and M. Saetta (2016). "Immune Inflammation and Disease Progression in Idiopathic Pulmonary Fibrosis." *PLoS One* **11**(5): e0154516.
- Bauer, Y., J. Tedrow, S. de Bernard, M. Birker-Robaczewska, K. F. Gibson, B. J. Guardela, P. Hess, A. Klenk, K. O. Lindell, S. Poirey, B. Renault, M. Rey, E. Weber, O. Nayler and N. Kaminski (2015). "A novel genomic signature with translational significance for human idiopathic pulmonary fibrosis." *Am J Respir Cell Mol Biol* **52**(2): 217-231.
- Beachboard, D. C., M. Park, M. Vijayan, D. L. Snider, D. J. Fernando, G. D. Williams, S. Stanley, M. J. McFadden and S. M. Horner (2019). "The small GTPase RAB1B promotes antiviral innate immunity by interacting with TNF receptor-associated factor 3 (TRAF3)." *J Biol Chem* **294**(39): 14231-14240.
- Behr, J. (2013). "The diagnosis and treatment of idiopathic pulmonary fibrosis." *Dtsch Arztebl Int* **110**(51-52): 875-881.
- Behr, J., A. Gunther, F. Bonella, J. Dinkel, L. Fink, T. Geiser, K. Geissler, S. Glaser, S. Handzhiev, D. Jonigk, D. Koschel, M. Kreuter, G. Leuschner, P. Markart, A. Prasse, N.

- Schonfeld, J. C. Schupp, H. Sitter, J. Muller-Quernheim and U. Costabel (2020). "[German Guideline for Idiopathic Pulmonary Fibrosis]." *Pneumologie* **74**(5): 263-293.
- Behr, J., A. Gunther, F. Bonella, J. Dinkel, L. Fink, T. Geiser, K. Geissler, S. Glaser, S. Handzhiev, D. Jonigk, D. Koschel, M. Kreuter, G. Leuschner, P. Markart, A. Prasse, N. Schonfeld, J. C. Schupp, H. Sitter, J. Muller-Quernheim and U. Costabel (2021). "S2K Guideline for Diagnosis of Idiopathic Pulmonary Fibrosis." *Respiration* **100**(3): 238-271.
- Beltramo, G., G. Thabut, N. Peron, P. Nicaise, A. Cazes, M. P. Debray, A. Joannes, Y. Castier, A. A. Mailleux, J. Frija, P. Pradere, A. Justet, R. Borie, M. C. Dombret, C. Taille, M. Aubier and B. Crestani (2018). "Anti-parietal cell autoimmunity is associated with an accelerated decline of lung function in IPF patients." *Respir Med* **135**: 15-21.
- Bjoraker, J. A., J. H. Ryu, M. K. Edwin, J. L. Myers, H. D. Tazelaar, D. R. Schroeder and K. P. Offord (1998). "Prognostic significance of histopathologic subsets in idiopathic pulmonary fibrosis." *Am J Respir Crit Care Med* **157**(1): 199-203.
- Bornstein, P. (1995). "Diversity of function is inherent in matricellular proteins: an appraisal of thrombospondin 1." *J Cell Biol* **130**(3): 503-506.
- Burgstaller, G., B. Oehrle, M. Gerckens, E. S. White, H. B. Schiller and O. Eickelberg (2017). "The instructive extracellular matrix of the lung: basic composition and alterations in chronic lung disease." *Eur Respir J* **50**(1).
- Burgstaller, G., A. Sengupta, S. Vierkotten, G. Preissler, M. Lindner, J. Behr, M. Konigshoff and O. Eickelberg (2018). "Distinct niches within the extracellular matrix dictate fibroblast function in (cell free) 3D lung tissue cultures." *Am J Physiol Lung Cell Mol Physiol* **314**(5): L708-L723.
- Burley, K., S. K. Westbury and A. D. Mumford (2018). "TUBB1 variants and human platelet traits." *Platelets* **29**(2): 209-211.
- Campbell, S. N., E. Rubio and A. L. Loschner (2014). "Clinical review of pulmonary manifestations of IgG4-related disease." *Ann Am Thorac Soc* **11**(9): 1466-1475.
- Chartrand, S., J. J. Swigris, L. Stanchev, J. S. Lee, K. K. Brown and A. Fischer (2016). "Clinical features and natural history of interstitial pneumonia with autoimmune features: A single center experience." *Respir Med* **119**: 150-154.
- Choi, J. H., X. Zhong, Z. Zhang, L. Su, W. McAlpine, T. Misawa, T. C. Liao, X. Zhan, J. Russell, S. Ludwig, X. Li, M. Tang, P. Anderton, E. M. Y. Moresco and B. Beutler (2020). "Essential cell-extrinsic requirement for PDIA6 in lymphoid and myeloid development." *J Exp Med* **217**(4).
- Collard, H. R., C. J. Ryerson, T. J. Corte, G. Jenkins, Y. Kondoh, D. J. Lederer, J. S. Lee, T. M. Maher, A. U. Wells, K. M. Antoniou, J. Behr, K. K. Brown, V. Cottin, K. R. Flaherty, J. Fukuoka, D. M. Hansell, T. Johkoh, N. Kaminski, D. S. Kim, M. Kolb, D. A. Lynch, J. L. Myers, G. Raghu, L. Richeldi, H. Taniguchi and F. J. Martinez (2016). "Acute Exacerbation of Idiopathic Pulmonary Fibrosis. An International Working Group Report." *Am J Respir Crit Care Med* **194**(3): 265-275.
- Cottin, V. (2016). "Idiopathic interstitial pneumonias with connective tissue diseases features: A review." *Respirology* **21**(2): 245-258.
- Cottin, V., N. A. Hirani, D. L. Hotchkiss, A. M. Nambiar, T. Ogura, M. Otaola, D. Skowasch, J. S. Park, H. K. Poonyagariyagorn, W. Wuyts and A. U. Wells (2018). "Presentation, diagnosis and clinical course of the spectrum of progressive-fibrosing interstitial lung diseases." *Eur Respir Rev* **27**(150).
- Coultas, D. B., R. E. Zumwalt, W. C. Black and R. E. Sobonya (1994). "The epidemiology of interstitial lung diseases." *Am J Respir Crit Care Med* **150**(4): 967-972.

- Cox, J. and M. Mann (2008). "MaxQuant enables high peptide identification rates, individualized p.p.b.-range mass accuracies and proteome-wide protein quantification." *Nat Biotechnol* **26**(12): 1367-1372.
- Cox, J., N. Neuhauser, A. Michalski, R. A. Scheltema, J. V. Olsen and M. Mann (2011). "Andromeda: a peptide search engine integrated into the MaxQuant environment." *J Proteome Res* **10**(4): 1794-1805.
- Cox, T. R. and J. T. Erler (2011). "Remodeling and homeostasis of the extracellular matrix: implications for fibrotic diseases and cancer." *Dis Model Mech* **4**(2): 165-178.
- Crawford, S. E., V. Stellmach, J. E. Murphy-Ullrich, S. M. Ribeiro, J. Lawler, R. O. Hynes, G. P. Boivin and N. Bouck (1998). "Thrombospondin-1 is a major activator of TGF-beta1 in vivo." *Cell* **93**(7): 1159-1170.
- Cyster, J. G. and C. C. Goodnow (1995). "Antigen-induced exclusion from follicles and anergy are separate and complementary processes that influence peripheral B cell fate." *Immunity* **3**(6): 691-701.
- de Lauretis, A., S. Veeraraghavan and E. Renzoni (2011). "Review series: Aspects of interstitial lung disease: connective tissue disease-associated interstitial lung disease: how does it differ from IPF? How should the clinical approach differ?" *Chron Respir Dis* **8**(1): 53-82.
- Degn, S. E., C. E. van der Poel and M. C. Carroll (2017). "Targeting autoreactive germinal centers to curb autoimmunity." *Oncotarget* **8**(53): 90624-90625.
- DePianto, D. J., S. Chandriani, A. R. Abbas, G. Jia, E. N. N'Diaye, P. Caplazi, S. E. Kauder, S. Biswas, S. K. Karnik, C. Ha, Z. Modrusan, M. A. Matthay, J. Kukreja, H. R. Collard, J. G. Egen, P. J. Wolters and J. R. Arron (2015). "Heterogeneous gene expression signatures correspond to distinct lung pathologies and biomarkers of disease severity in idiopathic pulmonary fibrosis." *Thorax* **70**(1): 48-56.
- Desai, O., J. Winkler, M. Minasyan and E. L. Herzog (2018). "The Role of Immune and Inflammatory Cells in Idiopathic Pulmonary Fibrosis." *Front Med (Lausanne)* **5**: 43.
- Distler, O., K. B. Highland, M. Gahlemann, A. Azuma, A. Fischer, M. D. Mayes, G. Raghu, W. Sauter, M. Girard, M. Alves, E. Clerisme-Beaty, S. Stowasser, K. Tetzlaff, M. Kuwana, T. M. Maher and S. T. Investigators (2019). "Nintedanib for Systemic Sclerosis-Associated Interstitial Lung Disease." *N Engl J Med* **380**(26): 2518-2528.
- Dobashi, N., J. Fujita, M. Murota, Y. Ohtsuki, I. Yamadori, T. Yoshinouchi, R. Ueda, S. Bandoh, T. Kamei, M. Nishioka, T. Ishida and J. Takahara (2000). "Elevation of anti-cytokeratin 18 antibody and circulating cytokeratin 18: anti-cytokeratin 18 antibody immune complexes in sera of patients with idiopathic pulmonary fibrosis." *Lung* **178**(3): 171-179.
- Donahoe, M., V. G. Valentine, N. Chien, K. F. Gibson, J. S. Raval, M. Saul, J. Xue, Y. Zhang and S. R. Duncan (2015). "Autoantibody-Targeted Treatments for Acute Exacerbations of Idiopathic Pulmonary Fibrosis." *PLoS One* **10**(6): e0127771.
- Doyle, T. J. and P. F. Dellaripa (2017). "Lung Manifestations in the Rheumatic Diseases." *Chest* **152**(6): 1283-1295.
- Dranoff, G. (2004). "Cytokines in cancer pathogenesis and cancer therapy." *Nat Rev Cancer* **4**(1): 11-22.
- Dreisin, R. B., M. I. Schwarz, A. N. Theofilopoulos and R. E. Stanford (1978). "Circulating immune complexes in the idiopathic interstitial pneumonias." *N Engl J Med* **298**(7): 353-357.
- Edwards, J. C. and G. Cambridge (2005). "Prospects for B-cell-targeted therapy in autoimmune disease." *Rheumatology (Oxford)* **44**(2): 151-156.

- Ellebrecht, C. T., V. G. Bhoj, A. Nace, E. J. Choi, X. Mao, M. J. Cho, G. Di Zenzo, A. Lanzavecchia, J. T. Seykora, G. Cotsarelis, M. C. Milone and A. S. Payne (2016). "Reengineering chimeric antigen receptor T cells for targeted therapy of autoimmune disease." *Science* **353**(6295): 179-184.
- Endo, Y., M. Matsushita and T. Fujita (2007). "Role of ficolin in innate immunity and its molecular basis." *Immunobiology* **212**(4-5): 371-379.
- Esser-von Bieren, J., I. Mosconi, R. Guet, A. Piersgilli, B. Volpe, F. Chen, W. C. Gause, A. Seitz, J. S. Verbeek and N. L. Harris (2013). "Antibodies trap tissue migrating helminth larvae and prevent tissue damage by driving IL-4/alpha-independent alternative differentiation of macrophages." *PLoS Pathog* **9**(11): e1003771.
- Fernandes, L., M. Nasser, K. Ahmad and V. Cottin (2019). "Interstitial Pneumonia With Autoimmune Features (IPAF)." *Front Med (Lausanne)* **6**: 209.
- Fernandez, I. E. and O. Eickelberg (2012). "New cellular and molecular mechanisms of lung injury and fibrosis in idiopathic pulmonary fibrosis." *Lancet* **380**(9842): 680-688.
- Fireman, E., N. Vardinon, M. Burke, S. Spizer, S. Levin, A. Endler, D. Stav, M. Topilsky, A. Mann, Y. Schwarz, S. Kivity and J. Greif (1998). "Predictive value of response to treatment of T-lymphocyte subpopulations in idiopathic pulmonary fibrosis." *Eur Respir J* **11**(3): 706-711.
- Fischer, A., K. M. Antoniou, K. K. Brown, J. Cadranel, T. J. Corte, R. M. du Bois, J. S. Lee, K. O. Leslie, D. A. Lynch, E. L. Matteson, M. Mosca, I. Noth, L. Richeldi, M. E. Streck, J. J. Swigris, A. U. Wells, S. G. West, H. R. Collard, V. Cottin and E. A. T. F. o. U. F. o. CTD-ILD (2015). "An official European Respiratory Society/American Thoracic Society research statement: interstitial pneumonia with autoimmune features." *Eur Respir J* **46**(4): 976-987.
- Fischer, A. and R. du Bois (2012). "Interstitial lung disease in connective tissue disorders." *Lancet* **380**(9842): 689-698.
- Flach, H., M. Rosenbaum, M. Duchniewicz, S. Kim, S. L. Zhang, M. D. Cahalan, G. Mittler and R. Grosschedl (2010). "Mzb1 protein regulates calcium homeostasis, antibody secretion, and integrin activation in innate-like B cells." *Immunity* **33**(5): 723-735.
- Fleischmajer, R. and A. Nedwich (1972). "Generalized morphea. I. Histology of the dermis and subcutaneous tissue." *Arch Dermatol* **106**(4): 509-514.
- Fujita, J., N. Dobashi, Y. Ohtsuki, I. Yamadori, T. Yoshinouchi, T. Kamei, M. Tokuda, S. Hojo, H. Okada and J. Takahara (1999). "Elevation of anti-cytokeratin 19 antibody in sera of the patients with idiopathic pulmonary fibrosis and pulmonary fibrosis associated with collagen vascular disorders." *Lung* **177**(5): 311-319.
- Gagnon, L., M. Leduc, J. F. Thibodeau, M. Z. Zhang, B. Grouix, F. Sarra-Bournet, W. Gagnon, K. Hince, M. Tremblay, L. Geerts, C. R. J. Kennedy, R. L. Hebert, A. Gutsol, C. E. Holterman, E. Kamto, L. Gervais, J. Ouboudinar, J. Richard, A. Felton, A. Laverdure, J. C. Simard, S. Letourneau, M. P. Cloutier, F. A. Leblond, S. D. Abbott, C. Penney, J. S. Duceppe, B. Zacharie, J. Dupuis, A. Calderone, Q. T. Nguyen, R. C. Harris and P. Laurin (2018). "A Newly Discovered Antifibrotic Pathway Regulated by Two Fatty Acid Receptors: GPR40 and GPR84." *Am J Pathol* **188**(5): 1132-1148.
- Gieseck, R. L., 3rd, M. S. Wilson and T. A. Wynn (2018). "Type 2 immunity in tissue repair and fibrosis." *Nat Rev Immunol* **18**(1): 62-76.
- Gregory, A. D., C. R. Kliment, H. E. Metz, K. H. Kim, J. Kargl, B. A. Agostini, L. T. Crum, E. A. Oczypok, T. A. Oury and A. M. Houghton (2015). "Neutrophil elastase promotes myofibroblast differentiation in lung fibrosis." *J Leukoc Biol* **98**(2): 143-152.
- Grund, D. and E. Siebert (2016). "[Pulmonary fibrosis in rheumatic diseases]." *Z Rheumatol* **75**(8): 795-808.



- Guler, S. A. and C. J. Ryerson (2018). "Unclassifiable interstitial lung disease: from phenotyping to possible treatments." *Curr Opin Pulm Med* **24**(5): 461-468.
- Gurtner, G. C., S. Werner, Y. Barrandon and M. T. Longaker (2008). "Wound repair and regeneration." *Nature* **453**(7193): 314-321.
- Hecker, L. and V. J. Thannickal (2011). "Nonresolving fibrotic disorders: idiopathic pulmonary fibrosis as a paradigm of impaired tissue regeneration." *Am J Med Sci* **341**(6): 431-434.
- Henry, M. T., K. McMahon, A. J. Mackarel, K. Prikk, T. Sorsa, P. Maisi, R. Sepper, M. X. Fitzgerald and C. M. O'Connor (2002). "Matrix metalloproteinases and tissue inhibitor of metalloproteinase-1 in sarcoidosis and IPF." *Eur Respir J* **20**(5): 1220-1227.
- Heukels, P., C. C. Moor, J. H. von der Thusen, M. S. Wijsenbeek and M. Kool (2019). "Inflammation and immunity in IPF pathogenesis and treatment." *Respir Med* **147**: 79-91.
- Hogan, B. L., C. E. Barkauskas, H. A. Chapman, J. A. Epstein, R. Jain, C. C. Hsia, L. Niklason, E. Calle, A. Le, S. H. Randell, J. Rock, M. Snitow, M. Krummel, B. R. Stripp, T. Vu, E. S. White, J. A. Whitsett and E. E. Morrisey (2014). "Repair and regeneration of the respiratory system: complexity, plasticity, and mechanisms of lung stem cell function." *Cell Stem Cell* **15**(2): 123-138.
- Hoyne, G. F., H. Elliott, S. E. Mutsaers and C. M. Prele (2017). "Idiopathic pulmonary fibrosis and a role for autoimmunity." *Immunol Cell Biol* **95**(7): 577-583.
- Hummelshoj, T., L. M. Fog, H. O. Madsen, R. B. Sim and P. Garred (2008). "Comparative study of the human ficolins reveals unique features of Ficolin-3 (Hakata antigen)." *Mol Immunol* **45**(6): 1623-1632.
- Hyldgaard, C., O. Hilberg, A. Muller and E. Bendstrup (2014). "A cohort study of interstitial lung diseases in central Denmark." *Respir Med* **108**(5): 793-799.
- Hynes, R. O. (2014). "Stretching the boundaries of extracellular matrix research." *Nat Rev Mol Cell Biol* **15**(12): 761-763.
- Ide, M., H. Ishii, H. Mukae, A. Iwata, N. Sakamoto, J. Kadota and S. Kohno (2008). "High serum levels of thrombospondin-1 in patients with idiopathic interstitial pneumonia." *Respir Med* **102**(11): 1625-1630.
- Idiopathic Pulmonary Fibrosis Clinical Research, N., G. Raghu, K. J. Anstrom, T. E. King, Jr., J. A. Lasky and F. J. Martinez (2012). "Prednisone, azathioprine, and N-acetylcysteine for pulmonary fibrosis." *N Engl J Med* **366**(21): 1968-1977.
- Ikezoe, K., T. Handa, K. Mori, K. Watanabe, K. Tanizawa, K. Aihara, T. Tsuruyama, A. Miyagawa-Hayashino, A. Sokai, T. Kubo, S. Muro, S. Nagai, T. Hirai, K. Chin and M. Mishima (2014). "Neutrophil gelatinase-associated lipocalin in idiopathic pulmonary fibrosis." *Eur Respir J* **43**(6): 1807-1809.
- Janeway, C. A., Jr. (2001). "How the immune system works to protect the host from infection: a personal view." *Proc Natl Acad Sci U S A* **98**(13): 7461-7468.
- John-Schuster, G., K. Hager, T. M. Conlon, M. Imler, J. Beckers, O. Eickelberg and A. O. Yildirim (2014). "Cigarette smoke-induced iBALT mediates macrophage activation in a B cell-dependent manner in COPD." *Am J Physiol Lung Cell Mol Physiol* **307**(9): L692-706.
- Juge, P. A., J. S. Lee, E. Ebstein, H. Furukawa, E. Dobrinskikh, S. Gazal, C. Kannengiesser, S. Ottaviani, S. Oka, S. Tohma, N. Tsuchiya, J. Rojas-Serrano, M. I. Gonzalez-Perez, M. Mejia, I. Buendia-Roldan, R. Falfan-Valencia, E. Ambrocio-Ortiz, E. Manali, S. A. Papis, T. Karageorgas, D. Boumpas, K. Antoniou, C. H. M. van Moorsel, J. van der Vis, Y. A. de Man, J. C. Grutters, Y. Wang, R. Borie, L. Wemeau-Stervinou, B. Wallaert, R. M. Flipo, H. Nunes, D. Valeyre, N. Saidenberg-Kermanac'h, M. C. Boissier, S. Marchand-Adam, A. Frazier, P. Richette, Y. Allanore, J. Sibilia, C. Dromer, C. Richez, T. Schaefferbeke, H. Liote, G. Thabut, N. Nathan, S. Amselem,

- M. Soubrier, V. Cottin, A. Clement, K. Deane, A. D. Walts, T. Fingerlin, A. Fischer, J. H. Ryu, E. L. Matteson, T. B. Niewold, D. Assayag, A. Gross, P. Wolters, M. I. Schwarz, M. Holers, J. J. Solomon, T. Doyle, I. O. Rosas, C. Blauwendraat, M. A. Nalls, M. P. Debray, C. Boileau, B. Crestani, D. A. Schwartz and P. Dieude (2018). "MUC5B Promoter Variant and Rheumatoid Arthritis with Interstitial Lung Disease." *N Engl J Med* **379**(23): 2209-2219.
- Jutel, M. and C. A. Akdis (2011). "Immunological mechanisms of allergen-specific immunotherapy." *Allergy* **66**(6): 725-732.
- Kahloon, R. A., J. Xue, A. Bhargava, E. Csizmadia, L. Otterbein, D. J. Kass, J. Bon, M. Soejima, M. C. Levesque, K. O. Lindell, K. F. Gibson, N. Kaminski, G. Banga, C. V. Oddis, J. M. Pilewski, F. C. Sciurba, M. Donahoe, Y. Zhang and S. R. Duncan (2013). "Patients with idiopathic pulmonary fibrosis with antibodies to heat shock protein 70 have poor prognoses." *Am J Respir Crit Care Med* **187**(7): 768-775.
- Kaji, K., N. Fertig, T. A. Medsger, Jr., T. Satoh, K. Hoshino, Y. Hamaguchi, M. Hasegawa, M. Lucas, A. Schnure, F. Ogawa, S. Sato, K. Takehara, M. Fujimoto and M. Kuwana (2014). "Autoantibodies to RuvBL1 and RuvBL2: a novel systemic sclerosis-related antibody associated with diffuse cutaneous and skeletal muscle involvement." *Arthritis Care Res (Hoboken)* **66**(4): 575-584.
- Kamal, A. H. M., J. J. Aloor, M. B. Fessler and S. M. Chowdhury (2019). "Cross-linking Proteomics Indicates Effects of Simvastatin on the TLR2 Interactome and Reveals ACTR1A as a Novel Regulator of the TLR2 Signal Cascade." *Mol Cell Proteomics* **18**(9): 1732-1744.
- Kelly, C. A., V. Saravanan, M. Nisar, S. Arthanari, F. A. Woodhead, A. N. Price-Forbes, J. Dawson, N. Sathi, Y. Ahmad, G. Koduri, A. Young and N. British Rheumatoid Interstitial Lung (2014). "Rheumatoid arthritis-related interstitial lung disease: associations, prognostic factors and physiological and radiological characteristics--a large multicentre UK study." *Rheumatology (Oxford)* **53**(9): 1676-1682.
- Khalil, N., H. Manganas, C. J. Ryerson, S. Shapera, A. M. Cantin, P. Hernandez, E. E. Turcotte, J. M. Parker, J. E. Moran, G. R. Albert, R. Sawtell, A. Hagerimana, P. Laurin, L. Gagnon, F. Cesari and M. Kolb (2019). "Phase 2 clinical trial of PBI-4050 in patients with idiopathic pulmonary fibrosis." *Eur Respir J* **53**(3).
- Kimura, T., Y. Ishii, K. Yoh, Y. Morishima, T. Iizuka, T. Kiwamoto, Y. Matsuno, S. Homma, A. Nomura, T. Sakamoto, S. Takahashi and K. Sekizawa (2006). "Overexpression of the transcription factor GATA-3 enhances the development of pulmonary fibrosis." *Am J Pathol* **169**(1): 96-104.
- King, T. E., Jr., W. Z. Bradford, S. Castro-Bernardini, E. A. Fagan, I. Glaspole, M. K. Glassberg, E. Gorina, P. M. Hopkins, D. Kardatzke, L. Lancaster, D. J. Lederer, S. D. Nathan, C. A. Pereira, S. A. Sahn, R. Sussman, J. J. Swigris, P. W. Noble and A. S. Group (2014). "A phase 3 trial of pirfenidone in patients with idiopathic pulmonary fibrosis." *N Engl J Med* **370**(22): 2083-2092.
- King, T. E., Jr., A. Pardo and M. Selman (2011). "Idiopathic pulmonary fibrosis." *Lancet* **378**(9807): 1949-1961.
- Kisseleva, T. and D. A. Brenner (2008). "Fibrogenesis of parenchymal organs." *Proc Am Thorac Soc* **5**(3): 338-342.
- Knuppel, L., Y. Ishikawa, M. Aichler, K. Heinzelmann, R. Hatz, J. Behr, A. Walch, H. P. Bachinger, O. Eickelberg and C. A. Staab-Weijnitz (2017). "A Novel Antifibrotic Mechanism of Nintedanib and Pirfenidone. Inhibition of Collagen Fibril Assembly." *Am J Respir Cell Mol Biol* **57**(1): 77-90.
- Kolahian, S., I. E. Fernandez, O. Eickelberg and D. Hartl (2016). "Immune Mechanisms in Pulmonary Fibrosis." *Am J Respir Cell Mol Biol* **55**(3): 309-322.
- Konigshoff, M., M. Kramer, N. Balsara, J. Wilhelm, O. V. Amarie, A. Jahn, F. Rose, L. Fink, W. Seeger, L. Schaefer, A. Gunther and O. Eickelberg (2009). "WNT1-inducible signaling protein-1

- mediates pulmonary fibrosis in mice and is upregulated in humans with idiopathic pulmonary fibrosis." *J Clin Invest* **119**(4): 772-787.
- Koski, C., J. Saharinen and J. Keski-Oja (1999). "Independent promoters regulate the expression of two amino terminally distinct forms of latent transforming growth factor-beta binding protein-1 (LTBP-1) in a cell type-specific manner." *J Biol Chem* **274**(46): 32619-32630.
- Kreuter, A., T. Krieg, M. Worm, J. Wenzel, P. Moinzadeh, A. Kuhn, E. Aberer, K. Scharffetter-Kochanek, G. Horneff, E. Reil, T. Weberschock and N. Hunzelmann (2016). "German guidelines for the diagnosis and therapy of localized scleroderma." *J Dtsch Dermatol Ges* **14**(2): 199-216.
- Kreuter, M., J. S. Lee, A. Tzouveleakis, J. M. Oldham, P. L. Molyneaux, D. Weycker, M. Atwood, K. U. Kirchgaessler and T. M. Maher (2021). "Monocyte Count as a Prognostic Biomarker in Patients with Idiopathic Pulmonary Fibrosis." *Am J Respir Crit Care Med* **204**(1): 74-81.
- Kulak, N. A., G. Pichler, I. Paron, N. Nagaraj and M. Mann (2014). "Minimal, encapsulated proteomic-sample processing applied to copy-number estimation in eukaryotic cells." *Nat Methods* **11**(3): 319-324.
- Kurosu, K., Y. Takiguchi, O. Okada, N. Yumoto, S. Sakao, Y. Tada, Y. Kasahara, N. Tanabe, K. Tatsumi, M. Weiden, W. N. Rom and T. Kuriyama (2008). "Identification of annexin 1 as a novel autoantigen in acute exacerbation of idiopathic pulmonary fibrosis." *J Immunol* **181**(1): 756-767.
- Larman, H. B., Z. Zhao, U. Laserson, M. Z. Li, A. Ciccia, M. A. Gakidis, G. M. Church, S. Kesari, E. M. Leproust, N. L. Solimini and S. J. Elledge (2011). "Autoantigen discovery with a synthetic human peptidome." *Nat Biotechnol* **29**(6): 535-541.
- Lee, J. H., D. H. Bhang, A. Beede, T. L. Huang, B. R. Stripp, K. D. Bloch, A. J. Wagers, Y. H. Tseng, S. Ryeom and C. F. Kim (2014). "Lung stem cell differentiation in mice directed by endothelial cells via a BMP4-NFATc1-thrombospondin-1 axis." *Cell* **156**(3): 440-455.
- Lee, J. S., E. J. Kim, K. L. Lynch, B. Elicker, C. J. Ryerson, T. R. Katsumoto, A. K. Shum, P. J. Wolters, S. Cerri, L. Richeldi, K. D. Jones, T. E. King, Jr. and H. R. Collard (2013). "Prevalence and clinical significance of circulating autoantibodies in idiopathic pulmonary fibrosis." *Respir Med* **107**(2): 249-255.
- Lefort, C. T., J. Rossaint, M. Moser, B. G. Petrich, A. Zarbock, S. J. Monkley, D. R. Critchley, M. H. Ginsberg, R. Fassler and K. Ley (2012). "Distinct roles for talin-1 and kindlin-3 in LFA-1 extension and affinity regulation." *Blood* **119**(18): 4275-4282.
- Lerner, A. and T. Matthias (2015). "Changes in intestinal tight junction permeability associated with industrial food additives explain the rising incidence of autoimmune disease." *Autoimmun Rev* **14**(6): 479-489.
- Leuschner, G. and J. Behr (2017). "Acute Exacerbation in Interstitial Lung Disease." *Front Med (Lausanne)* **4**: 176.
- Leuschner, G., C. H. Mayr, M. Ansari, B. Seeliger, M. Frankenberger, N. Kneidinger, R. A. Hatz, A. Hilgendorff, A. Prasse, J. Behr, M. Mann and H. B. Schiller (2021). "A proteomics workflow reveals predictive autoantigens in idiopathic pulmonary fibrosis." *medRxiv 2021.02.17.21251826*.
- Leuschner, G., F. Reiter, F. Stocker, A. Crispin, N. Kneidinger, T. Veit, F. Klenner, F. Ceelen, G. Zimmermann, H. Leuchte, S. Reu, J. Dinkel, J. Behr and C. Neurohr (2018). "Idiopathic Pulmonary Fibrosis Among Young Patients: Challenges in Diagnosis and Management." *Lung* **196**(4): 401-408.
- Lewis, S., A. Gifford and D. Baltimore (1984). "Joining of V kappa to J kappa gene segments in a retroviral vector introduced into lymphoid cells." *Nature* **308**(5958): 425-428.
- Lewis, S., A. Gifford and D. Baltimore (1985). "DNA elements are asymmetrically joined during the site-specific recombination of kappa immunoglobulin genes." *Science* **228**(4700): 677-685.

- Li, F. J., R. Surolia, H. Li, Z. Wang, T. Kulkarni, G. Liu, J. A. de Andrade, D. J. Kass, V. J. Thannickal, S. R. Duncan and V. B. Antony (2017). "Autoimmunity to Vimentin Is Associated with Outcomes of Patients with Idiopathic Pulmonary Fibrosis." *J Immunol* **199**(5): 1596-1605.
- Li, X., X. Cao, M. Guo, M. Xie and X. Liu (2020). "Trends and risk factors of mortality and disability adjusted life years for chronic respiratory diseases from 1990 to 2017: systematic analysis for the Global Burden of Disease Study 2017." *BMJ* **368**: m234.
- Liu, X., T. Kohyama, H. Wang, Y. K. Zhu, F. Q. Wen, H. J. Kim, D. J. Romberger and S. I. Rennard (2002). "Th2 cytokine regulation of type I collagen gel contraction mediated by human lung mesenchymal cells." *Am J Physiol Lung Cell Mol Physiol* **282**(5): L1049-1056.
- Liu, Y., F. Lu, L. Kang, Z. Wang and Y. Wang (2017). "Pirfenidone attenuates bleomycin-induced pulmonary fibrosis in mice by regulating Nrf2/Bach1 equilibrium." *BMC Pulm Med* **17**(1): 63.
- MacLennan, I. C. (1994). "Germinal centers." *Annu Rev Immunol* **12**: 117-139.
- Macosko, E. Z., A. Basu, R. Satija, J. Nemes, K. Shekhar, M. Goldman, I. Tirosh, A. R. Bialas, N. Kamitaki, E. M. Martersteck, J. J. Trombetta, D. A. Weitz, J. R. Sanes, A. K. Shalek, A. Regev and S. A. McCarroll (2015). "Highly Parallel Genome-wide Expression Profiling of Individual Cells Using Nanoliter Droplets." *Cell* **161**(5): 1202-1214.
- MacRae, I. J., E. Ma, M. Zhou, C. V. Robinson and J. A. Doudna (2008). "In vitro reconstitution of the human RISC-loading complex." *Proc Natl Acad Sci U S A* **105**(2): 512-517.
- Maher, T. M., U. Costabel, M. K. Glassberg, Y. Kondoh, T. Ogura, M. B. Scholand, D. Kardatzke, M. Howard, J. Olsson, M. Neighbors, P. Belloni and J. J. Swigris (2021). "Phase 2 trial to assess lebrikizumab in patients with idiopathic pulmonary fibrosis." *Eur Respir J* **57**(2).
- Mandel, T. E., R. P. Phipps, A. P. Abbot and J. G. Tew (1981). "Long-term antigen retention by dendritic cells in the popliteal lymph node of immunized mice." *Immunology* **43**(2): 353-362.
- Martinez, F. J., H. R. Collard, A. Pardo, G. Raghu, L. Richeldi, M. Selman, J. J. Swigris, H. Taniguchi and A. U. Wells (2017). "Idiopathic pulmonary fibrosis." *Nat Rev Dis Primers* **3**: 17074.
- Martino, M. M., P. S. Briquez, E. Guc, F. Tortelli, W. W. Kilarski, S. Metzger, J. J. Rice, G. A. Kuhn, R. Muller, M. A. Swartz and J. A. Hubbell (2014). "Growth factors engineered for super-affinity to the extracellular matrix enhance tissue healing." *Science* **343**(6173): 885-888.
- Mathai, S. K., B. S. Pedersen, K. Smith, P. Russell, M. I. Schwarz, K. K. Brown, M. P. Steele, J. E. Loyd, J. D. Crapo, E. K. Silverman, D. Nickerson, T. E. Fingerlin, I. V. Yang and D. A. Schwartz (2016). "Desmoplakin Variants Are Associated with Idiopathic Pulmonary Fibrosis." *Am J Respir Crit Care Med* **193**(10): 1151-1160.
- Meier, F. M., K. W. Frommer, R. Dinser, U. A. Walker, L. Czirjak, C. P. Denton, Y. Allanore, O. Distler, G. Riemekasten, G. Valentini, U. Muller-Ladner and E. Co-authors (2012). "Update on the profile of the EUSTAR cohort: an analysis of the EULAR Scleroderma Trials and Research group database." *Ann Rheum Dis* **71**(8): 1355-1360.
- Michalski, A., E. Damoc, J. P. Hauschild, O. Lange, A. Wieghaus, A. Makarov, N. Nagaraj, J. Cox, M. Mann and S. Horning (2011). "Mass spectrometry-based proteomics using Q Exactive, a high-performance benchtop quadrupole Orbitrap mass spectrometer." *Mol Cell Proteomics* **10**(9): M111 011015.
- Miyagawa, T., Y. Asano, Y. de Mestier, R. Saigusa, T. Taniguchi, T. Yamashita, K. Nakamura, M. Hirabayashi, S. Miura, Y. Ichimura, T. Takahashi, A. Yoshizaki, T. Miyagaki, M. Sugaya and S. Sato (2017). "Serum H-ficolin levels: Clinical association with interstitial lung disease in patients with systemic sclerosis." *J Dermatol* **44**(10): 1168-1171.
- Miyazono, K., A. Olofsson, P. Colosetti and C. H. Heldin (1991). "A role of the latent TGF-beta 1-binding protein in the assembly and secretion of TGF-beta 1." *EMBO J* **10**(5): 1091-1101.

- Moeller, A., K. Ask, D. Warburton, J. Gaudie and M. Kolb (2008). "The bleomycin animal model: a useful tool to investigate treatment options for idiopathic pulmonary fibrosis?" *Int J Biochem Cell Biol* **40**(3): 362-382.
- Morales, A. T., A. G. Cignarella, I. S. Jabeen, J. S. Barkin and M. Mirsaeidi (2019). "An update on IgG4-related lung disease." *Eur J Intern Med* **66**: 18-24.
- Moua, T., F. Maldonado, P. A. Decker, C. E. Daniels and J. H. Ryu (2014). "Frequency and implication of autoimmune serologies in idiopathic pulmonary fibrosis." *Mayo Clin Proc* **89**(3): 319-326.
- Moyron-Quiroz, J. E., J. Rangel-Moreno, K. Kusser, L. Hartson, F. Sprague, S. Goodrich, D. L. Woodland, F. E. Lund and T. D. Randall (2004). "Role of inducible bronchus associated lymphoid tissue (iBALT) in respiratory immunity." *Nat Med* **10**(9): 927-934.
- Muller, M., F. Fazi and C. Ciaudo (2019). "Argonaute Proteins: From Structure to Function in Development and Pathological Cell Fate Determination." *Front Cell Dev Biol* **7**: 360.
- Munthe-Fog, L., T. Hummelshoj, C. Honore, H. O. Madsen, H. Permin and P. Garred (2009). "Immunodeficiency associated with FCN3 mutation and ficolin-3 deficiency." *N Engl J Med* **360**(25): 2637-2644.
- Murphy-Ullrich, J. E. and M. Poczatek (2000). "Activation of latent TGF-beta by thrombospondin-1: mechanisms and physiology." *Cytokine Growth Factor Rev* **11**(1-2): 59-69.
- Murray, L. A., D. M. Habel, M. Hohmann, A. Camelo, H. Shang, Y. Zhou, A. L. Coelho, X. Peng, M. Gulati, B. Crestani, M. A. Sleeman, T. Mustelin, M. W. Moore, C. Ryu, A. D. Osafo-Addo, J. A. Elias, C. G. Lee, B. Hu, J. D. Herazo-Maya, D. A. Knight, C. M. Hogaboam and E. L. Herzog (2017). "Antifibrotic role of vascular endothelial growth factor in pulmonary fibrosis." *JCI Insight* **2**(16).
- Nakayama, T., K. Hirahara, A. Onodera, Y. Endo, H. Hosokawa, K. Shinoda, D. J. Tumes and Y. Okamoto (2017). "Th2 Cells in Health and Disease." *Annu Rev Immunol* **35**: 53-84.
- Nalysnyk, L., J. Cid-Ruzafa, P. Rotella and D. Esser (2012). "Incidence and prevalence of idiopathic pulmonary fibrosis: review of the literature." *Eur Respir Rev* **21**(126): 355-361.
- Nathan, S. D., O. A. Shlobin, N. Weir, S. Ahmad, J. M. Kaldjob, E. Battle, M. J. Sheridan and R. M. du Bois (2011). "Long-term course and prognosis of idiopathic pulmonary fibrosis in the new millennium." *Chest* **140**(1): 221-229.
- Neighbors, M., C. R. Cabanski, T. R. Ramalingam, X. R. Sheng, G. W. Tew, C. Gu, G. Jia, K. Peng, J. M. Ray, B. Ley, P. J. Wolters, H. R. Collard and J. R. Arron (2018). "Prognostic and predictive biomarkers for patients with idiopathic pulmonary fibrosis treated with pirfenidone: post-hoc assessment of the CAPACITY and ASCEND trials." *Lancet Respir Med* **6**(8): 615-626.
- Neurohr, C. and J. Behr (2015). "Changes in the current classification of IIP: A critical review." *Respirology* **20**(5): 699-704.
- Noble, P. W., C. Albera, W. Z. Bradford, U. Costabel, M. K. Glassberg, D. Kardatzke, T. E. King, Jr., L. Lancaster, S. A. Sahn, J. Szwarcberg, D. Valeyre, R. M. du Bois and C. S. Group (2011). "Pirfenidone in patients with idiopathic pulmonary fibrosis (CAPACITY): two randomised trials." *Lancet* **377**(9779): 1760-1769.
- Nutt, S. L., P. D. Hodgkin, D. M. Tarlinton and L. M. Corcoran (2015). "The generation of antibody-secreting plasma cells." *Nat Rev Immunol* **15**(3): 160-171.
- Oak, S. R., L. Murray, A. Herath, M. Sleeman, I. Anderson, A. D. Joshi, A. L. Coelho, K. R. Flaherty, G. B. Toews, D. Knight, F. J. Martinez and C. M. Hogaboam (2011). "A micro RNA processing defect in rapidly progressing idiopathic pulmonary fibrosis." *PLoS One* **6**(6): e21253.

- Oda, K., H. Ishimoto, S. Yamada, H. Kushima, H. Ishii, T. Imanaga, T. Harada, Y. Ishimatsu, N. Matsumoto, K. Naito, K. Yatera, M. Nakazato, J. Kadota, K. Watanabe, S. Kohno and H. Mukae (2014). "Autopsy analyses in acute exacerbation of idiopathic pulmonary fibrosis." *Respir Res* **15**: 109.
- Oldham, J. M., A. Adegunsoye, E. Valenzi, C. Lee, L. Witt, L. Chen, A. N. Husain, S. Montner, J. H. Chung, V. Cottin, A. Fischer, I. Noth, R. Vij and M. E. Streck (2016). "Characterisation of patients with interstitial pneumonia with autoimmune features." *Eur Respir J* **47**(6): 1767-1775.
- Oldham, J. M., L. J. Witt, A. Adegunsoye, J. H. Chung, C. Lee, S. Hsu, L. W. Chen, A. Husain, S. Montner, R. Vij, M. E. Streck and I. Noth (2018). "N-acetylcysteine exposure is associated with improved survival in anti-nuclear antibody seropositive patients with usual interstitial pneumonia." *BMC Pulm Med* **18**(1): 30.
- Olson, A. L., J. J. Swigris, D. B. Sprunger, A. Fischer, E. R. Fernandez-Perez, J. Solomon, J. Murphy, M. Cohen, G. Raghu and K. K. Brown (2011). "Rheumatoid arthritis-interstitial lung disease-associated mortality." *Am J Respir Crit Care Med* **183**(3): 372-378.
- Onishi, R. M. and S. L. Gaffen (2010). "Interleukin-17 and its target genes: mechanisms of interleukin-17 function in disease." *Immunology* **129**(3): 311-321.
- Parker, J. M., I. N. Glaspole, L. H. Lancaster, T. J. Haddad, D. She, S. L. Roseti, J. P. Fiening, E. P. Grant, C. M. Kell and K. R. Flaherty (2018). "A Phase 2 Randomized Controlled Study of Tralokinumab in Subjects with Idiopathic Pulmonary Fibrosis." *Am J Respir Crit Care Med* **197**(1): 94-103.
- Parra, E. R., R. A. Kairalla, C. R. Ribeiro de Carvalho, E. Eher and V. L. Capelozzi (2007). "Inflammatory cell phenotyping of the pulmonary interstitium in idiopathic interstitial pneumonia." *Respiration* **74**(2): 159-169.
- Pauling, J. D., G. Salazar, H. Lu, Z. E. Betteridge, S. Assassi, M. D. Mayes and N. J. McHugh (2018). "Presence of anti-eukaryotic initiation factor-2B, anti-RuvBL1/2 and anti-synthetase antibodies in patients with anti-nuclear antibody negative systemic sclerosis." *Rheumatology (Oxford)* **57**(4): 712-717.
- Peng, T., D. B. Frank, R. S. Kadzik, M. P. Morley, K. S. Rathi, T. Wang, S. Zhou, L. Cheng, M. M. Lu and E. E. Morrisey (2015). "Hedgehog actively maintains adult lung quiescence and regulates repair and regeneration." *Nature* **526**(7574): 578-582.
- Plovsing, R. R., R. M. Berg, L. Munthe-Fog, L. Konge, M. Iversen, K. Moller and P. Garred (2016). "Alveolar recruitment of ficolin-3 in response to acute pulmonary inflammation in humans." *Immunobiology* **221**(5): 690-697.
- Pratt, A. J. and I. J. MacRae (2009). "The RNA-induced silencing complex: a versatile gene-silencing machine." *J Biol Chem* **284**(27): 17897-17901.
- Prior, C. and P. L. Haslam (1992). "In vivo levels and in vitro production of interferon-gamma in fibrosing interstitial lung diseases." *Clin Exp Immunol* **88**(2): 280-287.
- Raghu, G., K. K. Brown, W. Z. Bradford, K. Starko, P. W. Noble, D. A. Schwartz, T. E. King, Jr. and G. Idiopathic Pulmonary Fibrosis Study (2004). "A placebo-controlled trial of interferon gamma-1b in patients with idiopathic pulmonary fibrosis." *N Engl J Med* **350**(2): 125-133.
- Raghu, G., K. K. Brown, U. Costabel, V. Cottin, R. M. du Bois, J. A. Lasky, M. Thomeer, J. P. Utz, R. K. Khandker, L. McDermott and S. Fatenejad (2008). "Treatment of idiopathic pulmonary fibrosis with etanercept: an exploratory, placebo-controlled trial." *Am J Respir Crit Care Med* **178**(9): 948-955.
- Raghu, G., H. R. Collard, J. J. Egan, F. J. Martinez, J. Behr, K. K. Brown, T. V. Colby, J. F. Cordier, K. R. Flaherty, J. A. Lasky, D. A. Lynch, J. H. Ryu, J. J. Swigris, A. U. Wells, J. Ancochea, D. Bouros, C. Carvalho, U. Costabel, M. Ebina, D. M. Hansell, T. Johkoh, D. S. Kim, T. E. King,

- Jr., Y. Kondoh, J. Myers, N. L. Muller, A. G. Nicholson, L. Richeldi, M. Selman, R. F. Dudden, B. S. Griss, S. L. Protzko, H. J. Schunemann and A. E. J. A. C. o. I. P. Fibrosis (2011). "An official ATS/ERS/JRS/ALAT statement: idiopathic pulmonary fibrosis: evidence-based guidelines for diagnosis and management." *Am J Respir Crit Care Med* **183**(6): 788-824.
- Raghu, G., F. J. Martinez, K. K. Brown, U. Costabel, V. Cottin, A. U. Wells, L. Lancaster, K. F. Gibson, T. Haddad, P. Agarwal, M. Mack, B. Dasgupta, I. P. Nnane, S. K. Flavin and E. S. Barnathan (2015). "CC-chemokine ligand 2 inhibition in idiopathic pulmonary fibrosis: a phase 2 trial of carlumab." *Eur Respir J* **46**(6): 1740-1750.
- Raghu, G., M. Remy-Jardin, J. L. Myers, L. Richeldi, C. J. Ryerson, D. J. Lederer, J. Behr, V. Cottin, S. K. Danoff, F. Morell, K. R. Flaherty, A. Wells, F. J. Martinez, A. Azuma, T. J. Bice, D. Bouros, K. K. Brown, H. R. Collard, A. Duggal, L. Galvin, Y. Inoue, R. G. Jenkins, T. Johkoh, E. A. Kazerooni, M. Kitaichi, S. L. Knight, G. Mansour, A. G. Nicholson, S. N. J. Pipavath, I. Buendia-Roldan, M. Selman, W. D. Travis, S. Walsh, K. C. Wilson, E. R. S. J. R. S. American Thoracic Society and S. Latin American Thoracic (2018). "Diagnosis of Idiopathic Pulmonary Fibrosis. An Official ATS/ERS/JRS/ALAT Clinical Practice Guideline." *Am J Respir Crit Care Med* **198**(5): e44-e68.
- Raghu, G., B. Rochweg, Y. Zhang, C. A. Garcia, A. Azuma, J. Behr, J. L. Brozek, H. R. Collard, W. Cunningham, S. Homma, T. Johkoh, F. J. Martinez, J. Myers, S. L. Protzko, L. Richeldi, D. Rind, M. Selman, A. Theodore, A. U. Wells, H. Hoogsteden, H. J. Schunemann, S. American Thoracic, s. European Respiratory, S. Japanese Respiratory and A. Latin American Thoracic (2015). "An Official ATS/ERS/JRS/ALAT Clinical Practice Guideline: Treatment of Idiopathic Pulmonary Fibrosis. An Update of the 2011 Clinical Practice Guideline." *Am J Respir Crit Care Med* **192**(2): e3-19.
- Raghu, G., B. van den Blink, M. J. Hamblin, A. W. Brown, J. A. Golden, L. A. Ho, M. S. Wijsenbeek, M. Vasakova, A. Pesci, D. E. Antin-Ozerkis, K. C. Meyer, M. Kreuter, D. Moran, H. Santin-Janin, F. Aubin, G. J. Mulder, R. Gupta and L. Richeldi (2019). "Long-term treatment with recombinant human pentraxin 2 protein in patients with idiopathic pulmonary fibrosis: an open-label extension study." *Lancet Respir Med* **7**(8): 657-664.
- Raghu, G., B. van den Blink, M. J. Hamblin, A. W. Brown, J. A. Golden, L. A. Ho, M. S. Wijsenbeek, M. Vasakova, A. Pesci, D. E. Antin-Ozerkis, K. C. Meyer, M. Kreuter, H. Santin-Janin, G. J. Mulder, B. Bartholmai, R. Gupta and L. Richeldi (2018). "Effect of Recombinant Human Pentraxin 2 vs Placebo on Change in Forced Vital Capacity in Patients With Idiopathic Pulmonary Fibrosis: A Randomized Clinical Trial." *JAMA* **319**(22): 2299-2307.
- Reijm, S., T. Kissel and R. E. M. Toes (2020). "Checkpoints controlling the induction of B cell mediated autoimmunity in human autoimmune diseases." *Eur J Immunol* **50**(12): 1885-1894.
- Richeldi, L., R. M. du Bois, G. Raghu, A. Azuma, K. K. Brown, U. Costabel, V. Cottin, K. R. Flaherty, D. M. Hansell, Y. Inoue, D. S. Kim, M. Kolb, A. G. Nicholson, P. W. Noble, M. Selman, H. Taniguchi, M. Brun, F. Le Maulf, M. Girard, S. Stowasser, R. Schlenker-Herceg, B. Disse, H. R. Collard and I. T. Investigators (2014). "Efficacy and safety of nintedanib in idiopathic pulmonary fibrosis." *N Engl J Med* **370**(22): 2071-2082.
- Rockey, D. C., P. D. Bell and J. A. Hill (2015). "Fibrosis--A Common Pathway to Organ Injury and Failure." *N Engl J Med* **373**(1): 96.
- Rosenbaum, M., V. Andreani, T. Kapoor, S. Herp, H. Flach, M. Duchniewicz and R. Grosschedl (2014). "MZB1 is a GRP94 cochaperone that enables proper immunoglobulin heavy chain biosynthesis upon ER stress." *Genes Dev* **28**(11): 1165-1178.
- Rosenberg, J. M. and P. J. Utz (2015). "Protein microarrays: a new tool for the study of autoantibodies in immunodeficiency." *Front Immunol* **6**: 138.
- Ryerson, C. J., T. H. Urbania, L. Richeldi, J. J. Mooney, J. S. Lee, K. D. Jones, B. M. Elicker, L. L. Koth, T. E. King, Jr., P. J. Wolters and H. R. Collard (2013). "Prevalence and prognosis of unclassifiable interstitial lung disease." *Eur Respir J* **42**(3): 750-757.

- Saito, A., H. Okazaki, I. Sugawara, K. Yamamoto and H. Takizawa (2003). "Potential action of IL-4 and IL-13 as fibrogenic factors on lung fibroblasts in vitro." *Int Arch Allergy Immunol* **132**(2): 168-176.
- Salinas, G. F., F. Braza, S. Brouard, P. P. Tak and D. Baeten (2013). "The role of B lymphocytes in the progression from autoimmunity to autoimmune disease." *Clin Immunol* **146**(1): 34-45.
- Scheltema, R. A. and M. Mann (2012). "SprayQc: a real-time LC-MS/MS quality monitoring system to maximize uptime using off the shelf components." *J Proteome Res* **11**(6): 3458-3466.
- Schiller, H. B., I. E. Fernandez, G. Burgstaller, C. Schaab, R. A. Scheltema, T. Schwarzmayr, T. M. Strom, O. Eickelberg and M. Mann (2015). "Time- and compartment-resolved proteome profiling of the extracellular niche in lung injury and repair." *Mol Syst Biol* **11**(7): 819.
- Schiller, H. B., C. H. Mayr, G. Leuschner, M. Strunz, C. Staab-Weijnitz, S. Preisendorfer, B. Eckes, P. Moinzadeh, T. Krieg, D. A. Schwartz, R. A. Hatz, J. Behr, M. Mann and O. Eickelberg (2017). "Deep Proteome Profiling Reveals Common Prevalence of MZB1-Positive Plasma B Cells in Human Lung and Skin Fibrosis." *Am J Respir Crit Care Med* **196**(10): 1298-1310.
- Schneider, F., K. L. Veraldi, M. C. Levesque, T. V. Colby and S. Y. E (2016). "IgG4-Related Lung Disease Associated with Usual Interstitial Pneumonia." *Open Rheumatol J* **10**: 33-38.
- Scott, M. K. D., K. Quinn, Q. Li, R. Carroll, H. Warsinske, F. Vallania, S. Chen, M. A. Carns, K. Aren, J. Sun, K. Koloms, J. Lee, J. Baral, J. Kropski, H. Zhao, E. Herzog, F. J. Martinez, B. B. Moore, M. Hinchcliff, J. Denny, N. Kaminski, J. D. Herazo-Maya, N. H. Shah and P. Khatri (2019). "Increased monocyte count as a cellular biomarker for poor outcomes in fibrotic diseases: a retrospective, multicentre cohort study." *Lancet Respir Med* **7**(6): 497-508.
- Shum, A. K., M. Alimohammadi, C. L. Tan, M. H. Cheng, T. C. Metzger, C. S. Law, W. Lwin, J. Perheentupa, H. Bour-Jordan, J. C. Carel, E. S. Husebye, F. De Luca, C. Janson, R. Sargur, N. Dubois, M. Kajosaari, P. J. Wolters, H. A. Chapman, O. Kampe and M. S. Anderson (2013). "BPIFB1 is a lung-specific autoantigen associated with interstitial lung disease." *Sci Transl Med* **5**(206): 206ra139.
- Sitaru, C., S. Mihai and D. Zillikens (2007). "The relevance of the IgG subclass of autoantibodies for blister induction in autoimmune bullous skin diseases." *Arch Dermatol Res* **299**(1): 1-8.
- Solomon, J. J., J. H. Chung, G. P. Cosgrove, M. K. Demoruelle, E. R. Fernandez-Perez, A. Fischer, S. K. Frankel, S. B. Hobbs, T. J. Huie, J. Ketzer, A. Mannina, A. L. Olson, G. Russell, Y. Tsuchiya, Z. X. Yunt, P. T. Zelarney, K. K. Brown and J. J. Swigris (2016). "Predictors of mortality in rheumatoid arthritis-associated interstitial lung disease." *Eur Respir J* **47**(2): 588-596.
- Staab-Weijnitz, C. A., I. E. Fernandez, L. Knuppel, J. Maul, K. Heinzelmann, B. M. Juan-Guardela, E. Hennen, G. Preissler, H. Winter, C. Neurohr, R. Hatz, M. Lindner, J. Behr, N. Kaminski and O. Eickelberg (2015). "FK506-Binding Protein 10, a Potential Novel Drug Target for Idiopathic Pulmonary Fibrosis." *Am J Respir Crit Care Med* **192**(4): 455-467.
- Strunz, M., L. M. Simon, M. Ansari, J. J. Kathiriya, I. Angelidis, C. H. Mayr, G. Tsidiridis, M. Lange, L. F. Mattner, M. Yee, P. Ogar, A. Sengupta, I. Kukhtevich, R. Schneider, Z. Zhao, C. Voss, T. Stoeger, J. H. L. Neumann, A. Hilgendorff, J. Behr, M. O'Reilly, M. Lehmann, G. Burgstaller, M. Konigshoff, H. A. Chapman, F. J. Theis and H. B. Schiller (2020). "Alveolar regeneration through a Krt8+ transitional stem cell state that persists in human lung fibrosis." *Nat Commun* **11**(1): 3559.
- Suda, T., Y. Kaida, Y. Nakamura, N. Enomoto, T. Fujisawa, S. Imokawa, H. Hashizume, T. Naito, D. Hashimoto, Y. Takehara, N. Inui, H. Nakamura, T. V. Colby and K. Chida (2009). "Acute exacerbation of interstitial pneumonia associated with collagen vascular diseases." *Respir Med* **103**(6): 846-853.
- Taille, C., S. Grootenboer-Mignot, C. Boursier, L. Michel, M. P. Debray, J. Fagart, L. Barrientos, A. Maillieux, N. Cigna, F. Tubach, J. Marchal-Somme, P. Soler, S. Chollet-Martin and B. Crestani



- (2011). "Identification of periplakin as a new target for autoreactivity in idiopathic pulmonary fibrosis." Am J Respir Crit Care Med **183**(6): 759-766.
- Taipale, J., K. Miyazono, C. H. Heldin and J. Keski-Oja (1994). "Latent transforming growth factor-beta 1 associates to fibroblast extracellular matrix via latent TGF-beta binding protein." J Cell Biol **124**(1-2): 171-181.
- Thakur, S. S., T. Geiger, B. Chatterjee, P. Bandilla, F. Frohlich, J. Cox and M. Mann (2011). "Deep and highly sensitive proteome coverage by LC-MS/MS without prefractionation." Mol Cell Proteomics **10**(8): M110 003699.
- Thannickal, V. J., Y. Zhou, A. Gaggar and S. R. Duncan (2014). "Fibrosis: ultimate and proximate causes." J Clin Invest **124**(11): 4673-4677.
- Thien, M., T. G. Phan, S. Gardam, M. Amesbury, A. Basten, F. Mackay and R. Brink (2004). "Excess BAFF rescues self-reactive B cells from peripheral deletion and allows them to enter forbidden follicular and marginal zone niches." Immunity **20**(6): 785-798.
- Thomeer, M. J., U. Costabe, G. Rizzato, V. Poletti and M. Demedts (2001). "Comparison of registries of interstitial lung diseases in three European countries." Eur Respir J Suppl **32**: 114s-118s.
- Todd, J. L., M. L. Neely, R. Overton, K. Durham, M. Gulati, H. Huang, J. Roman, L. K. Newby, K. R. Flaherty, R. Vinisko, Y. Liu, J. Roy, R. Schmid, B. Strobel, C. Hesslinger, T. B. Leonard, I. Noth, J. A. Belperio, S. M. Palmer and I.-P. R. investigators (2019). "Peripheral blood proteomic profiling of idiopathic pulmonary fibrosis biomarkers in the multicentre IPF-PRO Registry." Respir Res **20**(1): 227.
- Todd, N. W., R. G. Scheraga, J. R. Galvin, A. T. Iacono, E. J. Britt, I. G. Luzina, A. P. Burke and S. P. Atamas (2013). "Lymphocyte aggregates persist and accumulate in the lungs of patients with idiopathic pulmonary fibrosis." J Inflamm Res **6**: 63-70.
- Tonegawa, S. (1983). "Somatic generation of antibody diversity." Nature **302**(5909): 575-581.
- Travis, W. D., U. Costabel, D. M. Hansell, T. E. King, Jr., D. A. Lynch, A. G. Nicholson, C. J. Ryerson, J. H. Ryu, M. Selman, A. U. Wells, J. Behr, D. Bouros, K. K. Brown, T. V. Colby, H. R. Collard, C. R. Cordeiro, V. Cottin, B. Crestani, M. Drent, R. F. Dudden, J. Egan, K. Flaherty, C. Hogaboam, Y. Inoue, T. Johkoh, D. S. Kim, M. Kitaichi, J. Loyd, F. J. Martinez, J. Myers, S. Protzko, G. Raghu, L. Richeldi, N. Sverzellati, J. Swigris, D. Valeyre and A. E. C. o. I. I. Pneumonias (2013). "An official American Thoracic Society/European Respiratory Society statement: Update of the international multidisciplinary classification of the idiopathic interstitial pneumonias." Am J Respir Crit Care Med **188**(6): 733-748.
- Troy, L., I. Glaspole, N. Goh, C. Zappala, P. Hopkins, M. Wilsher, Y. Moodley and T. Corte (2014). "Prevalence and prognosis of unclassifiable interstitial lung disease." Eur Respir J **43**(5): 1529-1530.
- Tyanova, S., T. Temu, P. Sinitcyn, A. Carlson, M. Y. Hein, T. Geiger, M. Mann and J. Cox (2016). "The Perseus computational platform for comprehensive analysis of (prote)omics data." Nat Methods **13**(9): 731-740.
- Vekariya, U., K. Rawat, R. Saxena and R. K. Tripathi (2019). "Identification of MPhi specific POTEE expression: Its role in mTORC2 activation via protein-protein interaction in TAMs." Cell Immunol **335**: 30-40.
- Vidarsson, G., G. Dekkers and T. Rispiens (2014). "IgG subclasses and allotypes: from structure to effector functions." Front Immunol **5**: 520.
- Vij, R. and M. E. Streck (2013). "Diagnosis and treatment of connective tissue disease-associated interstitial lung disease." Chest **143**(3): 814-824.

- Vuga, L. J., J. R. Tedrow, K. V. Pandit, J. Tan, D. J. Kass, J. Xue, D. Chandra, J. K. Leader, K. F. Gibson, N. Kaminski, F. C. Scirba and S. R. Duncan (2014). "C-X-C motif chemokine 13 (CXCL13) is a prognostic biomarker of idiopathic pulmonary fibrosis." *Am J Respir Crit Care Med* **189**(8): 966-974.
- Wang, L., F. S. Wang and M. E. Gershwin (2015). "Human autoimmune diseases: a comprehensive update." *J Intern Med* **278**(4): 369-395.
- Wang, P. W., Y. C. Hung, T. H. Wu, M. H. Chen, C. T. Yeh and T. L. Pan (2017). "Proteome-based identification of apolipoprotein A-IV as an early diagnostic biomarker in liver fibrosis." *Oncotarget* **8**(51): 88951-88964.
- Wang, Q., X. Li, S. Ren, N. Cheng, M. Zhao, Y. Zhang, J. Li, W. Cai, C. Zhao, W. Cao and C. Zhou (2015). "Serum levels of the cancer-testis antigen POTEE and its clinical significance in non-small-cell lung cancer." *PLoS One* **10**(4): e0122792.
- Wells, A. U., J. Behr, U. Costabel, V. Cottin and V. Poletti (2012). "Triple therapy in idiopathic pulmonary fibrosis: an alarming press release." *Eur Respir J* **39**(4): 805-806.
- Wells, A. U. and C. P. Denton (2014). "Interstitial lung disease in connective tissue disease--mechanisms and management." *Nat Rev Rheumatol* **10**(12): 728-739.
- Wilson, M. S., S. K. Madala, T. R. Ramalingam, B. R. Gochuico, I. O. Rosas, A. W. Cheever and T. A. Wynn (2010). "Bleomycin and IL-1beta-mediated pulmonary fibrosis is IL-17A dependent." *J Exp Med* **207**(3): 535-552.
- Wuyts, W. A., C. Agostini, K. M. Antoniou, D. Bouros, R. C. Chambers, V. Cottin, J. J. Egan, B. N. Lambrecht, R. Lories, H. Parfrey, A. Prasse, C. Robalo-Cordeiro, E. Verbeken, J. A. Verschakelen, A. U. Wells and G. M. Verleden (2013). "The pathogenesis of pulmonary fibrosis: a moving target." *Eur Respir J* **41**(5): 1207-1218.
- Wynn, T. A. (2011). "Integrating mechanisms of pulmonary fibrosis." *J Exp Med* **208**(7): 1339-1350.
- Xue, J., D. J. Kass, J. Bon, L. Vuga, J. Tan, E. Csizmadia, L. Otterbein, M. Soejima, M. C. Levesque, K. F. Gibson, N. Kaminski, J. M. Pilewski, M. Donahoe, F. C. Scirba and S. R. Duncan (2013). "Plasma B lymphocyte stimulator and B cell differentiation in idiopathic pulmonary fibrosis patients." *J Immunol* **191**(5): 2089-2095.
- Yamauchi, T. and T. Moroishi (2019). "Hippo Pathway in Mammalian Adaptive Immune System." *Cells* **8**(5).
- Yang, Y., J. Fujita, S. Bandoh, Y. Ohtsuki, I. Yamadori, T. Yoshinouchi and T. Ishida (2002). "Detection of antivimentin antibody in sera of patients with idiopathic pulmonary fibrosis and non-specific interstitial pneumonia." *Clin Exp Immunol* **128**(1): 169-174.
- Yu, C., M. E. Gershwin and C. Chang (2014). "Diagnostic criteria for systemic lupus erythematosus: a critical review." *J Autoimmun* **48-49**: 10-13.
- Zhou, J. and P. Giannakakou (2005). "Targeting microtubules for cancer chemotherapy." *Curr Med Chem Anticancer Agents* **5**(1): 65-71.
- Zinkernagel, R. M. (2003). "On natural and artificial vaccinations." *Annu Rev Immunol* **21**: 515-546.

## Appendix: Permission to reuse figures and tables

- Figure 1: © 2011 Wynn et al. Originally published in *J Exp Med*. <https://doi.org/10.1084/jem.20110551>. Gratis reuse in dissertations.
- Figure 2: Copyright © ERS 2018. The *ERR* is published under the Creative Commons Attribution-NonCommercial 4.0 licence ("CC-BY-NC"), which allows for non-commercial reuse of content provided the source is acknowledged. DOI: 10.1183/16000617.0076-2018
- Figure 3: Reprinted with permission of the American Thoracic Society. Copyright © 2021 American Thoracic Society. All rights reserved. The American Journal of Respiratory and Critical Care Medicine is an official journal of the American Thoracic Society.
- Figure 4: Copyright © 2017, Macmillan Publishers Limited. Nature Reviews Disease Primers, Springer Nature. doi: 10.1038/nrdp.2017.74. The permit for reuse in this work is given.
- Figure 5: Copyright © 2004, Nature Publishing Group. Nature Reviews Cancer, Springer Nature. doi: 10.1038/nrc1252. The permit for reuse in this work is given.
- Figure 6: © 2015 The Association for the Publication of the Journal of Internal Medicine. <https://doi.org/10.1111/joim.12395>. The permit for reuse in this work is given.
- Figure 7: © 2020 Wiley-VCH GmbH. <https://doi.org/10.1002/eji.202048820>. The permit for reuse in this work is given.
- Figure 8: Reproduced with permission of the © ERS 2021: European Respiratory Journal Jun 2016, 47 (6) 1767-1775; DOI: 10.1183/13993003.01565-2015
- Figures 9-20: Reprinted with permission of the American Thoracic Society. Copyright © 2021 American Thoracic Society. All rights reserved. Schiller, H. B., C. H. Mayr, G. Leuschner, M. Strunz, C. Staab-Weijnitz, S. Preisendorfer, B. Eckes, P. Moinzadeh, T. Krieg, D. A. Schwartz, R. A. Hatz, J. Behr, M. Mann and O. Eickelberg (2017). "Deep Proteome Profiling Reveals Common Prevalence of MZB1-Positive Plasma B Cells in Human Lung and Skin Fibrosis."; *Am J Respir Crit Care Med*; **196**(10): 1298-1310. The American Journal of Respiratory and Critical Care Medicine is an official journal of the American Thoracic Society.
- Tables 4 and 5: Reprinted with permission of the American Thoracic Society. Copyright © 2021 American Thoracic Society. All rights reserved. Schiller, H. B., C. H. Mayr, G. Leuschner, M. Strunz, C. Staab-Weijnitz, S. Preisendorfer, B. Eckes, P. Moinzadeh, T. Krieg, D. A. Schwartz, R. A. Hatz, J. Behr, M. Mann and O. Eickelberg (2017). "Deep Proteome Profiling Reveals Common Prevalence of MZB1-Positive Plasma B Cells in Human Lung and Skin Fibrosis."; *Am J Respir Crit Care Med*; **196**(10): 1298-1310. The American Journal of Respiratory and Critical Care Medicine is an official journal of the American Thoracic Society.
- Figures 25-27, 29-32 and 34-39: The copyright holder for the preprint on medRxiv is the PhD student (author/funder), who has granted medRxiv a license to display the preprint in perpetuity.
- Tables 6-8: The copyright holder for the preprint on medRxiv is the PhD student (author/funder), who has granted medRxiv a license to display the preprint in perpetuity.

## Acknowledgements

A work such as this thesis can only be realized with the help of many others. First of all, I want to thank Dr. Herbert Schiller for supervising and mentoring me. I am very grateful for the scientific support, teaching and guidance throughout my time at the CPC and appreciate the opportunity to work on such a great translation research project.

To Prof. Dr. Jürgen Behr, for constant help, mentoring and encouragement. Also, I would like to thank the members of my thesis committee Prof. Dr. Vigo Heissmeyer and Prof. Dr. Heiko for their contribution to my thesis advisory committee, discussions and helpful advice. I would like to acknowledge all collaboration partners and co-authors of the autoantibody manuscript.

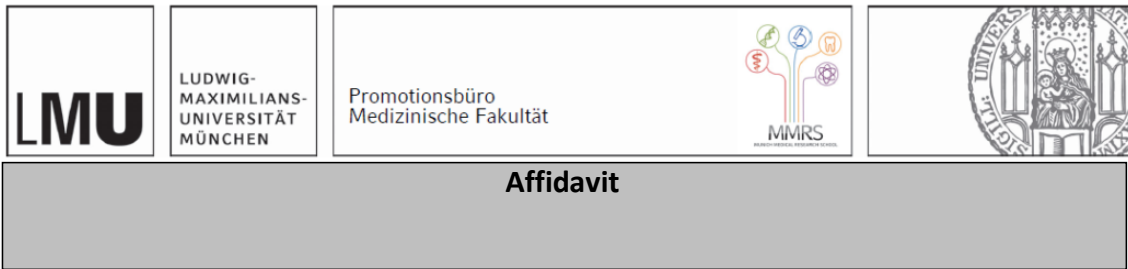
I am deeply grateful to all members of the Schiller Lab who contributed to an outstanding working atmosphere with helping hands, valuable advice, fruitful discussions and a lot of fun. Deep thanks to Christoph for the constant help from the first until the last day: without you, this work would have not been possible for me! Thank you also to Laura, Max, Ilias and Meshal for the wonderful time and your friendship.

Beyond, a big thank you to the CPC Research School „Lung Biology and Disease“, especially to PD Dr. Claudia Staab-Weijnitz, Dr. Doreen Franke, Dr. Cornelia Depner and Karin Herbert for the organization and excellent program. Further, I would like to acknowledge the CPC BioArchive with PD Dr. Anne Hilgendorff, Dr. Britta Peschel, Dr. Annika Frank, Dr. Marion Frankenberger and Daniela Dietel for their always prompt help.

To all patients who are willing to participate in clinical studies and physicians who take care of sample and clinical data collection.

Most importantly, I would like to thank my family and friends for their love and support. To my parents and sister who always support me in my life and my career. I would also like to thank my mom, Anita and Carolin for babysitting many hours so that I could work on my PhD thesis. Most importantly to Alex for always being by my side and to the best gifts in my life, Charlotte and Amelie.

## Affidavit



Dr. med. Leuschner, Gabriela Franziska

\_\_\_\_\_  
Surname, first name

\_\_\_\_\_  
Street

\_\_\_\_\_  
Zip code, town, country

I hereby declare, that the submitted thesis entitled:

**„B cell-mediated autoimmunity in idiopathic pulmonary fibrosis”**

is my own work. I have only used the sources indicated and have not made unauthorised use of services of a third party. Where the work of others has been quoted or reproduced, the source is always given.

I further declare that the submitted thesis or parts thereof have not been presented as part of an examination degree to any other university.

Landshut, 10.04.2022

\_\_\_\_\_  
place, date

Gabriela Leuschner

\_\_\_\_\_  
Signature doctoral candidate

## Confirmation of congruency



LUDWIG-  
MAXIMILIANS-  
UNIVERSITÄT  
MÜNCHEN

Promotionsbüro  
Medizinische Fakultät



**Confirmation of congruency between printed and electronic version of  
the doctoral thesis**

Dr. med. Leuschner, Gabriela Franziska

\_\_\_\_\_  
Surname, first name

\_\_\_\_\_  
Street

\_\_\_\_\_  
Zip code, town, country

I hereby declare, that the submitted thesis entitled:

**„B cell-mediated autoimmunity in idiopathic pulmonary fibrosis“**

is congruent with the printed version both in content and format.

Landshut, 10.04.2022

\_\_\_\_\_  
place, date

Gabriela Leuschner

\_\_\_\_\_  
Signature doctoral candidate

## **Curriculum vitae**

## List of publications

Dr. med. Gabriela Franziska Leuschner, née Wypior:

### Peer reviewed publications - in chronologic order

- Pestka A., Toth B., Kuhn C., Hofmann S., Wiest I., **Wypior G.**, Friese K., Jeschke U. 2011. Retinoid-X-receptor  $\alpha$  and retinoids are key regulators in apoptosis of trophoblasts of patients with recurrent miscarriages. *Journal of Molecular Endocrinology*
- Pavlik R.\*, **Wypior G.\***, Hecht S., Papadopoulos P., Kupka M., Thaler C., Wiest I., Pestka A., Friese K., Jeschke U. 2011. Induction of G Protein-Coupled Estrogen Receptor (GPER) and Nuclear Steroid Hormone Receptors by Gonadotropins in Human Granulosa Cells. *Journal of Histochemistry and Cell Biology*  
both authors contributed equally
- Rogenhofer N., Pavlik R., Jeschke U., **Wypior G.**, Ochsenkühn R., Thaler CJ. 2014. Effective Ovarian Stimulation in a Patient with Resistant Ovary Syndrome and Antigonadotrophin Antibodies. *American Journal of Reproductive Immunology*
- Kunisch R., Guder P., Schinke K., Nörenberg D., Ruf VC., Alig S., Bauer HJ., Kirchner SK., Kruger S., Noerenberg D., Singer K., Tiedt S., Weckbach L., **Wypior G.**, Angstwurm M. 2015. Reforming the Surgical Section of the Practical Year at Ludwig-Maximilians-University Munich. *Zentralbl. Chir.*
- **Leuschner G.\***, Wenter V.\*, Milger K., Zimmermann GS., Matthes S., Meinel F, Lehner S., Neurohr C., Behr J., Kneidinger N. 2016. Suspected pulmonary embolism in patients with pulmonary fibrosis: discordance between ventilation/perfusion SPECT and CT pulmonary angiography. *Respirology*  
both authors contributed equally
- Sabel BO, Plum JL, Kneidinger N, **Leuschner G.**, Koletzko L, Raziorrouh B, Schinner R, Kunz WG, Schoeppe F, Thierfelder KM, Sommer WH, Meinel FG. 2017. Structured reporting of CT examinations in acute pulmonary embolism. *J Cardiovasc Comput Tomogr.*
- Kneidinger N, Milger K, Janitza S, Ceelen F, **Leuschner G.**, Dinkel J, Königshoff M, Weig T, Schramm R, Winter H, Behr J, Neurohr C. 2017. Lung volumes predict survival in patients with chronic lung allograft dysfunction. *Eur Respir J.*
- Schiller, H., Mayr, C., **Leuschner, G.**, Strunz, M., Staab-Weijnitz, C., Preisendörfer, S., Eckes, B., Moinzadeh, P., Krieg, T., Hatz, R., Schwartz, D., Behr, J., Mann, M., Eickelberg, O. 2017. Deep proteome profiling reveals common prevalence of MZB1-positive plasma B cells in human lung and skin fibrosis. *AJRCCM. #*
- **Leuschner G.**, Stocker T., Veit T., Kneidinger N., Winter H., Schramm R., Weig T., Matthes S., Ceelen F., Arnold P., Munker D., Klenner F., Hatz R., Frankenberger M., Behr J., Neurohr C. 2017. Lung transplantation in idiopathic pulmonary fibrosis: the role of antifibrotic therapy. *Journal of Heart and Lung Transplantation.*
- Matthes S, Stadler J, Barton J, **Leuschner G**, Munker D, Arnold P, Villena-Hermoza H, Frankenberger M, Probst P, Koch A, Kneidinger N, Milger K, Behr J, Neurohr C. 2018. Asthma features in severe COPD: Identifying treatable traits. *Respir Med.*
- **Leuschner G.**, Reiter F, Stocker F, Crispin A, Kneidinger N, Veit T, Klenner F, Ceelen F, Zimmermann G, Leuchte H, Reu S, Dinkel J, Behr J, Neurohr C. 2018. Idiopathic Pulmonary Fibrosis Among Young Patients: Challenges in Diagnosis and Management. *Lung*



- Veit T, **Leuschner G**, Sisic A, Ceelen F, Munker D, Schmitzer M, Weig T, Michel S, Schneider C, Meiser B, Crispin A, Neurohr C, Behr J, Milger K, Kneidinger N. Pirfenidone exerts beneficial effects in patients with IPF undergoing single lung transplantation. 2019. *Am J Transplant*
- Schiopu SRI, Zacherl M, Todica A, Bartenstein P, Milger K, **Leuschner G**, Munker D, Bauer M, Massberg S, Behr J, Neurohr C, Huber BC, Kneidinger N. 2019. Feasibility and accuracy of SPECT myocardial perfusion imaging in end-stage lung disease. *J Nucl Cardiol*.
- Munker D, Arnold P, Veit T, **Leuschner G**, Ceelen F, Barnikel M, Schmitzer M, Barton J, Sonneck T, Milger K, Matthes S, Schiopu S, Kauke T, Weig T, Kneidinger N, Behr J, Neurohr C. 2020. Safety and Efficacy of Steroid Pulse Therapy for Acute Loss of FEV<sub>1</sub> in Lung Transplant Recipients After Exclusion of Acute Cellular Rejection. *Transplant Proc*
- Veit T, Munker D, **Leuschner G**, Mümmeler C, Sisic A, Kauke T, Schneider C, Irlbeck M, Michel S, Eser-Valerie D, Huber M, Barton J, Milger K, Meiser B, Behr J, Kneidinger N. 2020. High prevalence of falsely declaring nicotine abstinence in lung transplant candidates. *PLoS One*
- Behr J, Günther A, Bonella F, Dinkel J, Fink L, Geiser T, Geißler K, Gläser S, Handzhiev S, Jonigk D, Koschel D, Kreuter M, **Leuschner G**, Markart P, Prasse A, Schönfeld N, Schupp JC, Sitter H, Müller-Quernheim J, Costabel U. 2020. [German Guideline for Idiopathic Pulmonary Fibrosis]. *Pneumologie*
- **Leuschner G**, Lauseker M, Howanietz AS, Milger K, Veit T, Munker D, Schneider C, Weig T, Michel S, Barton J, Meiser B, Dinkel J, Neurohr C, Behr J, Kneidinger N. 2020. Longitudinal lung function measurements in single lung transplant recipients with chronic lung allograft dysfunction. *J Heart Lung Transplant*
- Veit T, Barnikel M, Crispin A, Kneidinger N, Ceelen F, Arnold P, Munker D, Schmitzer M, Barton J, Schiopu S, Schiller HB, Frankenberger M, Milger K, Behr J, Neurohr C, **Leuschner G**. 2020. Variability of forced vital capacity in progressive interstitial lung disease: a prospective observational study. *Respir Res*
- **Leuschner G**, Klotsche J, Kreuter M, Prasse A, Wirtz H, Pittrow D, Frankenberger M, Behr J, Kneidinger N; INSIGHTS-IPF Registry Group. 2020. Idiopathic pulmonary fibrosis in elderly patients: Analysis of the INSIGHTS-IPF Observational Study. *Frontiers in Medicine (Lausanne)*.
- Behr J, Günther A, Bonella F, Dinkel J, Fink L, Geiser T, Geissler K, Gläser S, Handzhiev S, Jonigk D, Koschel D, Kreuter M, **Leuschner G**, Markart P, Prasse A, Schönfeld N, Schupp JC, Sitter H, Müller-Quernheim J, Costabel U. 2021. S2K Guideline for Diagnosis of Idiopathic Pulmonary Fibrosis. *Respiration*
- Mayr CH, Simon LM, **Leuschner G**, Ansari M, Schniering J, Geyer PE, Angelidis I, Strunz M, Singh P, Kneidinger N, Reichenberger F, Silbernagel E, Böhm S, Adler H, Lindner M, Maurer B, Hilgendorff A, Prasse A, Behr J, Mann M, Eickelberg O, Theis FJ, Schiller HB. 2021. Integrative analysis of cell state changes in lung fibrosis with peripheral protein biomarkers. *EMBO Mol Med*.
- **Leuschner G\***, Mayr CH\*, Ansari M, Seelinger B, Frankenberger M, Kneidinger N, Hatz R, Hilgendorff A, Prasse A, Behr J, Mann M, Schiller HB. 2021. A proteomics workflow reveals predictive autoantigens in idiopathic pulmonary fibrosis. *medRxiv*. <https://doi.org/10.1101/2021.02.17.21251826>

\*both authors contributed equally

Preprint available online #

- Fischer DS, Ansari M, Wagner KI, Jarosch S, Huang Y, Mayr CH, Strunz M, Lang NJ, D'Ippolito E, Hammel M, Mateyka L, Weber S, Wolff LS, Witter K, Fernandez IE, **Leuschner G**, Milger K, Frankenberger M, Nowak L, Heinig-Menhard K, Koch I, Stoleriu MG, Hilgendorff A, Behr J, Pichlmair A, Schubert B, Theis FJ, Busch DH, Schiller HB, Schober K. 2021. Single-cell RNA sequencing reveals ex vivo signatures of SARS-CoV-2-reactive T cells through 'reverse phenotyping'. Nat Commun.

# publications included in this thesis.

#### Peer reviewed reviews - in chronologic order

- **Wypior G.**, Jeschke U., Kurpisz M., Szekeres-Bartho J. 2011. CRH family induced signal transduction processes in the mammalian ovary. Journal of Reproductive Immunology
- **Leuschner G.**, Behr J. 2017. Acute exacerbation in interstitial lung disease. Frontiers in Medicine (Lausanne).
- **Leuschner G.**, Neurohr C. 2018. Was der Rheumatologen vom Pneumologen lernen kann. Zeitschrift für Rheumatologie.
- **Leuschner G.**, Behr J. 2021. Neues zur Diagnostik und Therapie der idiopathischen Lungenfibrose (IPF). Atemwegs- und Lungenkrankheiten: Themenheft "Fibrosierende Lungenkrankheiten"